Synthesis and Reactivity of Alkylaluminum Adducts of Zirconium Ketene and Ketone Complexes

Thesis by

Robert M. Waymouth

In Partial Fulfillment of the Requirements

for the Degree of

Doctor of Philosophy

California Institute of Technology

Pasadena, California

1987

(Submitted November 24, 1986)

To Mom and Dad

ACKNOWLEDGEMENTS

I would like to acknowledge a number of people who have made my stay at Caltech enjoyable. First and foremost is my graduate advisor, Bob Grubbs. Working for Bob has been a pleasure. On top of exceptional science, his friendship, encouragement, and good example have been an invaluable part of my graduate education.

I would like to thank Dan Straus for many helpful discussions and for showing me the ropes. Many thanks to Doug Meinhart for early mornings on the Links and for his tireless and enthusiastic assistance on the NMR. To the members of the Grubbs group, thanks; it was a riot. Lou Cannizzo and Scott Youngquist have been great roommates and good friends.

I owe special thanks to my buddy Bill Tumas for his many contributions to this thesis and my overall degenerate state. I also thank Bill, Cindy, and Chester (the Dog) for many pleasurable skiing and rockclimbing excursions out of the smog of LA. Bill, Leigh Clawson, and Lou Cannizzo have read all or portions of this manuscript and made many helpful suggestions.

The x-ray crystallographic work was done in collaboration with Bernard Santarsiero, Bob Coots, and Mike Bronikowski. I thank Karl Clauser for excellent technical assistance. I acknowledge Caltech, W.R. Grace, and SOHIO for graduate fellowships that kept me in beer money.

Finally, I'd like to thank my brothers for being the dudes they are, Marcia, Donna, Grandad, and especially Mom and Dad, to whom this thesis is dedicated.

ABSTRACT

A family of alkylaluminum adducts of zirconium ketene and ketone complexes has been prepared. Treatment of dimeric bis(cyclopentadienyl)zirconium ketene complexes with alkylaluminum reagents affords trinuclear Zr_2Al bridging ketene complexes of formula $[Cp_2Zr(C,O\text{-}\eta^2\text{-}OCCHR)]_2(\mu\text{-}AlR_2)(\mu\text{-}X)$. X-Ray structural characterization of these complexes reveals several novel features. Two zirconium ketene ligands are spanned by symmetric dialkylaluminum and hydride, chloride, or methyl ligands to form slightly puckered 6-membered rings. A notable feature of these structures is the coordination of the bridging ligand X (H, Cl, or Me), which is characterized by a large Zr-X-Zr angle and an unusual hybridization for the bridging methyl group. The coordination of this methyl group represents a new bonding geometry for carbon, a trigonal-bipyramidal configuration between two metal centers. This geometry models intermediates in alkyl transmetallations that proceed with inversion and implies that transmetallations with inversion should be facile for electrophilic metal centers.

The bridging methyl complex $[Cp_2Zr(C,O\text{-}\eta^2\text{-}OCCHCH_2CMe_3)]_2(\mu\text{-}AlMe_2)(\mu\text{-}CH_3)$ reacts with acetylene to give an oxymetallacyclopentene. Carbonylation of the bridging methyl complex produces an acyl-enol complex—an unprecedented transformation for a group 4 ketene complex and one that is relevant to the behavior of ketene intermediates over Fischer-Tropsch catalysts.

Zirconium chloro acyl complexes react with alkylaluminum reagents to give alkylaluminum adducts of zirconium ketone complexes. Mechanistic studies of this reaction provide strong support for a stepwise mechanism involving transmetallation to form a zirconium alkyl acyl complex followed by reductive coupling of the zirconium alkyl and acyl ligands. A significant feature of these studies is the observation that aluminum reagents dramatically accelerate the reductive coupling of zirconium alkyl and acyl ligands.

The ketone complexes react readily with olefins, alkynes, and ketones in reactions that should prove useful in organic synthesis. Insertion of ethylene into the zirconium ketone ligand yields oxymetallacyclopentanes, which can hydrolyzed to tertiary alcohols. Insertion of alkynes into the zirconium ketone ligand affords oxymetallacyclopentenes. Terminal alkynes react with high regioselectivity to give oxymetallacyclopentenes with the alkyl substituent α to the metal center. Hydrolysis of these complexes yields tertiary allyl alcohols. The ketone complexes couple with organic ketones to give diolates. Hydrolysis of the diolates affords 1,2-diols. These results demonstrate that zirconium ketone complexes, in contrast to later transition metal ketone complexes, induce the reductive coupling of organic carbonyl substrates to give diolates, a reaction that may prove useful for the preparation of 1,2-diols.

Trinuclear Zr_2Al ketone complexes are formed in the reaction of two equivalents of alkyl acyl zirconium complexes and one equivalent of an aluminum reagent. These complexes appear structurally similar to the trinuclear Zr_2Al ketene complexes discussed above.

TABLE OF CONTENTS

LIST OF TABLES

LIST OF FIGURES AND SCHEMES

CHAPTER 2.

CHAPTER 3.

CHAPTER 1

Interaction of Transition Metal Centers with Lewis Acids

INTRODUCTION

The effects of the Lewis-acidic cocatalysts and metal oxide supports on the activity of transition metal catalysts is an area of considerable theoretical and experimental interest.[1,6] Main group Lewis acids, particularly alkylaluminum reagents, are widely used as cocatalysts in a number of industrially important catalytic processes such as Ziegler-Natta polymerization[2] and olefin metathesis.[3] Lewis acidic metal oxides such as SiO_2 and Al_2O_3 are also used as supports for heterogeneous polymerization, metathesis[4] and CO reduction catalysts.[5]

This thesis describes studies on the interactions between group 4 transition metal complexes and alkylaluminum reagents. Treatment of zirconium ketene and acyl complexes with alkylaluminum reagents afforded a new class of compounds, which serve as models for intermediates in CO reduction processes and which should also prove useful as reagents for the construction of carbon-carbon bonds. These studies reveal that molecular Lewis acids can dramatically affect the reactivity of coordinated ligands derived from carbon monoxide and provide further support for the proposal[6] that Lewis acids play a key role in the activation and reduction of CO.

This chapter presents a brief discussion of the interactions of transition metals with Lewis acids and describes some general features of Lewis acid and aluminum cocatalysts as they apply to three important areas: Ziegler-Natta polymerization, olefin metathesis, and CO reduction. The intent is not to present a review of these catalytic processes; excellent reviews are available elsewhere.[2-5] Rather, the present discussion will focus on the importance of interactions between Lewis acids and transition metal centers in these processes.

Ziegler-Natta Polymerization.[10] One of the prime motivations for studying the interactions of transition metal centers with Lewis acids is the remarkable activity of these bimetallic mixtures as olefin polymerization[2] and metathesis catalysts.[3]

Ziegler-Natta catalysis is a general description for a polymerization process employing catalysts consisting of an early transition metal halide and an alkylaluminum or alkylaluminum halide cocatalyst. These catalysts are believed to polymerize olefins via repeated coordination and insertion of olefins into the transition metal carbon bond as shown below.[11]

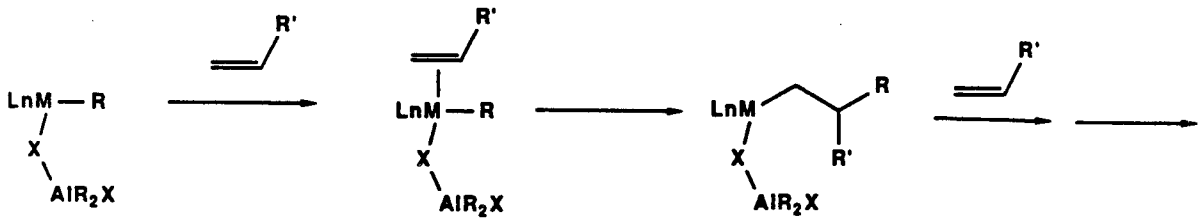

Although little is known concerning the precise role of the aluminum alkyl cocatalyst or the most active valence state of the transition metal for heterogeneous Ziegler-Natta catalysts, studies of homogeneous catalysts have provided considerable insight into the mechanisms of alkylaluminum-transition metal interactions.[2] Several general features are beginning to emerge concerning the nature of the active site and the role of the aluminum cocatalyst. There is now considerable literature precedent that the active site for the homogeneous Cp_2TiCl_2/AlR_xCl_{3-x} system is a Ti(IV) center[12-14] and that propagation involves insertion of the olefin into the transition metal carbon bond, not the aluminum carbon bond as was originally believed.[2,14]

An important function of an aluminum cocatalyst is to alkylate the transition metal center. The aluminum cocatalyst also appears to activate the metal alkyl bond for insertion of the olefin since few group 4 transition metal alkyls spontaneously polymerize olefins.[15,16] The presence of the aluminum cocatalyst appears to be required throughout polymerization since addition of strong Lewis bases quenches the polymerization process.[2] Several proposals have been offered to explain the role of the aluminum alkyl cocatalyst in activating the transition metal carbon bond for olefin

insertion. One proposal is that the aluminum center interacts with a ligand, usually a chlorine, thus affording a more electrophilic transition metal center. Whether or not a discrete metal cation is formed is still in dispute; nevertheless, several recent studies appear to support the proposal of a cationic or partially cationic active site, particularly studies by Dyachkovskii,[17] Eisch,[18] Clawson and Grubbs,[19] and Jordan.[20]

Although the mechanism of Ziegler-Natta polymerization and the role of aluminum cocatalysts are far from well established, the general features discussed above appear to be important for cocatalysis. Alkylaluminum complexes appear to be especially well suited as cocatalysts because they transmetallate readily with transition metal halides and are sufficiently Lewis acidic to activate transition metal centers through bridging ligand interactions or by abstracting a ligand from the transition metal center.

Metathesis. Olefin metathesis is a catalytic process involving the non-pairwise exchange of olefin double bonds, as shown below. The development of olefin metathesis catalysts closely paralleled the development of olefin polymerization catalysts and led to early confusion concerning the mechanistic relationship between the two processes.[3,19,21] Mechanistic studies have revealed some general features regarding the mechanism of olefin metathesis[3] and the role of main-group alkyl cocatalysts.[23–27] It is now generally accepted that the propagation steps for olefin metathesis involves the interconversion of transition metal carbene and metallacyclobutane intermediates as shown below. There are few cases where the mechanism of formation of the transition metal carbene and the role of the main group cocatalyst are well understood, but several functions of the cocatalyst appear to be important for metathesis: (1) As with Ziegler-Natta cocatalysts, an important function of a metathesis cocatalyst is to alkylate the transition metal center. (2) Another important function of the cocatalyst is to assist in the formation of the metal alkylidene by abstracting an α-hydrogen from the newly formed metal alkyl. (3) Coordination of the cocatalyst to the transition

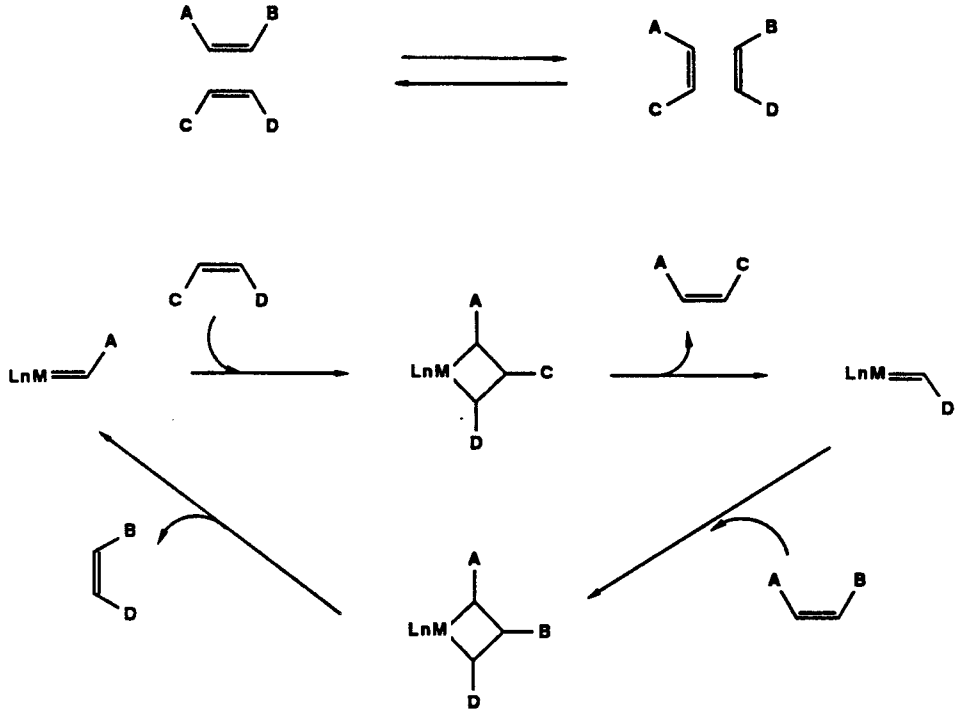

metal, although not always required for metathesis,[22] can in some cases stabilize the reactive alkylidene ligand.

One of the best defined olefin metathesis catalysts that illustrates some of the features discussed above is the bis(cyclopentadienyl)titanocene methylidene catalyst $Cp_2Ti{=}CH_2{\cdot}AlMe_2Cl$.[23] This catalyst is formed by treatment of Cp_2TiCl_2 with two equiv of $AlMe_3$ (eq 1).

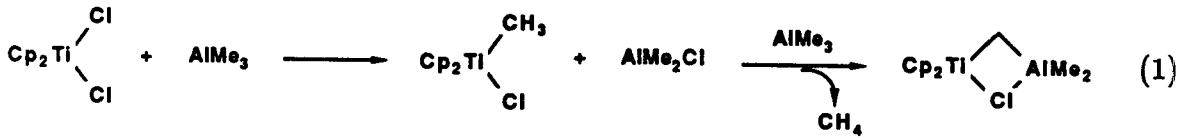

(1)

Mechanistic studies[24] on the reaction of Cp_2TiCl_2 with $AlMe_3$ reveal a stepwise pathway proceeding via initial transmetallation between Cp_2TiCl_2 and $AlMe_3$ to give $Cp_2TiMeCl$ and $AlMe_2Cl$. A subsequent step involving α-hydrogen abstraction

by $AlMe_3$ or $AlMe_2Cl$ yields the "protected" carbene $Cp_2Ti{=}CH_2{\cdot}AlMe_2Cl$. In this system, coordinated $AlMe_2Cl$ is not required for metathesis,[25] but it does help to stabilize the reactive methylidene fragment.

Consideration of the role of the alkylaluminum cocatalysts for olefin metathesis and Ziegler-Natta polymerization points out some striking similarities and some important differences. Following the alkylation step, common to both Ziegler-Natta polymerization and metathesis, there is a distinction in the role of the cocatalyst for the two processes. For the Ziegler-Natta process, the aluminum cocatalyst serves to activate the transition metal carbon bond for olefin insertion, whereas for olefin metathesis, the cocatalyst reacts with the transition metal carbon bond to form the transition metal carbene. This dichotomy in the role of the aluminum cocatalyst points out a fundamental mechanistic distinction[19] in the two processes: Ziegler-Natta polymerization is the reaction of an olefin with a transition metal carbon single bond,[11–15] and olefin metathesis is the reaction of an olefin with a transition metal carbon double bond.[3]

A remarkable feature of the titanium systems described above is that subtle changes in the nature and concentration of the aluminum cocatalyst give rise to mechanistically distinct catalytic processes: treatment of Cp_2TiCl_2 with $AlMeCl_2$ yields a polymerization catalyst,[12] while treatment with $AlMe_3$ affords an olefin metathesis catalyst.[22–28] One of the unique features of alkylaluminum reagents is that subtle changes in the number and type of halide and alkyl ligands can have a dramatic effect on their reactivity.

CO Reduction. The results discussed above point out some of the special features of aluminum reagents that render them ideally suited as cocatalysts for olefin polymerization and metathesis. The interaction between transition metals and alkylaluminum reagents also provides a good model for the interaction between transition metals and Lewis acidic oxide supports. Although few CO reduction catalysts employ

Lewis acid cocatalysts, many consist of later transition metals supported on metal oxide supports such as SiO_2, Al_2O_3, ZrO_2, TiO_2, ZnO, and ThO_2.[5] The role of the catalyst support in altering the activity of the catalyst and the degree to which the support actively participates in CO reduction is a matter of considerable interest and debate.[1,6] One of the experimental approaches to understanding Lewis acidic support effects is through model studies employing molecular Lewis acids. This approach has been pioneered by Shriver and coworkers, whose early studies investigated the coordination of Lewis acids to terminal and bridging carbonyls.[28] Stimulated by the results reported by Collman et al.[29] on the promotion of CO migratory insertion reactions by coordinated Li^+ and Na^+ ions, Shriver carried out a series of systematic investigations on the effects of Lewis acids on the rate of CO migratory insertion reactions.[6,7] As part of these investigations Shriver also demonstrated that alumina surfaces promote the migratory insertion of CO, thus providing indirect evidence that Lewis acidic metal oxides might play an active role in the activation of carbon monoxide.[7c]

There are now a number of reports in the literature documenting the effects of Lewis acids on the migratory insertion of CO, particularly for the later transition metals such as Fe, Mn, Re, and Mo.[6-9] These studies provide a good model for the interactions between later transition metals and Lewis acidic oxide supports and the cooperativity that may be an important feature of the catalyst-support interface. Another important consideration relating to the effects of Lewis acids to CO reduction is the activity of metal oxides such as ZrO_2, ThO_2, HfO_2, LaO_2, Nb_2O_5, and ZnO as CO reduction catalysts.[30] These Lewis acidic metal oxides reduce CO under very mild conditions and show high selectivities for branched hydrocarbon products.[30] A recent mechanistic proposal suggested that branching over these catalysts is due to the formation of ketene, ketone and aldehyde intermediates on the metal oxide catalyst.[31] This mechanistic proposal was based on product analysis and on homogeneous model studies reported by a number of laboratories, notably those of Bercaw,[32] Floriani,[33] Erker,[34] Marks,[35] and Grubbs.[36]

Scope of Thesis. Model studies strongly implicate Lewis acidic centers as sites for CO activation and reduction and underscore the need for further research in this area. One of the aims of this thesis is to address the effects of Lewis acids on the reactivity of ligands derived from carbon monoxide. In particular, this thesis presents results that address the effects of alkylaluminum reagents on the reactivity of zirconium ketene, ketone, and acyl complexes. The interactions between these complexes and aluminum reagents provide a good model for the bonding and reactivity of ketene, ketone and acyl intermediates on heterogenous CO reduction catalysts.

Chapter 2 describes the synthesis and reactivity of trinuclear Zr_2Al bridging ketene complexes prepared from reactions of dimeric ketene complexes with alkylaluminum reagents. Structural studies of these complexes reveal several remarkable features, the most notable of which is a trigonal-bipyramidal bridging methyl group between two zirconium centers. The configuration of this methyl group points out the dramatic effects that electrophilic metal centers have on the reactivity of coordinated alkyl groups. Another feature of the trinuclear bridging ketene complexes is a Zr-O-Al-O-Zr structural framework that supports the bridging ketene ligands. Strong Zr-O-Al interactions dominate the reactivity of the complexes reported throughout this thesis and provide important information regarding the reactivity of alkyl ligands bound to metal oxide surfaces.

Chapter 3 describes the synthesis and reactivity of zirconium ketone complexes prepared by treating zirconium chloro acyl complexes with alkylaluminum reagents. Mechanistic studies revealed that alkylaluminum reagents promote the reductive coupling of alkyl and acyl ligands to give ketone complexes. These studies have important implications regarding the reactivity of acyl intermediates and the role of ketone complexes as precursors to branched products produced over CO reduction catalysts.

The reactivity of these ketone complexes suggests that they will be useful as reagents in organic synthesis. In particular, the ketone complexes react with a variety

of unsaturated substrates such as olefins, alkynes, and ketones. The reaction of the ketone complexes with organic ketones to give diolates implies that zirconium complexes, in conjunction with alkylaluminum reagents, might be developed into versatile reagents for the cross-coupling of organic ketones and aldehydes.

REFERENCES

1. (a) Baker, R.J.; Tauster, S.J.; Eds. *Strong Metal Support Interactions* ACS Symposium Series 298: Washington, D.C., 1986.. (b) Imelik, B.; Naccache, C.; Condurier, G.; Praliand, H.; Meriandeau, P.; Martin, G.A.; Vedrine, J.C.; Eds. *Metal-Support and Metal-Additive Effects in Catalysis* Elsevier: New York, 1982.

2. (a) Sinn, H.; Kaminsky, W. *Adv. Organomet. Chem.* **1980**, *18*, 99-149. (b) Pino, P.; Mulhaupt, R. *Angew. Chem., Int. Ed. Eng.* **1980**, *19*, 857-875. (c) Boor, J. *Ziegler-Natta Catalysis and Polymerizations* Academic Press: London; 1983.

3. (a) Ivin, K.J. *Olefin Metathesis* Academic Press: London; 1983. (b) Grubbs, R.H. *Comprehensive Organometallic Chemistry* Wilkinson, G.; Stone, F.G.A.; Abel, E.W., Eds.; Pergamon Press: Oxford, 1982, Vol 9, p. 499.

4. (a) Iwasawa, Y. *Tailored Metal Catalysts* Reidel: Boston, 1986.(b) Yermakov, Y.I.; Kuznetsov, B.N.; Zakharov, V.A., Eds. *Catalysis by Supported Complexes* Elsevier: Amsterdam, 1981.

5. (a) Rofer-Depoorter, C.K. *Chem. Rev.* **1981**, *81*, 447-474. (b) Masters, C. *Adv. Organomet. Chem.* **1979**, *17*, 61-103. (c) Anderson, R.B. *The Fischer-Tropsch Synthesis* Academic Press: New York, 1984.

6. Shriver, D.F. In *Catalytic Activation of Carbon Monoxides* Ford, P.C., Ed.; ACS Symposium Series 152: Washington, D.C., 1981, pp.1-19.

7. (a) Richmond, T.G.; Shriver, D.F. *Inorg. Chem.* **1982**, *21*, 1272. (b) Butts, S.B.; Strauss, S. H.; Holt, E.M.; Stimson, R.E.; Alcock, N.W.; Shriver, D.F. *J. Am. Chem. Soc.* **1980**, *102*, 5093. (c) Correa, F.; Nakamura, R.; Stimson, R.E.; Burwell, Jr., R.L.; Shriver, D.F. *Ibid.* **1980**, *102*, 5112.

8. (e) Labinger, J.A.; Miller, J.S. *J. Am. Chem. Soc.* **1982**, *104*, 6856. (b) Labinger, J.A.; Bonfiglio, J.N.; Grimmett, D.L.; Masuo, T.; Shearin, E.; Muller, J.S.

Organometallics **1983**, *2*, 733-740. (c) Lindner, E.; von Au, G. *Angew. Chem., Int. Ed. Eng.* **1980**, *19*, 824.

9. (a) Powell, J.; Kuksis, A.; May, C.J.; Nyburg, S.C.; Smith, S.J. *J. Am. Chem. Soc.* **1981**, *103*, 5941. (b) McLain, S.J. *J. Am. Chem. Soc.* **1983**, *105*, 6355.

10. For a historical review of the development of Ziegler-Natta polymerization see: McMillan, F.M. *The Chain Straighteners* MacMillan Press: London, 1979.

11. An alternate mechanism involving metal carbene intermediates has been proposed for the propagation step in Ziegler-Natta systems, but this mechanism has received little experimental support. Ivin, K.J.; Rooney, J.J.; Green, M.L.H.; Mahtab, R. *J. Chem. Soc., Chem. Commun.* **1978**, 604.

12. (a) Breslow, D.S.; Newberg, N.R. *J. Am. Chem. Soc.* **1959**, *81*, 81. (b) Breslow, D.S.; Newberg, N.R. *Ibid.* **1957**, *79*, 5072.

13. Homogeneous Ti(III) centers will also polymerize ethylene, but at slower rates. Natta, G.; Pino, P.; Mazzanti, G.; Giannini, U. *J. Am. Chem. Soc.* **1957**, *79*, 2975. For heterogeneous Ziegler-Natta catalysts, there is considerable evidence that Ti(III) sites are also active for polymerization (ref. 2).

14. Fink, G.; Rottler, R.; Schnell, D.; Zoller, W. *J. Appl. Polym. Sci.* **1976**, *20*, 2779.

15. (a) Chien, J.C.W.; Wu, J.C.; Rausch, M. *J. Am. Chem. Soc.* **1981**, *103*, 1180.(b) Ballard, D.G.H.; Dawkins, J.V.; Key, J.M.; van Lienden, P.W. *Makromol. Chem.* **1973**, *165*, 173.

16. Recently, a family of homogeneous group 3 and lanthanide polymerization catalysts have been developed which do not require Lewis acid cocatalysts. (a) Thompson, M.E.; Bercaw, J.E. *Pure Appl. Chem.* **1984**, *56*, 1-11. (b) Watson, P.L.; Parshall, G.N. *Acc. Chem. Res.* **1985**, *18*, 51-56, and refs. therein. See also: (c) Schmidt, G.F.; Brookhart, M *J. Am. Chem. Soc.* **1985**, *107*, 1443.

17. Dyachkovskii, F.S.; Shilova, A.K.; Shilov, A.E. *J. Polym. Sci., Part C* **1967**, *16*, 2333-2339.

18. Eisch, J.J.; Piotrowski, A.M.; Brownstein, S.K.; Gabe, E.J.; Lee, F.L. *J. Am. Chem. Soc.* **1985**, *107*, 7219-7221.

19. Clawson, L.; Soto, J.; Buchwald, S.L.; Stiegerwald, M.L.; Grubbs, R.H. *J. Am. Chem. Soc.* **1985**, *107*, 3377. Clawson, L.; Grubbs, R.H., unpublished results.

20. Jordan, R.F.; Dasher, W.E.; Echols, S.F. *J. Am. Chem. Soc.* **1986**, *108*, 1718-1719.

21. Banks, R.L. *Catalysis (London)* **1981**, *4*, 100-129.

22. Shrock has reported a family of tungsten oxo alkylidenes whose metathesis activity is enhanced by Lewis Acids. Wengrovius, J.; Schrock, R.R.; Churchill, M.R.; Missert, J.R.; Young, W.J. *J. Am. Chem. Soc.* **1980**, *102*, 4515.

23. (a) Tebbe, F.N.; Parshall, G.W.; Reddy, G.S. *J. Am. Chem. Soc.* **1978**, *100*, 3611. (b) Tebbe, F.N.; Parshall, G.W.; Ovenall, D.W. *Ibid.* **1979**, *101*, 5074. (c) Howard, T.R.; Lee, J.B.; Grubbs, R.H. *Ibid.* **1980**, *102*, 6876. (d) Ott, K.C.; Lee, J.B; Grubbs, R.H. *Ibid.* **1982**, *104*, 2942.

24. Ott, K.C.; deBoer, E.J.M.; Grubbs, R.H. *Organometallics* **1984**, *3*, 223.

25. Treatment of **2** with olefins in the presence of a strong base generates metallacyclobutanes which are active metathesis catalysts in the absence of alkylaluminums(ref. 24, 26, 27).

26. (a) Gilliom, L.R.; Grubbs, R.H. *J. Am. Chem. Soc.* **1986**, *108*, 733-742. (b) Lee, J.B.; Ott, K.C.; Grubbs, R.H. *J. Am. Chem. Soc.* **1982**, *104*, 7491. (c) Lee, J.B.; Gajda, G.J.; Schaefer, W.P.; Howard, T.R.; Ikayira, T.; Straus, D.A.; Grubbs, R.H. *J. Am. Chem. Soc.* **1981**, *103*, 7318.

27. Straus, D.A.; Grubbs, R.H. *J. Mol. Cat.* **1985**, *28*, 9.

28. Horwitz, C.P.; Shriver, D.F. *Adv. Organomet. Chem.* **1984**, *23*, 219-305.

29. Collman, J.P.; Finke, R.G.; Cawse, J.N.; Brauman, J.I. *J. Am. Chem. Soc.* **1978**, *100*, 4766-4772.

30. (a) Onishi, T.; Abe, H.; Maruya, K.; Domen, K. *J. Chem. Soc., Chem. Commun.* **1986**, 103. (b) Maruya, K.; Inaba, A.; Maehashi, T.; Domen, K.; Onishi, T. *J. Chem. Soc., Chem. Commun.* **1985**, 487. (d) Wang, G.; Hattori, H.; Itoh, H.; Tanabe, K. *J. Chem. Soc., Chem. Commun.* **1982**, 1256. (e) Saussey, J.; Lavalley, J-C.; Lamotte, J.; Rais, T. *J. Chem. Soc., Chem. Commun.* **1982**, 278.

31. Mazenec, T.J. *J. Catal.* **1986**, *98*, 115-125.

32. (a) Wolczanski, P.T.; Bercaw, J.E. *Acc. Chem. Res.* **1980**, *13*, 121. (b) Barger, P.T.; Santarsiero, B.D.; Armantrout, J.; Bercaw, J.E *J. Am. Chem. Soc.* **1984**, *106*, 5178 and refs. therein.

33. Gamboratta, S.; Floriani, C.; Chiesi-Villa, A.; Guastini, C. *J. Am. Chem. Soc.* **1983**, *105*, 1690.

34. Erker, G.; Kropp, K. *Chem. Ber.* **1982**, *115*, 2437.

35. Moloy, K.G.; Fagan, P.J.; Manriquez, J.M.; Marks, T.J. *J. Am. Chem. Soc.* **1986**, *108*, 56-67 and refs. therein.

36. (a) Straus, D.A.; Grubbs, R.H. *J. Am. Chem. Soc.* **1982**, *104*, 5499. (b) Ho, S.C.H.; Straus, D.A.; Armantrout, J.; Schaefer, W.P.; Grubbs, R.H.; Bercaw, J.E. *J. Am. Chem. Soc.* **1984**, *106*, 2210. (c) Moore, E.J.; Straus, D.A.; Armantrout, J.; Santarsiero, B.D.; Grubbs, R.H.; Bercaw, J.E. *J. Am. Chem. Soc.* **1983**, *105*, 2068.

CHAPTER 2

Trinuclear Zr_2Al μ-Ketene Complexes Containing Bridging Ligands

INTRODUCTION

Transition metal ketene complexes have been implicated as intermediates in heterogeneous CO reduction[1] and have been demonstrated to be involved in stoichiometric CO reduction processes.[2,4d] Ketene complexes also show considerable promise as intermediates in organic synthesis.[3] We have recently developed an efficient and general route to early transition metal ketene complexes.[4] Deprotonation of Group 4 acyl-halide metallocenes[5] cleanly affords ketene complexes in high yield (eq. 1).[6]

(1)

The monomeric bis-(η^5-pentamethylcyclopentadienyl) zirconocene ketene complexes, and oligomeric bis-(η^5-cyclopentadienyl) titanocene ketene complexes prepared by this route are reactive toward olefins and other substrates under mild conditions.[4a,d] We envisioned that an olefin or acetylene insertion reaction might be synthetically useful if applied to the readily prepared bis-(η^5-cyclopentadienyl) zirconocene ketene complexes (eq. 2).[7] However, these zirconocene ketene complexes are exceptionally inert, apparently due to the formation of strongly bound dimers. These complexes are inert even when generated in the presence of potential substrates.[4b]

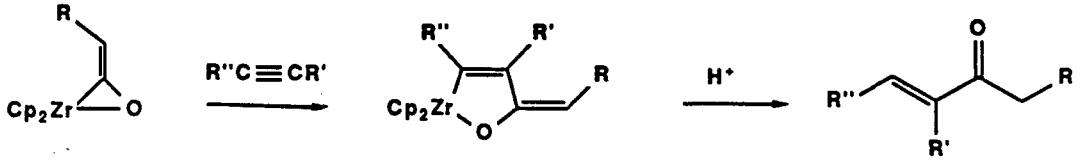

(2)

To develop the chemistry of these complexes, we have investigated their reactivity toward aluminum reagents[10] with two objectives in mind: (1) to activate[9] Zr ketene complexes toward insertion reactions of potential synthetic utility and (2) to study the role of ketene complexes[1,4d] and Lewis acids[11] in Fischer-Tropsch model systems. In a preliminary communication,[12] we reported the crystal structure of the bridging methyl compound **3** prepared by treating the ketene dimer **1a** with $AlMe_3$. A unique structural feature of this compound is a trigonal-bipyramidal bridging methyl ligand. Herein we report details of the synthesis, structure, and reactivity of this novel compound. In addition, we report our studies on the analogous bridging chloride (**7a**) and bridging hydride (**10**) compounds prepared by treating **1a** with Me_2AlCl and Et_2AlH, respectively. The greater stability of **7a** and **10** has enabled us to characterize an intermediate in the reaction sequence (Scheme I-III) and rationalize the reactivity of these compounds in terms of the lability of the bridging ligands.

RESULTS

Preparation of 1a,b.[4a,b] Treatment of the acyl complex (Cp = η^5-cyclopentadienyl) $Cp_2Zr(Cl)C(O)CH_2CH_2C(CH_3)_3$[8b] with a strong, bulky base such as $NaN(Si(CH_3)_3)_2$ affords the ketene dimer **1a** (eq. 1, M=Zr, R′=CH_2CMe_3, R=H) in high yield (quantitative by ^1H NMR).[4] The deprotonation is highly stereoselective. Monitoring the reaction by ^1H NMR at room temperature reveals the following isomeric ratios for the dimer: 76% **(Z,Z)-1a**, 22% **(Z,E)-1a**, and 2% **(E,E)-1a**.[13] These stereochemical assignments were based on NMR data and on crystallographic studies on complexes derived from stereochemically pure samples of **(Z,Z)-1a** (vide infra).[13] Compound **(Z,Z)-1a** can be isolated in 75% yield by this route.

The parent ketene complex **1b** (eq. 1, M = Zr, R = H, R' = H) was prepared by treating the acyl complex $Cp_2Zr(Cl)COCH_3$[15] with $NaN(Si(CH_3)_3)_2$. Complex **1b** has not been completely characterized due to its low solubility, but is assumed to be oligomeric. Spectral comparison (^1H, ^{13}C NMR, IR) with its titanium[4a] and bis (η^5-pentamethylcyclopentadienyl)zirconium[4d] analogs along with characterization of its $AlMe_2Cl$ derivative (vida infra) supports its assignment as the unsubstituted ketene complex of zirconocene.

Preparation of 2,3. The ketene dimer **1a** reacts instantly at 25°C with 1 equivalent of $AlMe_3$ in toluene to afford the adduct **2** (Scheme I). Complex **2** could not be isolated, but was observed spectroscopically. The NMR spectra of **2** (Table 2) exhibit inequivalent cyclopentadienyl, ketene, and methyl resonances. The methyl resonances appear in the ^1H NMR as slightly broad singlets in a ratio of 2:1, indicating that these groups do not exchange at 25°C on the NMR time scale. The inequivalent methyl groups also have different $^1J_{CH}$ coupling constants, 110.5 Hz and 125.7 Hz (Table 2).

Complex **2** is unstable under vacuum; evacuating solutions of **2** regenerate the ketene dimer **1a** and $AlMe_3$. Treatment of **2** with Lewis bases (Et_2O, THF, pyridine) generates **1a** and the $AlMe_3$·Lewis base adduct. In toluene at room temperature, **2** slowly isomerizes to **3** in approximately 9 h at 25°C (Scheme I). If **2** is formed in the presence of excess $AlMe_3$, the isomerization is faster, requiring approximately 1 h at 25°C. Complex **3** does not react cleanly with excess $AlMe_3$ but does decompose faster in the presence of that reagent.

SCHEME I

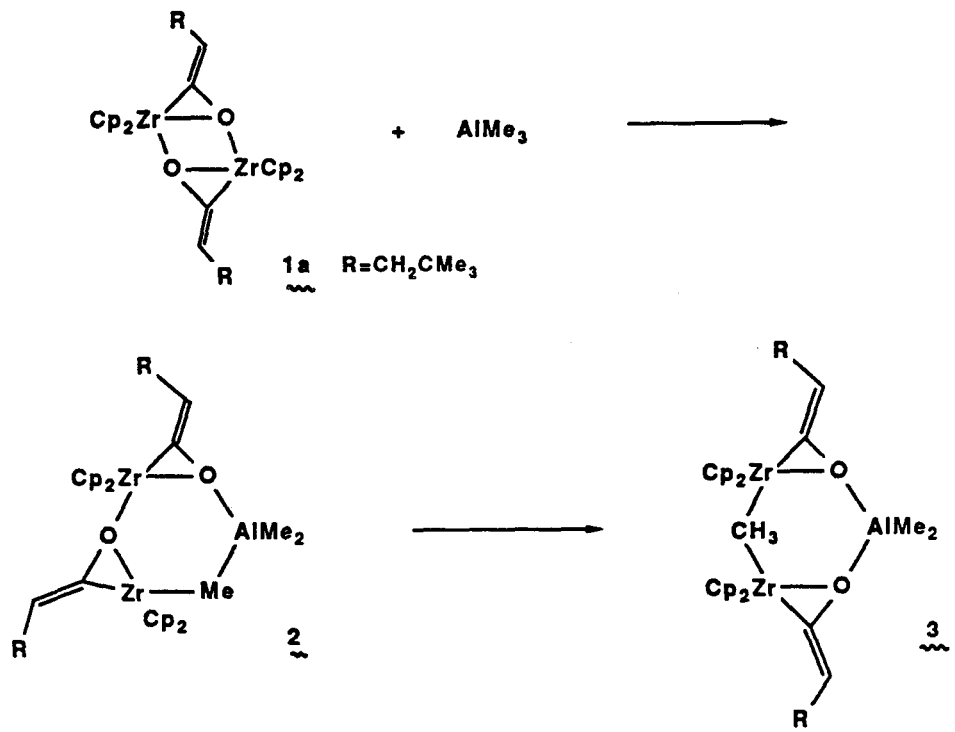

Complex **3** is a colorless crystalline compound which is stable at 25°C in aromatic solvents but decomposes slowly ($t_{1/2}$ = 2.5 h) at 60°C to unidentified products. The NMR spectra of **3** exhibit equivalent cyclopentadienyl and ketene resonances along with inequivalent methyl resonances in a ratio of 2:1. The appearance of a sharp singlet at -9.24 ppm in the ^{13}C NMR spectrum implies that one of the methyl groups is no longer bonded to aluminum.[16] In addition, this methyl group exhibits an anomalously high $^1J_{CH}$ coupling constant of 136.2 Hz. Typical $^1J_{CH}$ coupling

constants for terminally bound alkyl groups of zirconium fall in the range of 116-120 Hz.

An ORTEP diagram of **3** is given in Figure 1 and relevant bond angles and lengths are given in Figure 2. Additional bond angles and lengths are given in Table 1. The structure reveals two zirconocene ketene monomers connected via nearly symmetric dialkylaluminum and methyl bridges. The zirconium atoms in **3** adopt pseudotetrahedral configurations if the Cp and ketene ligands are considered to occupy single coordination sites. The angles between the equatorial ligands, calculated from the midpoint of the C-O bond to the methyl C atom, average to 99.4°, similar to the angle of 95.6° reported for dimethylzirconocene.[17]

A remarkable feature of the structure is the Zr-CH_3-Zr bridge. The carbon atom adopts a distorted trigonal-bipyramidal configuration between the two zirconium centers. The positions of the hydrogen atoms (determined from a difference Fourier map and refined),[12] in conjunction with the high $^1J_{CH}$ coupling constant observed in the $^{13}C\{^1H\}$ NMR spectrum, suggest an sp^2-hybridized configuration for this methyl group. The H-C-H angles of 119(4)°, 117(4)°, and 122(4)° are consistent with this formulation. Another unusual feature of this alkyl bridge is the large Zr-CH_3-Zr angle of 147.8(3)°. Typical values for bridging alkyl groups are less than 90°.[18] The Zr-C bond lengths to the methyl group are not unusually long[19] but differ from one another by approximately 0.1 Å. This difference is reflected in the slight displacement (0.08 Å) of the carbon atom out of the hydrogen atom plane. (For a typical sp^3-hybridized methyl group, the carbon atom is displaced 0.3 Å out of the carbon atom plane.) The origin of this dissymmetry is unclear but might be attributed to crystal packing forces.

The bond angles and lengths of the ketene ligand are typical of those for structurally characterized zirconium ketene complexes.[4,20] As with other early transition

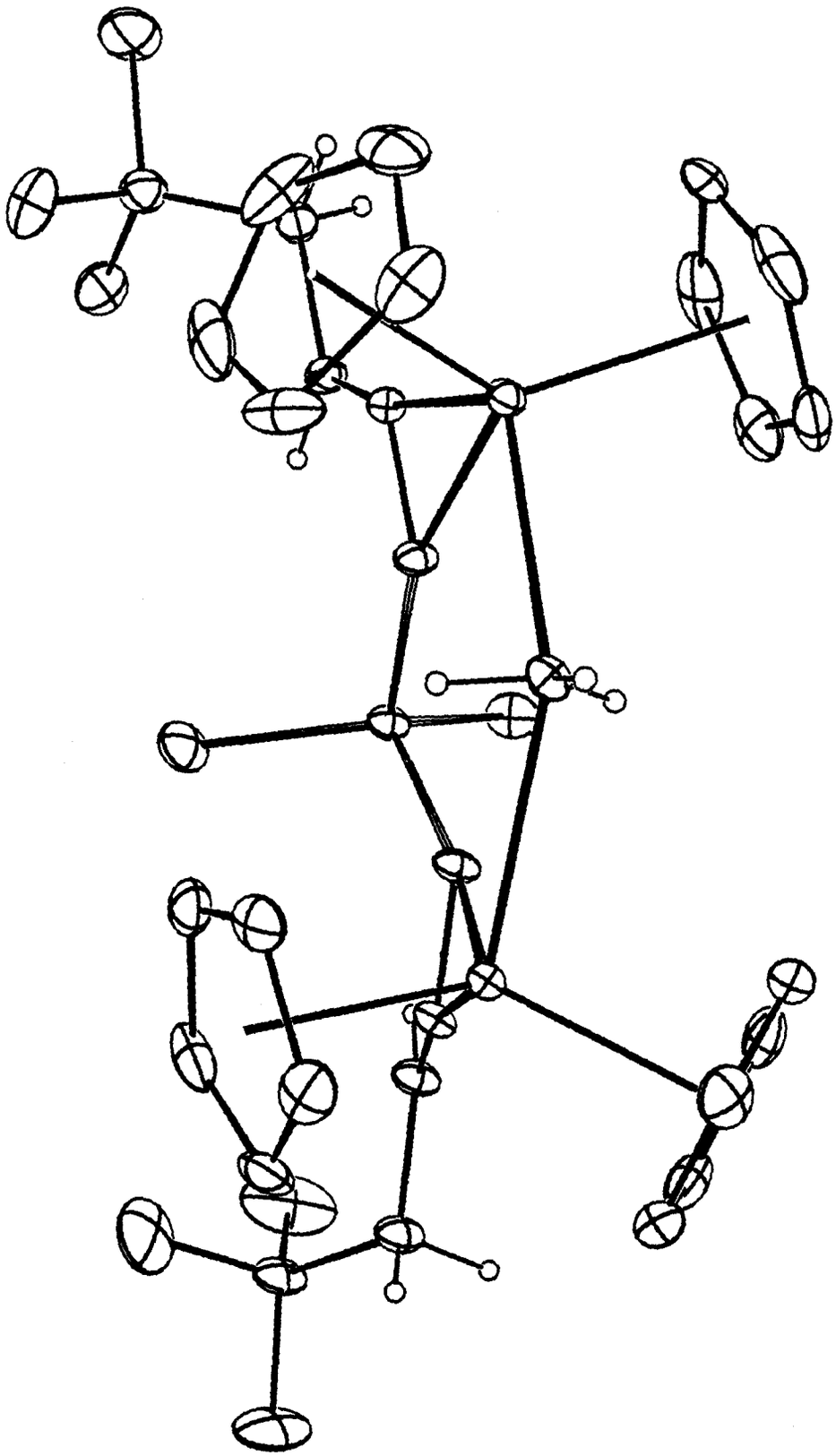

Figure 1. ORTEP Diagram of **3**.

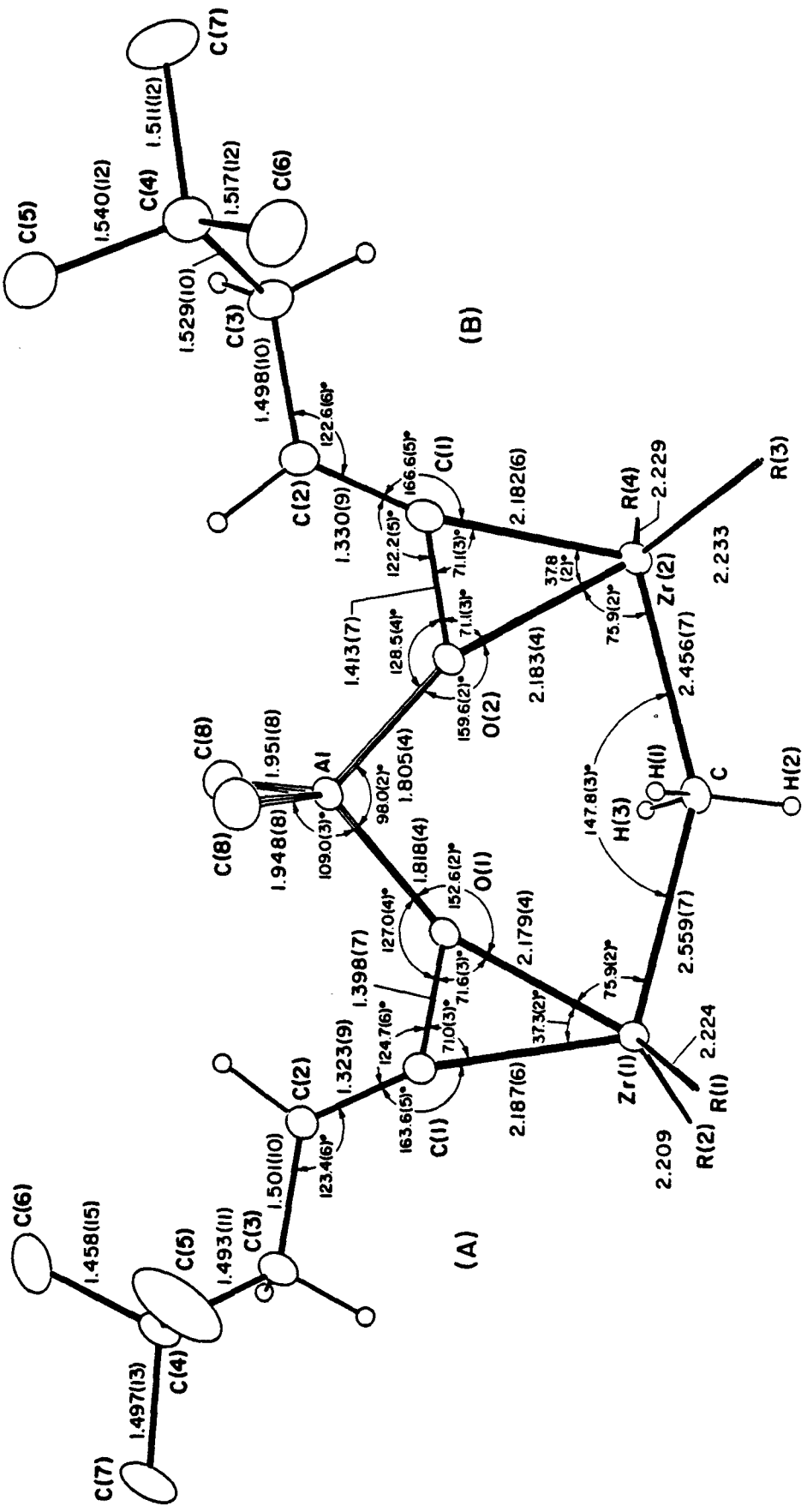

Figure 2. ORTEP Diagram of **3** with Selected Bond Angles and Lengths.

metal ketene complexes,[4,20,21] large M-C-C angles (163.6(5)°, 166.6(5)°), short M-C distances (2.187(6), 2.182(6) Å), and long C-O distances (1.398(7), 1.413(7) Å) point toward significant metallaoxirane character in the η^2-CO portion of the ketene ligand.[22] Due to the limited number of structurally characterized zirconium ketene complexes, it is difficult to assess the effect of the Lewis acid on the bonding properties of the ketene ligand. However, the C-O bond lengths of **3** are slightly longer than those of ketene complexes without coordinated Lewis acids.[23]

Coordination at aluminum is a distorted tetrahedron. The C(8)-Al-O angles are closest to typical tetrahedral values at 109.6(3)° and 109.0(2)°, but the C(8)-Al-C(8) angle is larger at 120.5(3)° and the O(1)-Al-O(2) angle smaller at 98.0(2)° . This type of coordination for aluminum has recently been observed by Atwood for ($AlMe_2(OPh)_2$).[24] The Al-C distances of 1.948(8) Å and 1.951(8) Å are normal, but the Al-O distances of 1.818(4) Å and 1.805(4) Å fall on the short side of the range normally observed for O-bonded alkylaluminum complexes.[24]

Reactivity of 3. Treatment of **3** with pyridine (eq. 3) regenerates the dimer **1a** and the pyr·$AlMe_3$ adduct after 12 h at 25°C. The stronger Lewis base 4-dimethylaminopyridine (DMAP) reacts rapidly (eq. 4) with **3** to give two products by ^{1}H NMR. One product was spectroscopically characterized as the ketene·$AlMe_3$·DMAP adduct **11** by comparison with the analogous $AlMe_2Cl$ adduct **8** (vide infra). The other product formed was assigned as the ketene·DMAP adduct **12**.

Treatment of **3** with excess acetylene in toluene yields **4** and its adduct **4**·$AlMe_3$ in nearly quantitative yield by ^{1}H NMR (eq. 5). Performing the reaction in the presence of an equivalent of THF affords **4** exclusively (under these conditions **4**·$AlMe_3$ is converted to **4**). This reaction is best run in the presence of a Lewis base to inhibit the polymerization of acetylene by $AlMe_3$.[26] The structure given for **4** is supported

(3)

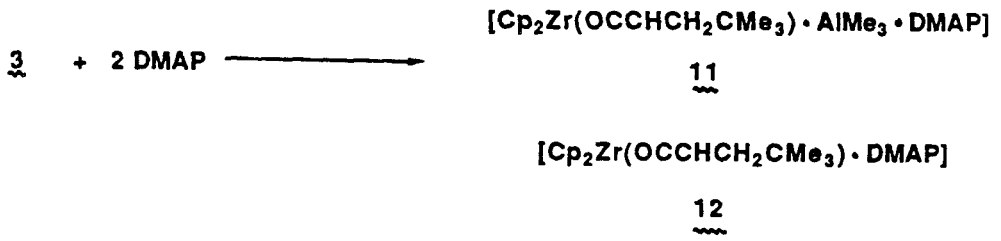

(4)

by spectral and analytical data. In particular, in the ^{1}H NMR spectrum, the exocyclic vinyl proton appears as a broad triplet of doublets with allylic coupling to the α-vinyl proton of 1.4 Hz. Although **3** reacts cleanly with acetylene, it does not react with ethylene or substituted acetylenes under similar conditions.

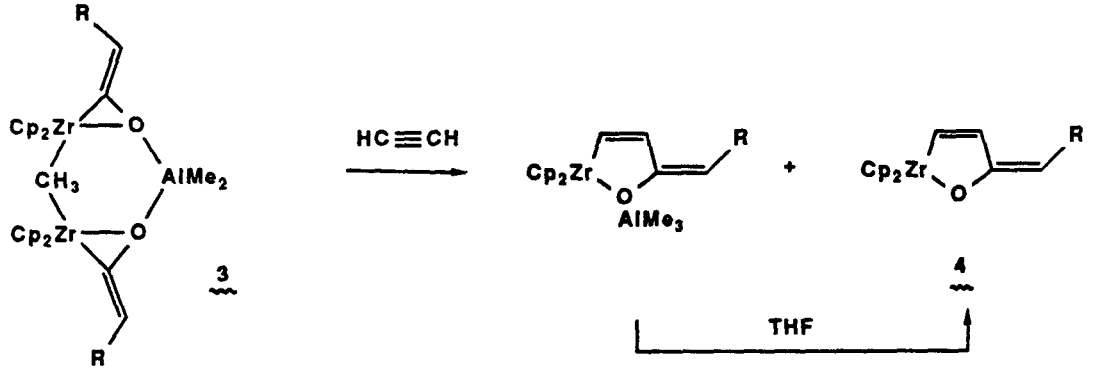

(5)

Toluene solutions of **3** react after 3 h at 45°C under 50 psi of carbon monoxide to afford the acyl complex **5** (eq. 6). The structure of **5** was assigned on the basis of its ^{1}H, ^{13}C NMR, and IR spectra. The solution IR spectra (C_6D_6) of **5** displays an absorption at 1440 cm^{-1} which we assign as the acyl carbonyl stretching frequency. Similar carbonyl stretching frequencies have been observed previously for transition metal acyl complexes coordinated to Lewis acids,[9b] thus suggesting that the acyl

oxygen of **5** is coordinated to the other Lewis-acidic zirconium center. The $^1J_{CH}$ coupling constant of 120 Hz for the zirconium methyl group implies that it occupies a terminal position.

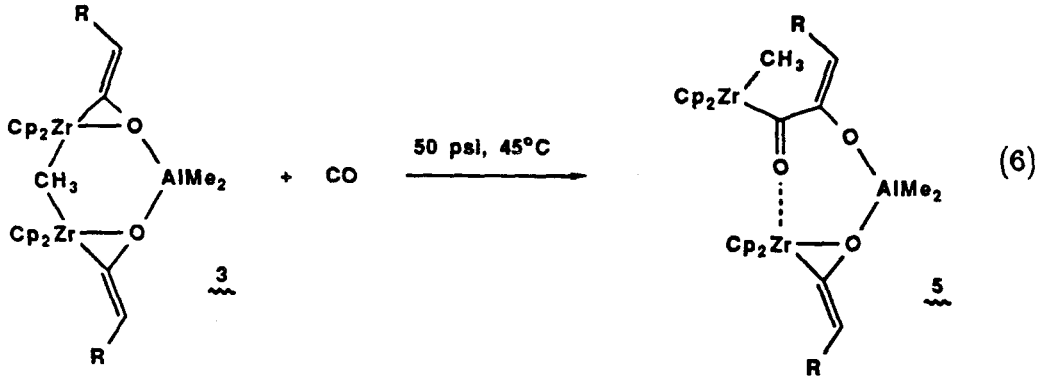

(6)

Preparation and Reactivity of 6a, 7a,b. The stable zirconocene ketene dimer **1a** reacts instantly with 1 equivalent of $AlMe_2Cl$ in toluene to yield the isolable adduct **6a** (Scheme II). Inequivalent cyclopentadienyl and ketene-ligand resonances in the ^1H and ^{13}C NMR spectra (Table 2) support its formulation as the $AlMe_2Cl$-bridged adduct. This colorless crystalline compound undergoes slow thermal rearrangement (18-20 h, 25°C) to the more symmetric complex **7a**. The rearrangement is catalyzed by Lewis bases such as THF or pyridine (instantaneous, 1 equiv., 25°C). Treatment of the dimer **1a** with $AlMe_2Cl$·THF etherate affords only **7a** (3 days, 25°C); **6a** is not observed by ^1H NMR. The dimer **1a** reacts only with 1 equivalent of $AlMe_2Cl$, as neither **6a** nor **7a** react further with that reagent.

The unsubstituted complex **7b** can also be prepared from the oligomeric **1b** (eq. 7). Complex **7b** forms upon addition of $AlMe_2Cl$ to **1b** (1 h, 25°C). In this case, an intermediate adduct analogous to **6a** was not observed.

Complexes **7a,b** are colorless crystalline compounds that are stable indefinitely in aromatic solvents at 25°C under an inert atmosphere. Complex **7a** slowly decomposes at 110°C ($t_{1/2}$=4.5 h) to unidentified products.

SCHEME II

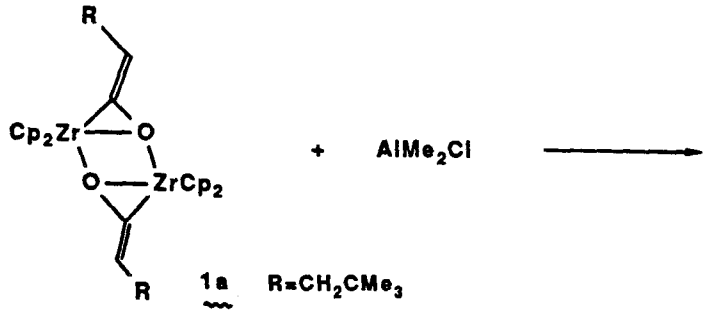

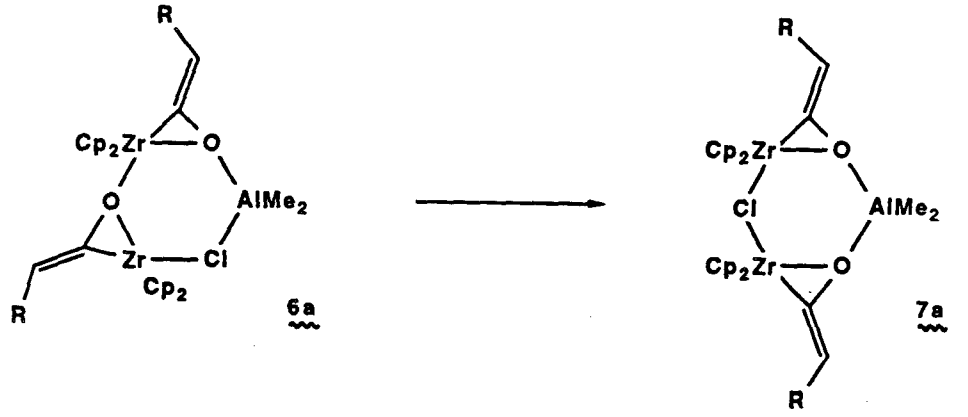

X-ray quality crystals of **7a** were obtained by slowly cooling a toluene-pentane solution of **7a**. Crystal and intensity data collection information is given in Table 1 of Appendix 1, along with fractional atom coordinates and Gaussian Amplitudes (Tables 5-7, Appendix 1). An ORTEP diagram of **7a** is given in Figure 3; selected bond angles and lengths are presented in Table 1.

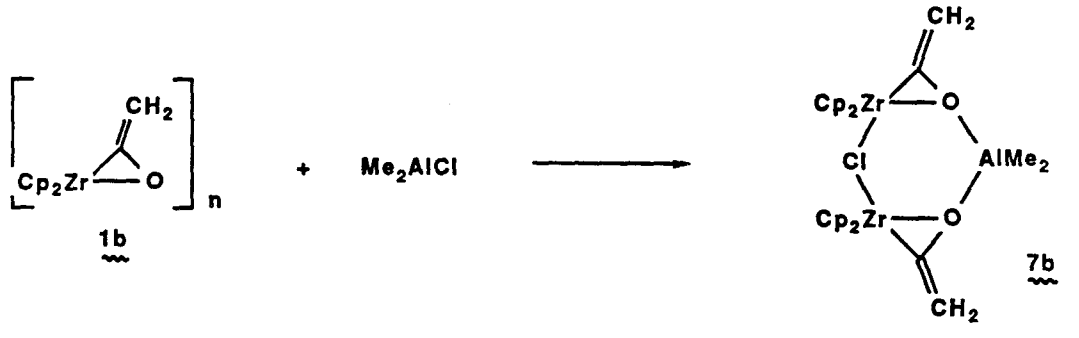

(7)

The structure of **7a** is remarkably similar to that of **3**. The bond angles and lengths of the ketene ligands are similar to those of **3**, as are the bond lengths and angles about the 6-membered ring. The coordination about the chlorine atom is

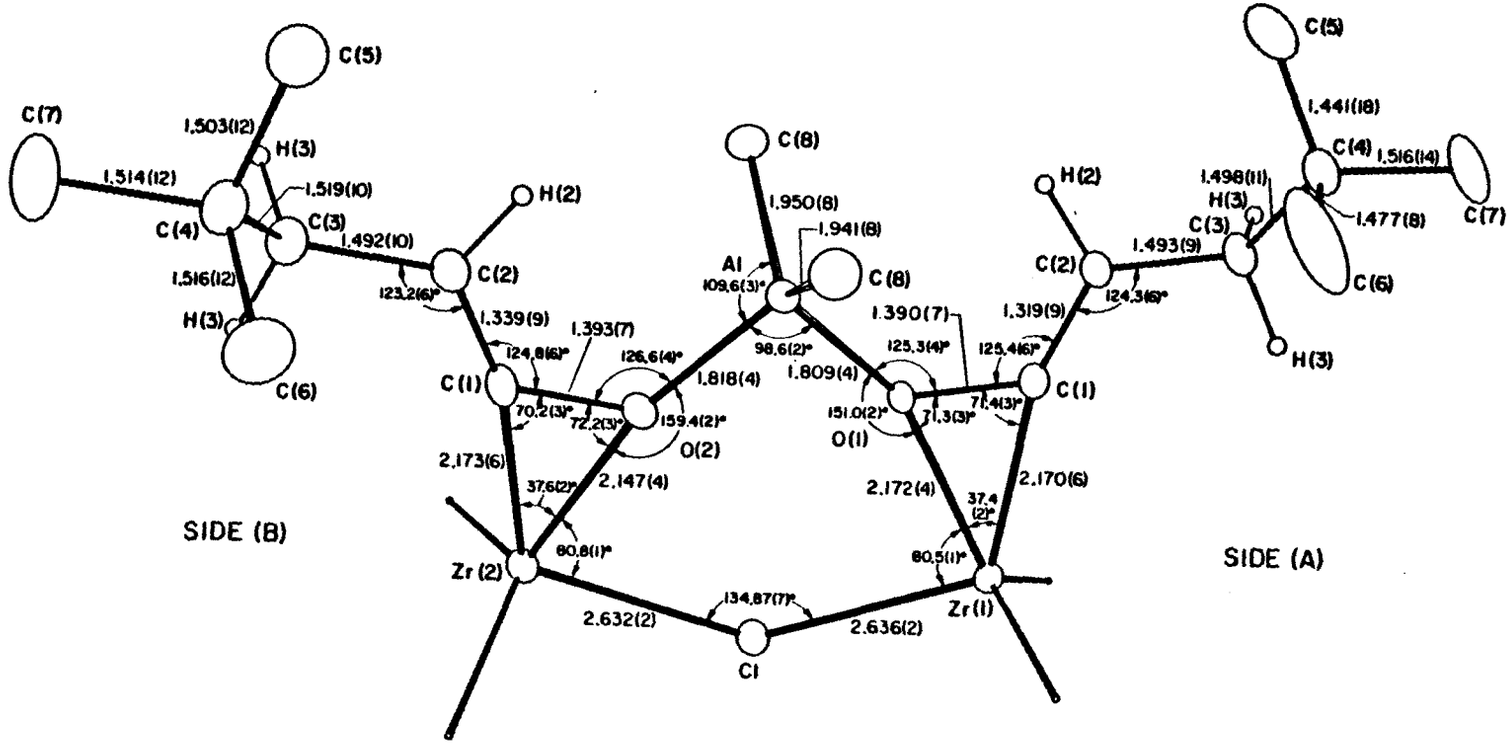

Figure 3. ORTEP Diagram of **7a** with Selected Bond Lengths and Angles.

slightly different from that of the methyl group in **3**. The chlorine atom is bonded symmetrically between the two zirconium centers. The Zr-Cl bond distances are analogous to those of other bridging zirconium chloride complexes,[27] but the Zr-Cl-Zr angle is large at 134.87(7)° (see Discussion Section). The Zr-Zr distance of 4.864(1) Å is just slightly longer than that of **3** and implies little direct M-M interaction.

Complex **7a** is stable in the presence of pyridine but reacts with 2 equivalents of the stronger Lewis base 4-dimethylaminopyridine (DMAP) to afford the complex **8** (ca. 50% yield ^{1}H NMR) and another product, which is apparently the ketene·DMAP adduct **12** (eq. 8).

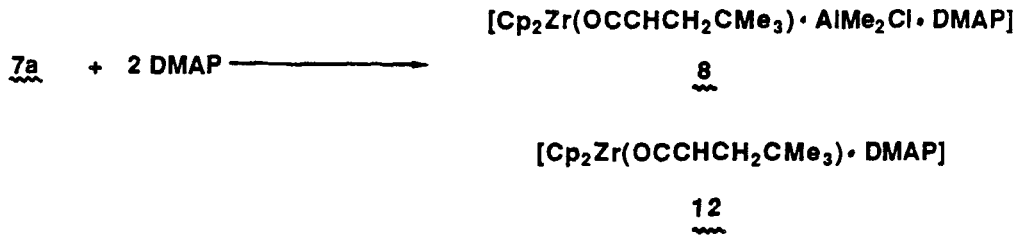

(8)

The structures of **8** and its $AlMe_3$ analogue **11** (vide supra) were difficult to assign on the basis of spectral data. Analytical data on **8** indicate one DMAP and one Me_2AlCl molecule per zirconium. A solution molecular weight determination indicated a monomeric species. The appearance of two inequivalent methyl signals in a ratio of 6:3 in the ^{1}H NMR and a methyl signal at 15.1 ppm in the ^{13}C NMR spectrum for the $AlMe_3$ adduct **11** are consistent with the structure given below.

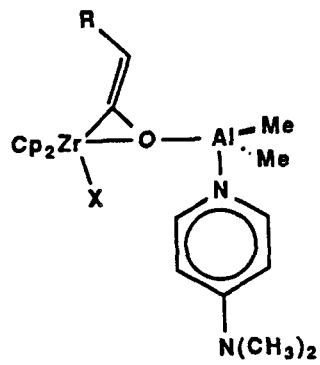

In contrast to the μ-CH_3 complex **3**, the μ-Cl complex **7a** does not react with either acetylene or carbon monoxide. Solutions of **7a** in toluene-d_8 in sealed NMR tubes remain unchanged under several atmospheres of these reagents after weeks at 25°C.

Preparation of 9,10. Complex **1a** reacts instantly with Et_2AlH to afford the adduct **9** (Scheme III). A broad resonance at -1.59 ppm, inequivalent cyclopentadienyl and ketene ligand resonances in the ^1H NMR spectrum (Table 2), and a broad absorption at 1800 cm^{-1} in the IR spectrum support its formulation as an adduct containing an Al-H-Zr bridge.[28]

Complex **9** is a colorless crystalline compound that shows no tendency to isomerize in toluene at 25°C. Crystals of **9** were obtained from the concentrated pentane washings of the crude product **9**. A summary of crystal and intensity data collection information is given in the Appendix. Fractional atom coordinates and Gaussian Amplitudes are presented in Tables 10-13 of the Appendix. The bridging hydrogen atom was located from a difference map and refined.

The structure of **9** (Fig. 4) reveals a roughly planar 6-membered ring formed from one Et_2AlH and two Zr ketene molecules. The bond angles and lengths of the ketene ligands are similar to those of the other three complexes. The Al-H and Zr-H distances are not unusual, but the C(1A)-Zr-H angle is slightly larger than the analogous angles for the other three complexes (Table 1). An interesting result of the structure determination is the equivalence (within experimental error) of the two Zr-O distances at 2.193(4) and 2.194(4) Å. The M-M distances of 3.835(2) Å (Al-Zr(1)), 3.573(2) Å (Al-Zr(2)), and 4.263(1) Å (Zr(1)-Zr(2)) imply little direct M-M interaction.

Heating toluene solutions of **9** establishes an equilibrium between **9** and its symmetric isomer **10** (Scheme III). An equilibrium ratio of 1:1.35 (**9:10**) is obtained upon heating isolated samples of **9** or **10** at 100°C overnight.

SCHEME III

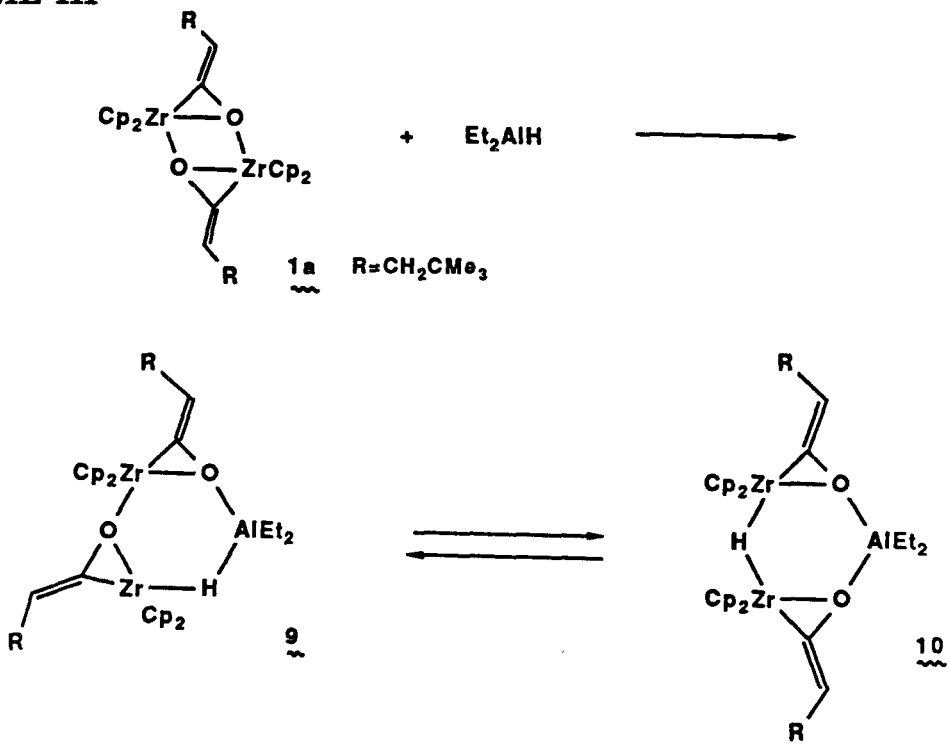

Compound **10** was isolated by washing **9** away from a solid mixture of **9** and **10**. This compound is a colorless crystalline material that exhibits equivalent cyclopentadienyl and ketene resonances and a sharp hydride resonance at -3.03 ppm in the ^1H NMR (Table 2). This compound is stable indefinitely in aromatic solvents at 25°C; heating toluene solutions of **10** to 120°C reestablishes the **9-10** equilibrium but does not result in significant decomposition after several weeks.

Recrystallization of **10** from Et_2O/hexane affords x-ray suitable crystals. A summary of crystal and intensity data collection is given in Appendix 1. An ORTEP diagram of **10** is given in Figure 5; selected bond lengths and angles are presented in Figure 5 and Table 1.

Complex **10** crystallizes in space group C2/c on a crystallographic C2 axis passing through the hydrogen and aluminum atoms. The bridging hydrogen atom was located from a difference map and refined (see Experimental Section).

The molecule adopts a puckered 6-membered ring conformation similar to that

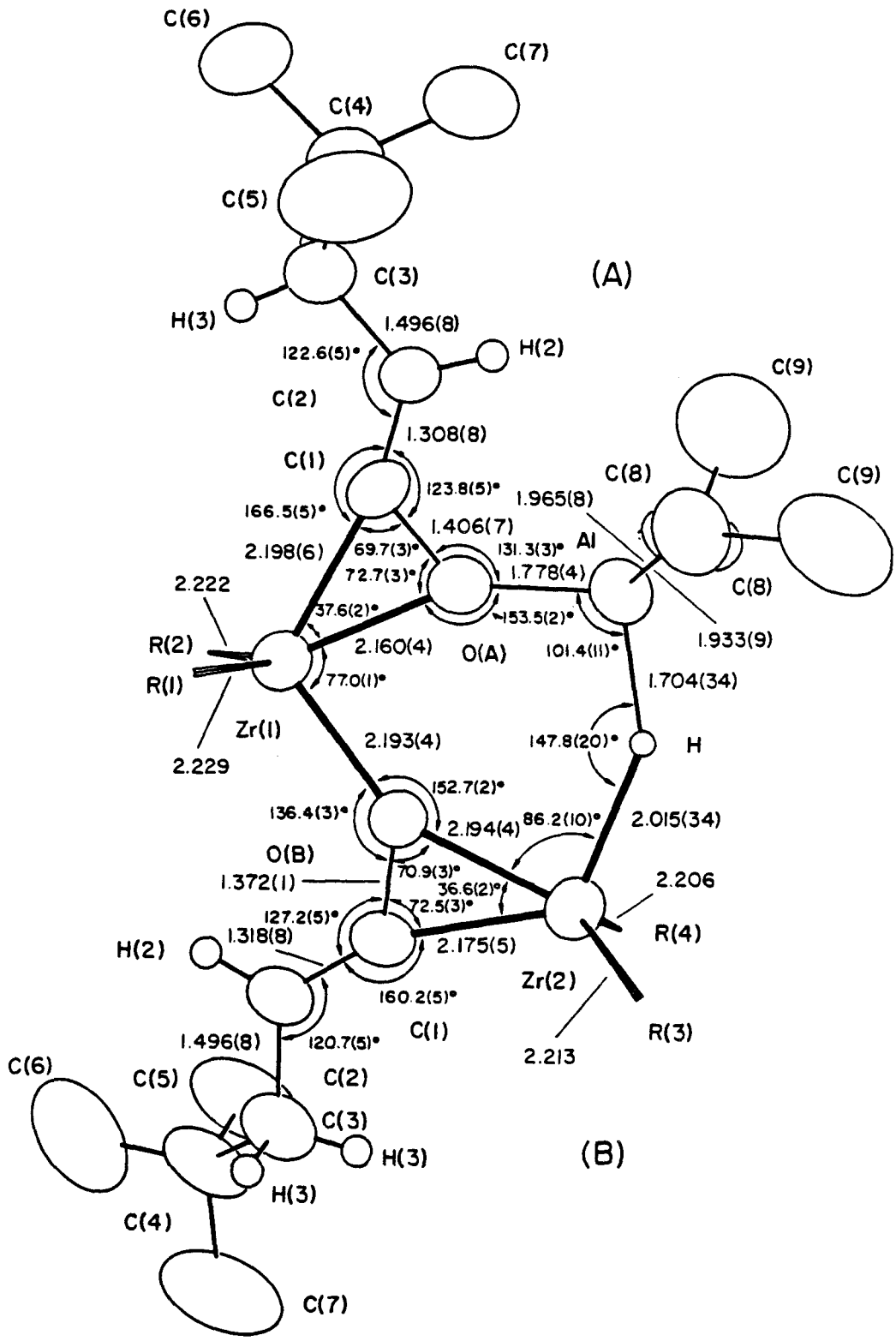

Figure 4. ORTEP Diagram of **9** with Selected Bond Lengths and Angles.

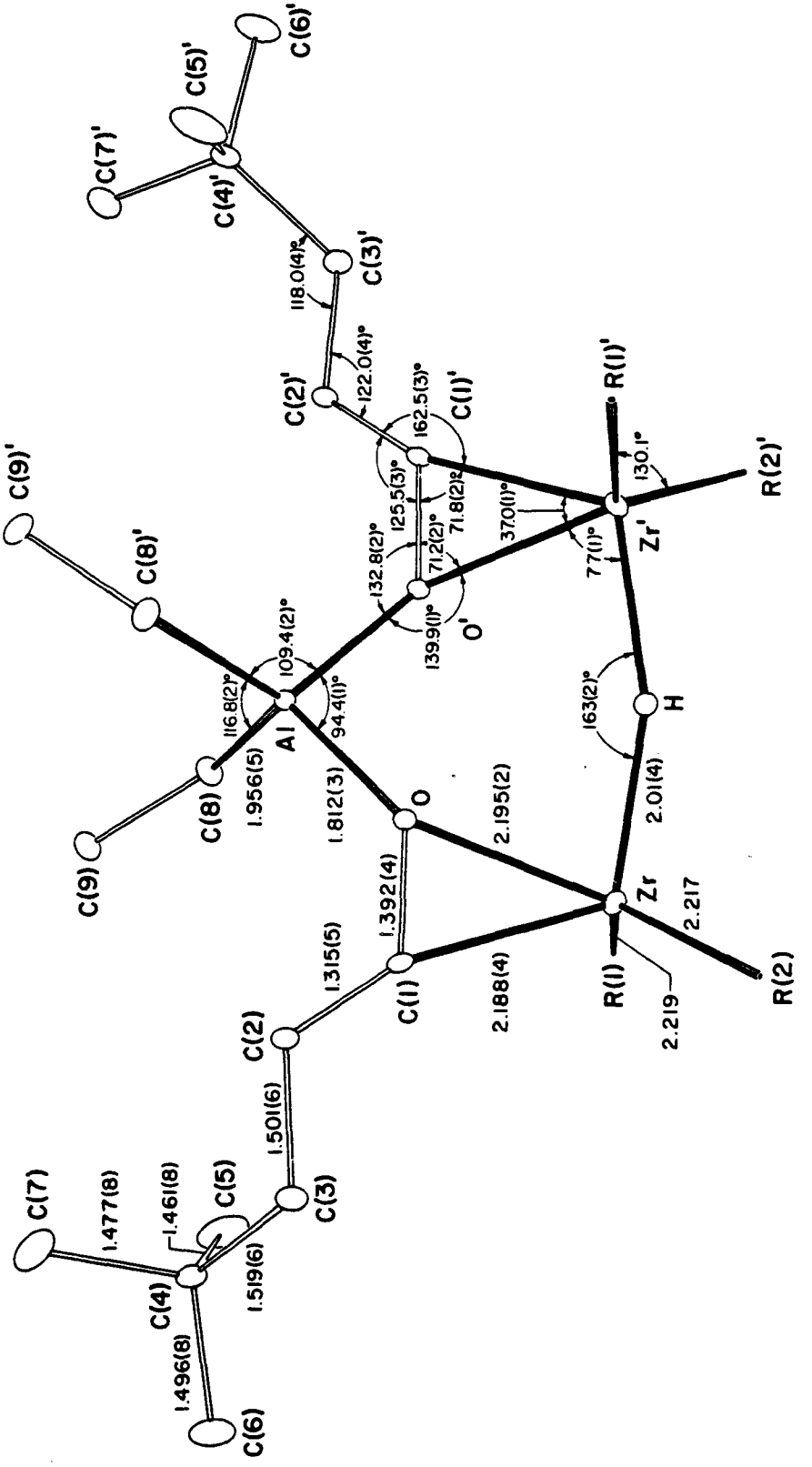

Figure 5. ORTEP Diagram of 10 with Selected Bond Lengths and Angles.

Table 1. Selected Bond Lengths (Å) and Angles (°).

	3 (μ-CH_3)		**7a** (μ-Cl)		**9**(μ-H)		**10**(μ-H)
	Fragment A	**Fragment B**	**Fragment A**	**Fragment B**	**Fragment A**	**Fragment B**	
			Bond Lengths				
Zr-Zr	4.817(1)		4.864(1)		4.263(1)		3.976(1)
Zr-X	2.559(7)	2.456(7)	2.636(2)	2.632(2)		2.014(34)	2.01(4)
Al-X	3.739(8)		3.986(2)			1.703(34)	3.94(4)
Zr-C(1)	2.187(6)	2.183(6)	2.170(6)	2.173(6)	2.198(6)	2.175(5)	2.188(4)
Zr(1)-O	2.179(4)		2.172(4)		2.160(4)	2.193(4)	2.195(2)
Zr(2)-O		2.183(4)		2.147(4)		2.194(4)	2.195(2)
C(1)-O	1.398(7)	1.413(7)	1.390(7)	1.393(7)	1.406(7)	1.372(6)	1.392(4)
Al-O	1.818(4)	1.805(4)	1.809(4)	1.818(4)	1.778(4)		1.812(3)
Al-C(8)	1.948(8)	1.951(8)	1.941(8)	1.950(8)	1.933(9)	1.965(9)	1.956(5)
C(1)-C(2)	1.323(9)	1.330(9)	1.319(9)	1.339(9)	1.308(8)	1.318(8)	1.315(5)
C(2)-C(3)	1.501(10)	1.498(10)	1.493(9)	1.492(10)	1.496(8)	1.496(8)	1.501(6)
C(3)-C(4)	1.493(11)	1.529(10)	1.498(11)	1.519(10)	1.527(9)	1.549(10)	1.519(6)
C-H(1)	0.94(5)						
C-H(2)	0.98(5)						
C-H(3)	0.86(5)						
			Bond Angles				
Zr-X-Zr	147.8(3)		134.87(7)			152.6(1)[a]	163(2)
O-Al-O	98.0(2)		98.6(2)				94.4(1)
Zr-O-Al	152.6(2)	159.6(2)	151.0(2)	159.4(2)	153.5(2)		139.9(1)
Cp-M-Cp	129.7	130.1	129.6	130.2	130.8	131.4	130.1
X-Zr-C(1)	113.2(2)	113.5(2)	117.7(2)	118.4(2)		122.8(9)	113.9(11)
Zr-C(1)-C(2)	163.6(5)	166.6(5)	162.8(5)	164.9(5)	166.4(5)	160.2(5)	162.5(3)
H(1)-C-H(2)	119(4)						
H(2)-C-H(3)	122(4)						
H(3)-C-H(1)	117(4)						
Zr-C-H(1)	74(3)	80(3)					
Zr-C-H(2)	99(3)	111(3)					
Zr-C-H(3)	81(3)	93(3)					

[a] X = O(B)

in **3** and **7a**; however, the angles about the ring differ substantially from those of **3** and **7a**. In particular, the O-Al-O angle is approximately 4° smaller at 94.4(1)° and the Zr-O-Al angle smaller by approximately 20° at 139.9(1)°. The significance of these differences in ring conformation for **10** is considered in the Discussion Section.

The bond angles and lengths of the ketene ligands for **10** are symmetry related and analogous to those of **3**, **9** and **7a**. The Zr-H bond lengths of 2.01(4) Å are normal for bridging hydrides of zirconium,[29,30] but the Zr-H-Zr angle is unusually large. Although typical M-H-M angles[31] are less than 140°, larger angles have recently been observed between Lewis acidic metal centers, particularly titanium,[32] zirconium,[33] and aluminum.[33b]

The Zr-Zr distances of 3.975(1) Å are long for any significant metal-metal interaction[27] but is substantially shorter than those observed for **3** or **7a** (See Discussion Section). Complexes **9** and **10** are thermally robust and chemically inert. They do not react under several atmospheres of CO or CO/H_2 mixtures, even at elevated temperatures. They are both stable in the presence of excess acetylene and do not react with excess Et_2AlH or with Lewis bases such as THF, pyridine, or 4-dimethylaminopyridine.

DISCUSSION

Synthesis. The addition of alkylaluminum reagents to the ketene dimer **1a** (Schemes I-III) affords a family of alkylaluminum-ketene complexes with novel structural characteristics. This reaction is surprisingly general and involves the formation of an adduct resulting from the addition of an Al-X bond into a Zr-O dative bond of the dimer. The μ-$AlMe_3$ adduct **2** is unstable to vacuum and could not be isolated. The complexes **6a** and **9** could be isolated and in the case of **9** crystallographically characterized. The crystal structure of **9** provides some indication why these intermediates do not react further with the aluminum reagent. From Figure 4, it can be seen that the cyclopentadienyl rings of Zr(1) and the hydrogen atom H(3) sterically inhibit attack at the Zr(1)-O(B) bond.

Thermal rearrangement of complexes **2**, **6a**, and **9** proceeds via transmetallation and migration of the X group (X = CH_3, Cl, H) to a symmetric, or nearly symmetric, position between the two zirconium centers. The mechanism of this transformation and the role of Lewis bases in the isomerization **6a** to **7a** are still not well understood.

Structure. The structures of **3**, **7a**, and **9** share several common features. The dialkyl aluminum center is chelated by the oxygen atoms of two ketene ligands. The structural constraints of this chelation have a dramatic effect on the coordination environment of the bridging ligand X (X = CH_3, Cl, H). Two highly Lewis acidic zirconium centers are structurally disposed such that they are able to stabilize unusual coordination geometries for the bridging ligands. Two features of this coordination are noteworthy: the large M-X-M angles for these complexes, and the hybridization of the methyl group in **3**.

For the majority of transition metal bridging chloride[27] and alkyl complexes,[23] M-X-M angles are less than 90°. For transition metal bridging hydrides these angles can be larger[31] (angles up to 180° have been reported where one or both of the

metals are aluminum),[33] but the vast majority prefer angles less than 140°. This preference for sharp M-X-M angles appears to be due to a tendency on the part of metal complexes to adopt a "closed" bonding configuration (A), where there is significant M-M overlap.[31] For the complexes reported here, large M-X-M angles (from 136° to 162°) and large Zr-Zr bond distances (from 3.9 Å to 4.8 Å) suggest that the bonding description for these bridging ligands is better described via an "open" bonding configuration (B).

A B

As a consequence of the large M-X-M angle, the methyl group of **3** is forced to adopt a trigonal-bipyramidal configuration between the two zirconium centers. The Zr-C-Zr angle is not 180° as might be expected for a trigonal-bipyramidal methyl group, but is 147.8(3)°. We attribute this to the disposition of the zirconium bonding orbitals. The zirconium orbitals available for bonding to the methyl group[34] are derived from orbitals of a_1 symmetry. The orientation of the ketenes in **3** is such that these orbitals are directed away from the aluminum atom. Maximum overlap is achieved via a bent "banana" bond as illustrated in Figure 6. This 3-center 2-electron bond utilizes a carbon p-orbital as in C, which contrasts the more typical bonding description D offered for the majority of bridging hydrocarbyl groups.

The methyl group of **3** appears to be a pentacoordinate carbanion of approximate D_3h symmetry. A trigonal-bipyramidal geometry for carbon[35–38] has recently been discussed theoretically for $CH_3Li_2^+$.[35] In addition, several examples have recently

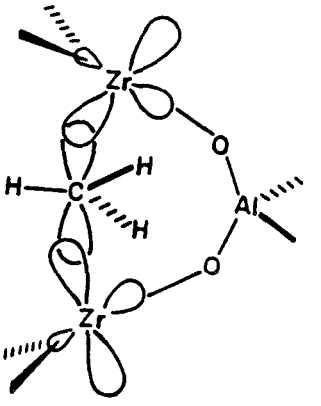

Figure 6.

appeared in the literature,[36–38] particularly involving electrophilic metal centers, where large M-C-M angles imply a similar type of coordination for the bridging carbon atoms. A noteworthy example is the complex $(PhCH_2^-Na^+)_4(TMEDA)_2$ prepared by Schleyer et al.,[36] for which the benzyl anion was shown crystallographically to be in a trigonal-bipyramidal configuration between the two sodium atoms.

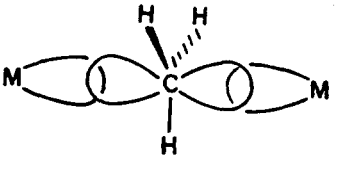

C

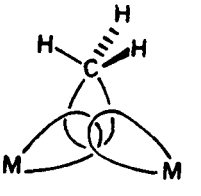

D

The present work, and the examples listed above, suggest that this type of coordination for carbon may be general for metal centers where steric constraints disfavor a bonding mode as in D. The effects of this coordination on the reactivity of the alkyl ligand are unknown and warrant further investigation. The structure of **3** should be helpful in the development of bimetallic systems specifically designed to favor this type of coordination.

Model for Alkyl Transfer. Bridging ligands serve as structural models for intermediates in ligand transfer processes. The methyl group of **3** represents an intermediate in an alkyl transfer process that proceeds with inversion. Many bimolecular electrophilic substitution (S_E2) reactions proceed with retention of configuration at carbon,[39] but selected examples proceed with inversion.[40] The transfer of an alkyl group from an alkylcobalamine to a mercury(II) center has been shown to proceed with inversion.[41] This alkyl transfer undoubtedly proceeds through an intermediate or transition state of configuration similar to the methyl group of **3**.

In a more closely related system, **3** serves as a direct model for the proposed transition state that equilibrates the isomers of the aldehyde complexes prepared by Schwartz,[42] Erker,[43] and Floriani.[44] In this case, NMR studies on the chiral aldehyde complex indicated that the isomerization proceeds with inversion at the carbon center.[42a] These results point out that alkyl transmetallations are likely to proceed with inversion[45] between metal centers where steric and electronic constraints disfavor a transition state analogous to D.

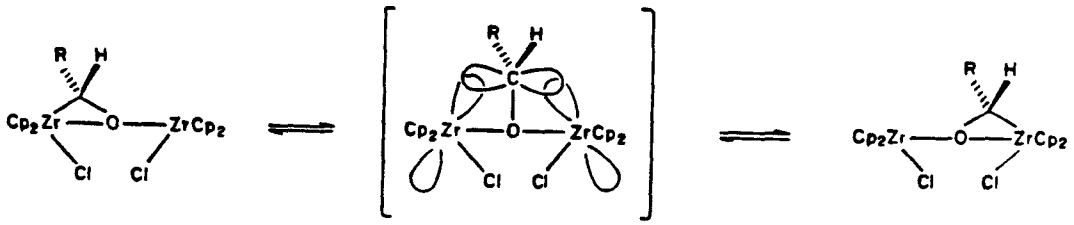

Structural Comparisons. The Zr-Zr distances of **3**, **7a**, and **10** appear to be influenced by the size of the bridging ligand. The chloride and methyl ligands are of similar size and the Zr-Zr distances of the complexes containing these ligands are correspondingly similar (4.864 (1) and 4.817(1) Å, respectively, Table 1). For the

hydride complex, where the bridging ligand is smaller, the Zr-Zr distance is approximately 0.9 Å shorter at 3.975(1) Å. Larger M-X-M angles and smaller O-Al-O angles also appear to correspond with smaller bridging ligands and shorter Zr-Zr distances.

One feature of the hydride complex that may be a consequence of the shorter Zr-Zr distance is the amount of puckering in the 6-membered ring (Fig. 7). The degree of puckering is measured by considering the angles between the planes defined by the atoms of the ketene ligands (Zr, O, C(1), C(2), C(3)). For **3** and **7a**, these angles are 21(6)° and 22(6)°, respectively. For **10**, this angle is much larger at 36(5)°. We attribute the increased puckering of the ring in the hydride complex **10** to an increase in the non-bonded contacts between the Cp ligands on adjacent zirconium centers as the Zr-Zr distance decreases. To minimize non-bonded contacts between adjacent Cp ligands, the zirconium centers must twist with respect to each other, causing an increased distortion in the 6-membered ring. As can be seen from Figure 7, the Cp ligands of **7a** are almost eclipsed, while those of **10** are staggered.

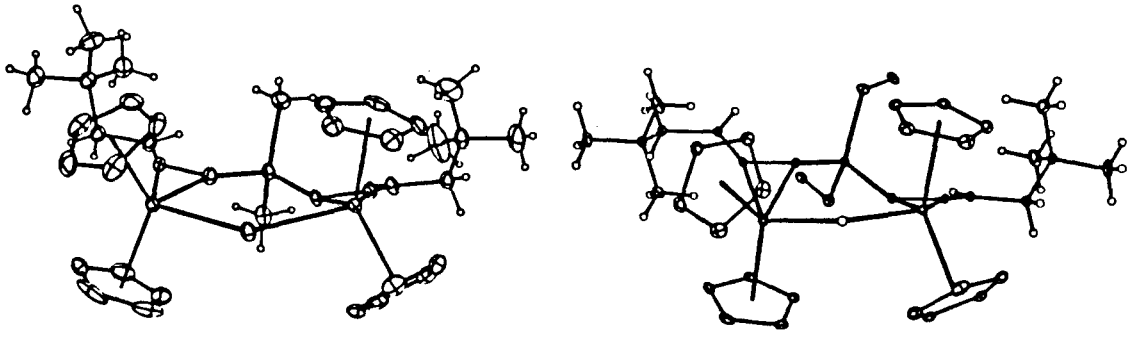

Figure 7. ORTEP Drawings of **7a** and **10**.

Reactivity. The complexes formed from the addition of alkylaluminum reagents to the ketene dimer **1a** exhibit different reactivities depending on the bridging ligand X (X = CH_3, Cl, H). This difference in reactivity was first probed using Lewis bases. Of the initial adducts **2**, **6a**, and **9**, the μ-$AlMe_3$ complex **2** reacts with the mild Lewis base Et_2O to give **1a** and $AlMe_3 \cdot Et_2O$. In contrast, neither **6a** nor **9** reacts with Et_2O, but the μ-Cl **6a** reacts instantly with the stronger Lewis bases THF or pyridine to give **7a**. The μ-H **9** does not react with THF or pyridine. The symmetric complexes **3**, **7a**, and **10** are stable to Et_2O, but the μ-CH_3 compound **3** reacts slowly with pyridine (12 h, 25°C) to yield the dimer **1a** and pyridine·$AlMe_3$. In contrast, the μ-Cl **7a** and μ-H **10** are stable to pyridine. The μ-CH_3 **3** and μ-Cl **7a** complexes both react with 4-dimethylaminopyridine; the μ-H complex **10** does not. In contrast to the other reactions with Lewis bases, the product from the reactions of **3** and **7a** with DMAP is not the dimer **1a**, but the Lewis base adducts **11** and **8**, respectively. Another product is apparently formed and, although not isolated, is assigned as the ketene DMAP adduct $Cp_2Zr(OCCHCH_2CMe_3)$·DMAP **12**.

The reactivity of complexes **3**, **7a**, and **10** toward unsaturated substrates is also sensitive to the nature of the bridging ligand. The μ-CH_3 compound **3** is the only one observed to react with unsaturated substrates. Group 4 ketene complexes react with a variety of unsaturated substrates including olefins, acetylenes,[4] aldehydes,[46] and organic ketenes.[19] An open coordination site is presumed to be a prerequisite for these insertion reactions. For the complexes described, it is likely that dissociation of the ligand bridge provides the necessary open coordination site. Dissociation of the chloride or hydride bridge is expected to be less facile than the methyl bridge,[47] and thus the reactivity of these compounds appears to reflect the lability of the bridging ligands with respect to dissociation. The results from the reactions with Lewis bases and unsaturated substrates allow the following order of reactivity to be established: μ-CH_3 (**3**) > μ-Cl (**7a**) > μ-H (**10**).

Treatment of the μ-CH_3 **3** with acetylene generates two products, the cyclic enolate **4** and its $AlMe_3$ adduct **4**·$AlMe_3$. The reaction probably proceeds by cleavage of the methyl bridge followed by coordination and insertion of acetylene into one of the ketene ligands (Scheme IV) . Migration of the methyl group back to aluminum via an intermediate such as **3'** results in a second acetylene insertion to generate **4**·$AlMe_3$. The formation of **4** via **3** provides one route to the desired activation of ketene dimer **1a** (eq. 2). Although low yield of **4** (20% from **1a**) limits the usefulness of this strategy, our results further demonstrate the effectiveness of using alkylaluminum reagents to coordinate and stabilize reactive organometallic species.[48]

SCHEME IV

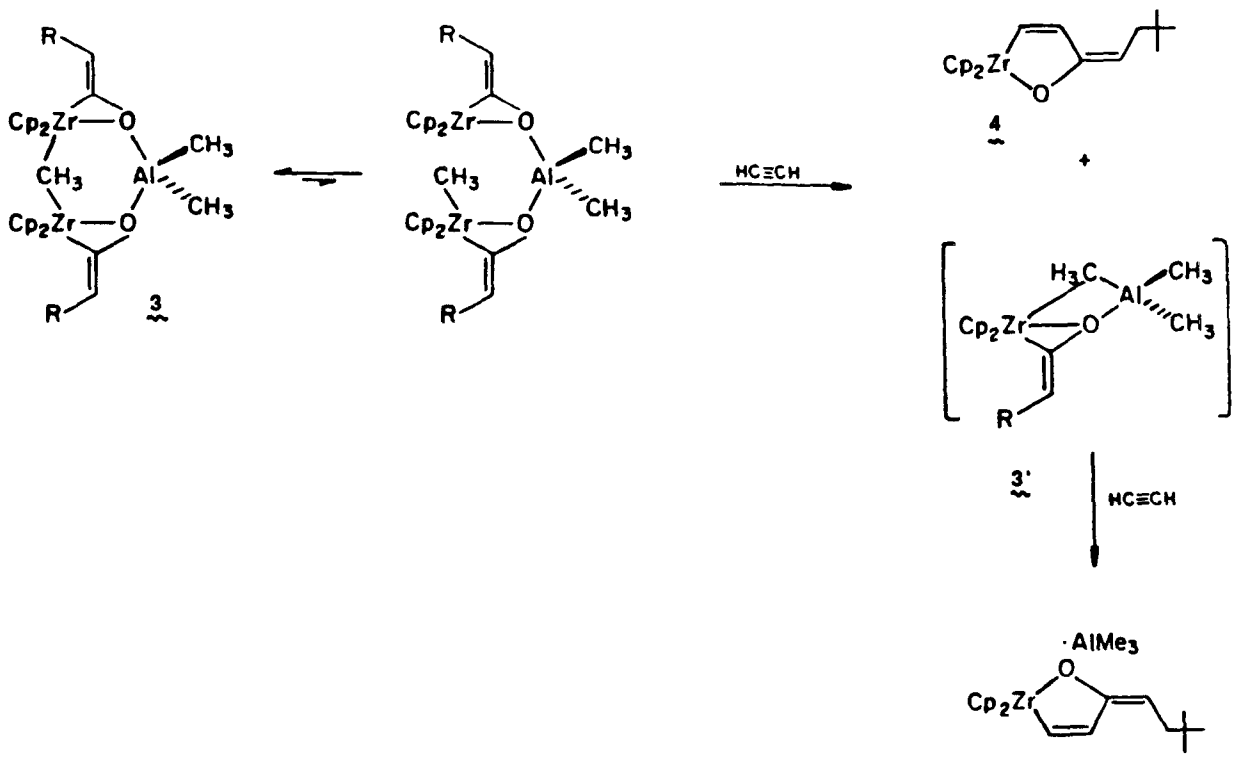

Metal-bound ketene complexes have been proposed as intermediates in CO reduction processes.[1,2] Several homogeneous systems have been developed that model the production of metal-bound ketenes via the coupling of metal-methylenes and CO.[2,50] However, the reactivity of metal ketene complexes under Fischer-Tropsch

conditions is less well investigated, particularly with regard to further carbon-carbon bond formation.[49-51]

The carbonylation of **3** to **5** models a key carbon-carbon bond forming step of a CO reduction sequence involving metal ketene intermediates. The insertion of CO into one of the ketene ligands is an unprecedented transformation for a metal-bound ketene complex[52] and may be due to the effect of the aluminum species in this system. Aluminum species have been used as cocatalysts in homogeneous CO reduction systems,[11] and aluminum oxides are widely used as catalyst supports in heterogeneous systems. However, the role of these supports in CO reduction is not well established.[53] Our results support the suggestion[53b] that Lewis-acidic supports play an active role in promoting CO reduction.

A related observation concerns the relevance of reaction (6) to CO reduction over heterogeneous metal oxide catalysts.[54] Maruya et al.[54a] have shown that metal oxides of Groups 3, 4, and 5 are active Fischer-Tropsch catalysts. The Zr-O-Al-O-Zr structural framework of complexes **3**, **7a**, and **10** provides a homogeneous model for such surfaces, and the carbonylation of **3** models the insertion of CO into a metal oxide bound alkylidene.

Summary. We have demonstrated that the zirconocene ketene complex **1a** reacts with a variety of alkylaluminum reagents to afford trinuclear bridging ketene complexes. Single crystal x-ray diffraction studies of all three members of this series have provided useful structural comparisons of these molecules. The chelating arrangement of the aluminum atom and the ketene ligands provides a unique coordination environment for the bridging chloride, hydride and methyl ligands. In particular, the methyl group of **3** represents a new coordination mode for carbon between metal centers. The trigonal-bipyramidal configuration of this methyl group models the transition state of transmetallation reactions that proceed with inversion.

Despite the large number of transmetallation reactions observed between early transition metals, a clear picture of the stereochemistry of such reactions has not yet emerged.[8b,45] Our results imply that the stereochemistry of transmetallation reactions is highly dependent on the steric and electronic properties of the metal centers, and transmetallations with inversion can be the dominant pathway, especially at highly oxidized metal centers.

The reactivity of these molecules appears to be dominated by the availability of open coordination sites at the metal centers. For **3**, where an open coordination site becomes available by dissociating the methyl bridge, facile insertion reactions are observed. The reaction of **3** with CO models a key chain carrying step in CO reduction processes over Lewis-acidic and metal-oxide catalyst surfaces.

Table 2. NMR Data[a]

assignment	chemical shift, multiplicity, coupling constant			
	^1H		^{13}C	
(Z,Z)-[$Cp_2Zr(OCCHCH_2C(CH_3)_3]_2$ (1a)				
C_5H_5	5.88 s		109.0	
$OCCHCH_2C(CH_3)_3$			187.8 dt	$^2J_{CH}$ = 8.1
				$^3J_{CH}$ = 8.1
$OCCHCH_2C(CH_3)_3$	5.68 t	J = 7.3	99.9 d	$^1J_{CH}$ = 146
$OCCHCH_2C(CH_3)_3$	2.13 d	J = 7.3	44.6 t	$^1J_{CH}$ = 127
$OCCHCH_2C(CH_3)_3$			31.4	
$OCCHCH_2C(CH_3)_3$	1.17 s		30.0 q	$^1J_{CH}$ = 124
(Z,E)-[$Cp_2Zr(OCCHCH_2C(CH_3)_3)]_2$ (1a)				
C_5H_5	5.89 s		108.8	
	5.82 s		109.3	
$OCCHCH_2C(CH_3)_3$			187.0 dt	$^2J_{CH}$ = 8.1
				$^3J_{CH}$ = 8.1
			185.2 dt	$^2J_{CH}$ = 11.0
				$^3J_{CH}$ = 5.4
$OCCHCH_2C(CH_3)_3$	5.59 t	J = 7.3	101.0	
	4.55 t	J = 7.3	99.1	
$OCCHCH_2C(CH_3)_3$	2.16 d	J = 7.3	44.3	
	2.14 d	J = 7.3	44.3	
$OCCHCH_2C(CH_3)_3$			31.8	
			31.5	
$OCCHCH_2C(CH_3)_3$	1.18 s		29.9	
	1.16 s		29.8	

Table 2. (Continued)

assignment	chemical shift, multiplicity, coupling constant				
	^1H			^{13}C	
$[Cp_2Zr(OCCH_2)]_n$ (1b)					
C_5H_5	5.84	s		109.4	
$OCCH_2$				*e*	
$OCCH_2$	5.25	s		87.1	
	4.40	s			
$[Cp_2Zr(OCCHCH_2C(CH_3)_3)]_2(\mu\text{-}Al(CH_3)_3)$ (2)[b]					
C_5H_5	5.84	s		108.8	
	5.48	s		107.9	
$OCCHCH_2C(CH_3)_3$				187.3	s
				180.6	s
$OCCHCH_2C(CH_3)_3$	6.22	t	J = 7.3	101.8	d $^1J_{CH} = 146$
	5.67	t	J = 7.3	99.5	d $^1J_{CH} = 144$
$OCCHCH_2C(CH_3)_3$	2.20	d	J = 7.3	45.5	t $^1J_{CH} = 120$
	2.07	d	J = 7.3	45.1	t $^1J_{CH} = 122$
$OCCHCH_2C(CH_3)_3$				32.2	s
				32.1	s
$OCCHCH_2C(CH_3)_3$	1.21	s		30.7	q $^1J_{CH} = 123$
	1.19	s		30.6	q
$Al(CH_3)_2$	-0.11	s		-6.9	q $^1J_{CH} = 110.5$
Zr-CH_3-Al	-0.46	s		-16.2	q $^1J_{CH} = 125.7$

Table 2. (Continued)

assignment	chemical shift, multiplicity, coupling constant				
	^1H			^{13}C	
$[Cp_2Zr(OCCHCH_2C(CH_3)_3)]_2(\mu\text{-}CH_3)(\mu\text{-}Al(CH_3)_2)$ (3)					
C_5H_5	5.64	s		107.1 m	$^1J_{CH} = 171.3$
$OCCHCH_2C(CH_3)_3$				178.3 d	$^2J_{CH} = 7.3$
$OCCHCH_2C(CH_3)_3$	6.05	t	J = 7.3	102.1 d	$^1J_{CH} = 147.9$
$OCCH_2C(CH_3)_3$	2.14	d	J = 7.3	44.9 t	$^1J_{CH} = 123.7$
$OCCHCH_2C(CH_3)_3$				31.6 s	
$OCCHCH_2C(CH_3)_3$	1.14	s		30.0 q	$^1J_{CH} = 124.5$
Zr-CH_3-Zr	-0.19	s		-9.2 q	$^1J_{CH} = 136.2$
$Al(CH_3)_2$	-0.46	s		*c*	
$Cp_2ZrOC(CHCH_2C(CH_3)_3)CHCH$ (4)					
C_5H_5	5.88	s		110.0 m	$^1J = 170$
$OC(CHCH_2C(CH_3)_3)CHCH$				167.0 s	
$OC(CHCH_2C(CH_3)_3)CHCH$	4.89	td	$^3J = 8.3$	103.0 d	$^1J = 147$
					$^4J = 1.4$
$OC(CHCH_2C(CH_3)_3)CHCH$	2.21	d	$^3J = 8.3$	42.9 t	$^1J = 125$
$OC(CHCH_2C(CH_3)_3)CHCH$				32.3 s	
$OC(CHCH_2C(CH_3)_3)CHCH$	1.10	s		29.7 q	$^1J = 123$
$OC(CHCH_2C(CH_3)_3)CHCH$	7.05	d	$^3J = 11.2$	*f*	
$OC(CHCH_2C(CH_3)_3)CHCH$	7.37	dd	$^3J = 11.2$	187.9 d	$^1J = 133$
					$^4J = 1.4$

Table 2. (Continued)

	chemical shift, multiplicity, coupling constant			
assignment	^1H		^{13}C	

$[Cp_2Zr(C^aH_3)C^bOC^c(C^dHC^eH_2C^f(C^gH_3)_3)]OAl(C^hH_3)_2[Cp_2Zr(OC^iC^jHC^kH_2C^l(C^mH_3)_3)]$ (5)

C_5H_5	5.85	s	108.4		
	5.46	s	108.6		
a	0.56	s	18.4	q	$^1J = 120.1$
b			297.5	s	
c			157.0	s	
d	6.13	t	109.0		
e	2.71	d	40.7	t	$^1J = 123$
f			31.5	s	
g	1.05	s	29.9	q	$^1J = 124$
h	-0.53	s	-7.6	q	$^1J = 112$
i			183.9	s	
j	6.11	t	99.8		
k	2.29	d	44.8		
l			31.2		
m	1.15	s	29.7		

Table 2. (Continued)

	chemical shift, multiplicity, coupling constant			
assignment	^{1}H		^{13}C	
(Z,Z)-[$Cp_2Zr(OCCHCH_2C(CH_3)_3)]_2(\mu$-$ClAl(CH_3)_2$) (6a)				
C_5H_5	5.85 s		109.0	
	5.67 s		*c*	
$OCCHCH_2C(CH_3)_3$			188.8 dt	$^2J_{CH} = 7.3$
				$^3J_{CH} = 7.3$
			183.3 dt	$^2J_{CH} = 8.8$
				$^3J_{CH} = 7.3$
$OCCHCH_2C(CH_3)_3$	6.16 t	J = 7.3	103.4	
	d		99.6	
$OCCHCH_2C(CH_3)_3$	2.14 d	J = 7.3	45.0	
	2.07 d	J = 7.3	44.7	
$OCCHCH_2C(CH_3)_3$			31.9	
			c	
$OCCHCH_2C(CH_3)_3$	1.18 s		30.3	
	1.16 s		30.0	
$Al(CH_3)_2Cl$	-0.08 s		-6.49	
(Z,Z)-[$Cp_2Zr(OCCHCH_2(CH_3)_3)]2(\mu$-Cl)($\mu$-$Al(CH_3)_2$) (7a)				
C_5H_5	5.77 s		109.1	
$OCCHCH_2C(CH_3)_3$			179.5 dt	$^2J_{CH} = 8.8$
				$^3J_{CH} = 7.3$
$OCCHCH_2C(CH_3)_3$	6.15 t	J = 7.3	102.6	
$OCCHCH_2C(CH_3)_3$	2.09 d	J = 7.3	44.8	
$OCCHCH_2C(CH_3)_3$			31.6	
$OCCHCH_2C(CH_3)_3$	1.14 s		29.9	
$Al(CH_3)_2$	-0.25 s		*c*	

Table 2. (Continued)

assignment	chemical shift, multiplicity, coupling constant			
	^{1}H		^{13}C	
(Z,E)-7a				
C_5H_5	5.79 s		109.5	
	5.75 s		109.3	
OCCHCH$_2$C(CH$_3$)$_3$			178.8 dt	$^2J_{CH}$ = 8.8
				$^3J_{CH}$ = 7.3
			178.8 dt	$^2J_{CH}$ = 8.8
				$^3J_{CH}$ = 5.9
OCCHCH$_2$C(CH$_3$)$_3$	6.17 t	J = 7.3	103.4	
	4.74 t	J = 7.8	103.3	
OCCHCH_2C(CH$_3$)$_3$	2.47 d	J = 7.8	45.4	
	2.09 d	J = 7.3	45.2	
OCCHCH$_2C$(CH$_3$)$_3$			32.6	
			32.1	
OCCHCH$_2$C(CH_3)$_3$	1.14 s		30.5	
	1.14 s		30.1	
[Cp$_2$Zr(OCCH$_2$)]$_2$(μ-Cl)(μ-Al(CH$_3$)$_2$) (7b)				
C_5H_5	5.70 s		109.5	
OCCH$_2$			187.5	
OCCH_2	5.78 d	J = 1.5	90.0	
	4.57 d	J = 1.5		
Al(CH_3)$_2$	-0.21 s		*c*	

Table 2. (Continued)

assignment	chemical shift, multiplicity, coupling constant			
	^1H			^{13}C
$[Cp_2Zr(OCCHCH_2C(CH_3)_3)](C_7H_{10}N_2)(Al(CH_3)_2Cl)$ (8)				
C_5H_5	5.95	s		109.3
$OCCHCH_2C(CH_3)_3$				186.3
$OCCHCH_2C(CH_3)_3$	6.15	t		101.5
$OCCHCH_2C(CH_3)_3$	2.26	d		44.9
$OCCHCH_2C(CH_3)_3$				31.7
$OCCHCH_2C(CH_3)_3$	1.20	s		30.1
$Al(CH_3)_2$	0.01	s		-7.7
$C_7H_{10}N$	8.13	d		147.1
	5.71	d		106.4
				155.3
	1.92	s		38.1
$[Cp_2Zr(OCCHCH_2C(CH_3)_3)]_2(\mu\text{-}HAl(CH_2CH_3)_2)$ (9)				
C_5H_5	5.76	s		108.5
	5.60	s		105.5
$OCCHCH_2C(CH_3)_3$				188.1
				183.0
$OCCHCH_2C(CH_3)_3$	6.11	t	J = 7.3	103.2
	d			100.7
$OCCHCH_2C(CH_3)_3$	2.21	d	J = 7.3	45.6
	2.20	d	J = 7.3	44.9
$OCCHCH_2C(CH_3)_3$				32.2
				32.0
$OCCHCH_2C(CH_3)_3$	1.23	s		30.7
	1.20	s		30.6
$HAl(CH_2CH_3)_2$	-1.59			
$HAl(CH_2CH_3)_2$	0.49	q	J = 7.8	-2.7
$HAl(CH_2CH_3)_2$	1.56	t	J = 7.8	10.8

Table 2. (Continued)

assignment	chemical shift, multiplicity, coupling constant		
	^{1}H		^{13}C
$[Cp_2Zr(OCCHCH_2C(CH_3)_3)]_2(\mu$-H)($\mu$-Al($CH_2CH_3)_2$) (10)			
C_5H_5	5.68 s		106.4
OCCHCH$_2$C(CH$_3$)$_3$			175.7
OCCHCH$_2$C(CH$_3$)$_3$	6.14 t	J = 7.3	103.4
OCCHCH_2C(CH$_3$)$_3$	2.20 d	J = 7.3	44.9
OCCHCH$_2C$(CH$_3$)$_3$			31.7
OCCHCH$_2$C(CH_3)$_3$	1.17 s		30.0
Zr-H-Zr	-3.03 s		
Al-(CH_2CH$_3$)$_2$	0.29 q	J = 7.8	*c*
Al(CH$_2CH_3$)$_2$	1.55 t	J = 7.8	10.1
$[Cp_2Zr(OCCHCH_2C(CH_3)_3)]_2(C_7H_{10}N_2)(Al(CH_3)_3)$ (11)			
C_5H_5	5.79 s		106.9
OCCHCH$_2$C(CH$_3$)$_3$			190.1
OCCHCH$_2$C(CH$_3$)$_3$	*d*		102.1
OCCHCH_2C(CH$_3$)$_3$	2.34 d	J = 7.3	45.5
OCCHCH$_2C$(CH$_3$)$_3$			30.4
OCCHCH$_2$C(CH_3)$_3$	1.18 s		30.2
Zr-CH_3	0.0 s		15.1 s
Al-(CH_3)$_2$	-0.13 s		-8.5 br
$C_7H_{10}N_2$	8.24 d	J = 5.7	149.0
	5.95 d	J = 5.7	106.7
	2.13 s		38.3

Table 2. (Continued)

assignment	chemical shift, multiplicity, coupling constant		
	^{1}H		^{13}C
$[Cp_2Zr(OCCHCH_2C(CH_3)_3)]\cdot(C_7H_{10}N_2)$ (12)			
C_5H_5	5.75 s		106.5
$OCCHCH_2C(CH_3)_3$			186.2
$OCCHCH_2C(CH_3)_3$	4.88 d	J = 7.3	99.9
$OCCHCH_2C(CH_3)_3$	2.88 t	J = 7.3	44.6
$OCCHCH_2C(CH_3)_3$			31.7
$OCCHCH_2C(CH_3)_3$	1.35 s		30.1
$C_7H_{10}N_2$	8.24 d	J = 5.7	150.9
	5.95 d	J = 5.7	106.6
	2.13 s		38.3

[a] ^{1}H and ^{13}C NMR spectra taken in benzene-d_6 at ambient temperature unless otherwise indicated. Chemical shifts are reported in ppm relative to TMS or to residual protons/carbons in solvent. Coupling constants are reported in Hz. [b] Recorded in toluene-d_8 at -10°C. [c]Not resolved at 22.5 MHz. [d]Not Observed at 90 MHz. [e]Not resolved at 100.5 MHz. [f]Obscured by benzene solvent resonance.

EXPERIMENTAL SECTION

General Considerations. All manipulations were carried out under argon using standard Schlenk techniques or in a nitrogen-filled glovebox equipped with a -40°C freezer. Argon was purified by passage through columns of Chemalog RS-11 catalyst and Linde 4 Å molecular sieves. Toluene, benzene, diethyl ether, pentane, THF, and hexane, including NMR solvents, were stirred over CaH_2 and transferred onto sodium benzophenone ketyl. Solvents dried in this manner were vacuum transferred and stored under argon in flasks equipped with Teflon screw valves. $AlMe_2Cl$ was purchased from Texas Alkyls and was used neat or as prepared solutions in C_6D_6. Et_2AlH was obtained from Texas Alkyls as a 6% solution in heptane. Heptane was removed in vacuo to afford neat Et_2AlH, which was used without further purification. 2,2-Dimethyl-1-butene was obtained from Aldrich, distilled from CaH_2 and stored over molecular sieves. $NaN(Si(CH_3)_3)_2$ was prepared by refluxing freshly distilled $HN(Si(CH_3)_3)_2$ (Analabs) with NaH in toluene under argon for 24 h. Carbon monoxide (Matheson) and ^{13}C-labeled CO (99% , MRC-Mound) were used as received.

^1H NMR spectra were recorded in C_6D_6, $CDCl_3$, or C_7D_8 using residual protio-solvent resonances as an internal reference on Varian EM-390, JEOL FX-90Q, JEOL GX400, or Bruker WM-500 spectrometers. ^{13}C NMR spectra were obtained on the JEOL instruments. IR spectra were recorded as nujol mulls or in solution in C_6D_6 on a Beckman IR-4240 or Shimadzu IR-435 instrument. Elementary analyses were performed at the California Institute of Technology Analytical Facility, Dornis and Kolbe Microanalytical Laboratory, or MicAnal Laboratories. All reactions were carried out at room temperature unless otherwise indicated.

Procedures. **$[Cp_2Zr(C,O\text{-}\eta^2\text{-}OCCHCH_2CMe_3)]_2$ (1a).** This complex was prepared by the method of Straus.[4a] A mixture of 3.727 g (10.0 mmol) of the acyl complex $Cp_2Zr(Cl)C(O)CH_2CH_2C(CH_3)_3$[8b] and 1.880 g (10.0 mmol) of $NaN(Si(CH_3)_3)_2$ was dissolved in 75 mL of benzene. A gelatinous yellow mixture formed and was stirred for 2.5 h. The mixture was filtered through a pad of Celite on a coarse frit and washed repeatedly with benzene. The clear yellow filtrate was stripped of solvent and washed with two 15 mL portions of pentane to afford **(Z,Z)-1a** as a pale yellow powder (2.476 g, 7.42 mmol). The washings were stripped of solvent to yield 0.425 gm (0.60 mmol) of a yellow powder that was identified as **(Z,E)-1a** by ^1H and ^{13}C NMR (80% purity by ^1H NMR). **(Z,Z)-1a** IR (solution C_6D_6): 2950 (s), 2900 (s), 2860 (s), 1690 (w), 1620 ($\nu_{C=C}$, m), 1475 (m), 1460 (m), 1385 (m), 1360 (s), 1290 (w), 1250 (m), 1195 (w), 1085 (s), 1040 (vs), 1015 (vs), 990 (vs), 900 (m), 875 (m), 790 (s) cm-1.

$[Cp_2Zr(C,O\text{-}\eta^2\text{-}OCCH_2)]_n$ (1b).[4b] A mixture of 2.793 g (9.34 mmol) of the acyl $Cp_2Zr(Cl)C(O)Me$[14] and 1.737 g (9.47 mmol) of $NaN(Si(CH_3)_3)_2$ was suspended in 50 mL of toluene at -50°C. A yellow suspension formed and was allowed to warm to room temperature and stir for 2 h. After the reaction mixture was allowed to settle overnight at -20°C, the orange supernantant was cannulated off and the resulting off-white powder was washed with two 5 mL portions of toluene and one 5 mL portion of ether to yield 2.593 g of **1b** as a 1:1 mixture with NaCl. This material was used without further purification. IR (nujol): 2900 (s), 2850 (s), 1595 (m), 1530 (m), 1460 (m), 1375 (w), 1350 (w), 1075 (m), 1050 (m), 940 (s), 810 (s), 790 (s), 765 (s) cm-1.

$[Cp_2Zr(C,O\text{-}\eta^2\text{-}OCCHCH_2CMe_3)]_2(\mu\text{-}AlMe_3)$ (2). To an NMR tube charged with **1a** (21 mg, 0.031 mmol) at -40°C was added 0.450 mL of a 0.067 M solution of $AlMe_3$ in toluene-d_8. At -10°C, the proton NMR spectrum indicated the immediate formation of **2**. The ^{13}C and $^{13}C\{^1H\}$ NMR spectra were recorded at -10°C to prevent isomerization of **2** to **3**.

$[Cp_2Zr(C,O\text{-}\eta^2\text{-}OCCHCH_2CMe_3)]_2(\mu\text{-}AlMe_2)(\mu\text{-}Me)$ (3). The ketene dimer **1a** (0.818 g, 1.226 mmol) in 8 mL benzene was treated with 0.12 mL (1.25 mmol) of neat $AlMe_3$ via syringe. The yellow solution was stirred for 8 h at 25°C and the solvent removed in vacuo to afford a waxy solid. This solid was washed with two 5 mL portions of pentane to give **3** as a white powder (0.517 g, 0.699 mmol). Crystals suitable for x-ray analysis were obtained by the addition of 6 mL of pentane to 4 mL of a 0.17 M toluene solution of **3**. The resulting cloudy solution was quickly filtered through a pad of Celite on a fine frit and placed in a 10°C refrigerator overnight to afford beautiful colorless needles of **3**. IR (Nujol): 2910 (vs), 2850 (vs), 1625 ($\nu_{C=C}$, m), 1382 (m), 1375 (m), 1360 (s), 1325 (w), 1290 (w), 1260 (w), 1240 (w), 1195 (w), 1180 (m), 1165 (m), 1030 (m), 1010 (s), 970 (s), 900 (m), 870 (m), 800 (vs). Anal. Calcd. for $C_{37}H_{53}O_2AlZr_2$: C, 60.12; H, 7.23. Found: C, 59.99; H, 7.19.

X-ray Structure Determination of 3. A small prism of **3** was mounted approximately along *c* in a glass capillary under N_2. A series of oscillation and Weissenberg photographs indicated monoclinic symmetry and the space group $P2_1/c$ (*0k0* absent for *k* odd, *h0l* absent for *l* odd); data were collected on an Enraf-Nonius CAD4 diffractometer (graphite monochromator and MoKα radiation λ = 0.71073 Å). The unit cell parameters (Table 1, Appendix 1) were obtained by least-squares refinement of 25 2θ-values. The total, 10114 (+h,±k,±l), yielded an averaged data set 6573 reflections upon deletion of 87 for overlap; 5216 had I > 0 and 3380 had I > 3 σ(I). The four check reflections indicated no decomposition, and the data were reduced to F^2. The position of the two independent Zr atoms were derived from the Patterson map, and the subsequent Fourier map phased on these two atom revealed the remainder of the structure. The bridging methyl hydrogen atoms and those on the *t*-butyl group were located from difference maps; all other H-atoms were introduced into the model with fixed coordinates at idealized positions with isotropic U = 0.101 $Å^2$. Least-squares refinement of the atomic coordinates and U's (anisotropic for all

non-H atoms and isotropic for H(1), H(2), and H(3)) minimizing $\Sigma w\Delta^2$ with weights $w = \sigma^{-2}(F_o^2)$ gave $R_F = 0.0813$ (for $I > 0$, $R_F = 0.042$ for $I > 3\sigma(I)$) and the goodness–of-fit = 1.63 (p = 391 parameters); the maximum shift/error ratio is 0.50, the average < 0.10, and the maximum deviations in the $\Delta\rho$ map are close to the Zr atoms and are less than 1.1 e $Å^{-3}$. All calculations were carried out on a VAX 11/780 computer using the CRYRM system of programs. The form factors for all atoms were taken from Table 2.2B, *International Tables for X-Ray Crystallography* (1974); those for Zr and Al were corrected for anomalous dispersion.

Reaction of 3 with Pyridine. A 27 mg (0.037 mmol) sample of **3** was placed in a 5 mm NMR tube, dissolved in benzene-d_6 and capped with a rubber septum. To this solution was added 9.0 μL (0.112 mmol) pyridine. After 12 h the NMR spectrum indicated complete formation of **1a** (Table 2) and Me_3Al·pyr (δ = -0.31 ppm, C_6D_6).

Reaction of 3 with 4-Dimethylaminopyridine. A 20 mg (0.027 mmol) sample of **3** was combined with 7 mg (0.057 mmol) of 4-dimethylaminopyridine and dissolved in C_6D_6. After 15 min the ^1H NMR indicated the formation of Cp_2Zr(C,O-η^2-$OCCHCH_2CMe_3$)·$AlMe_3$·DMAP **11** and another product assigned as Cp_2Zr(C,O-η^2-$OCCHCH_2CMe_3$)·DMAP **12**.

$Cp_2ZrOC(CHCH_2CMe_3)CHCH$ (4). A 0.385 g (0.521 mmol) sample of **3** was weighed into a medium Schlenk tube and dissolved in 10 mL of benzene. To this yellow solution was added 0.05 mL (0.616 mmol) of THF. Argon was evacuated from the Schlenk tube and replaced with an atmosphere of acetylene which had been passed through a -78°C trap (CAUTION: Purified acetylene is highly shock sensitive and explosive).[55] The clear yellow solution turned metallic green and then dark grey, suggesting the formation of polyacetylene. The reaction mixture was stirred for 1.5 h at 25°C and filtered through a fine frit to yield a clear yellow solution. Removal of solvent in vacuo gave a waxy yellow solid, which was washed with 5 mL Et_2O and 5 mL pentane to afford **4** as a white powder (0.150 g, 0.417 mmol). IR (Nujol): 2900

(s), 2850 (s), 1610 ($\nu_{C=C}$, m), 1360 (m), 1285 (w), 1200 (w), 1190 (w), 1140 (w), 1040 (m), 1010 (m), 825 (m), 800 (s), 780 (m) cm-1. Anal. Calcd. for $C_{19}H_{24}OZr$: C, 63.46; H, 6.73. Found: C, 63.44; H, 6.70.

$Cp_2Zr(CH_3)COC(CHCH_2CMe_3)OAlMe_2$-[$Cp_2Zr(C,O$-$\eta^2$-$OCCHCH_2$-$CMe_3$)] (5). A 20 mL benzene solution of **3** (1.014 g, 1.37 mmol) was placed in a glass pressure bottle, warmed to 45°C in an oil bath, flushed twice with carbon monoxide, and pressurized to 50 psi with carbon monoxide. After being stirred for 2 h at 45°C, the dark orange solution was transferred to a Schlenk tube. Solvent was removed in vacuo to afford a waxy orange residue. This residue was washed with three 5 mL portion of hexane to yield **5** as a light yellow powder (0.657 g, 0.856 mmol). IR (solution C_6D_6): 2950 (s), 2930 (s), 2860 (s), 2820 (m), 1610 ($\nu_{C=C}$, m), 1470 (m), 1440 ($\nu_{C=O}$, s), 1385 (w), 1360 (m), 1325 (w), 1285 (m), 1255 (w), 1240 (w), 1225 (w), 185 (s), 1150 (m), 1100 (w), 1090 (m) , 1040 (s), 1015 (vs), 990 (vs), 900 (m), 800 (vs) cm-1. Anal. Calcd. for $C_{38}H_{53}O_3Zr_2Al$: C, 59.49; H, 6.96. Found: C, 59.51; H, 6.89.

[$Cp_2Zr(C,O$-η^2-$OCCHCH_2CMe_3$)]$_2$(μ-$AlMe_2Cl$) (6a). Me_2AlCl (0.074 mL, 0.796 mmol) was added dropwise via syringe to an 8 mL precooled (-40°C), stirred toluene solution of **1a** (0.530 gm, 0.794 mmol). The resulting yellow solution was allowed to warm to room temperature and was stirred for 30 min. Toluene was removed in vacuo and the resultant yellow waxy solid washed twice with 5 mL of hexane to give **6a** (0.422 gm, 0.555 mmol) as an off-white powder. Running the reaction (0.809 mmol **1a**) in 3.5 mL of toluene and slowly cooling to -50°C afforded colorless crystals of **6a** suitable for analysis (0.448 mmol, 55%). IR (solution C_6D_6): 2950 (s), 2900 (s), 2860 (s), 1710 (bw), 1620 ($\nu_{C=C}$, m), 1475 (m), 146 0 (m), 1390 (m), 1360 (s), 1290 (w), 1260 (m), 1190 (m), 1150 (w), 1085 (m), 1070 (m), 1035 (s), 1015 (s), 990 (s), 900 (m), 875 (m), 810 (s), 790 (s) cm-1. Anal. Calcd. for $C_{36}H_{50}O_2ClZr_2Al$: C, 56.93; H, 6.63; Cl, 4.67. Found: C, 56.97; H, 6.60; Cl, 4.65.

$[Cp_2Zr(C,O\text{-}\eta^2\text{-}OCCHCH_2CMe_3)]_2(\mu\text{-}AlMe_2)(\mu\text{-}Cl)$ (7a). A solution of **1a** (0.818 g, 1.23 mmol) in 30 mL of toluene was treated with 0.11 mL (1 .18 mmol) of neat Me_2AlCl followed by 0.095 mL (1.18 mmol) of pyridine via syringe. The pale yellow solution was stirred for 1 h, solvent was removed in vacuo and the pale yellow residue washed with two 5 mL portions of pentane to yield **7a** as a white powder (0.678 g, 0.893 mmol). Crystals suitable for X-ray diffraction were obtained by layering pentane onto a concentrated (0.3 M) toluene solution of **7a** and cooling slowly to -20°C. IR (solution C_6D_6): 3100 (w), 2950 (s), 2900 (s), 2860 (s), 2820 (m), 1710 (w), 1670 (w), 1620 ($\nu_{C=C}$, m), 1595 (w), 1475 (m), 1460 (m), 1435 (m), 1385 (m), 1360 (s), 1290 (w), 1260 (m), 1180 (s), 1110 (mbr), 1095 (mbr), 1080 (mbr), 1060, 1030 (s), 1015 (s), 985 (m), 970 (s), 900 (m), 875 (m) cm-1. Anal. Calcd. for $C_{36}H_{50}O_2ClZr_2Al$: C, 56.93; H, 6.63; Cl, 4.67. Found: C, 56.95; H, 6.67; Cl, 4.75.

X-ray Structure Determination of $[Cp_2Zr(C,O\text{-}\eta^2\text{-}OC\dot{C}HCH_2CMe_3)]_2$-$(\mu\text{-}AlMe_2)(\mu\text{-}Cl)$ (7a). A thin crystalline plate (0.057 x 0.184 x 0.342 mm) of **7a** was mounted approximately along c in a glass capillary under N_2. A series of oscillation and Weissenberg photographs indicated monoclinic symmetry and the space group $P2_1/c$ (*0k0* absent for *k* odd, *h0l* absent for *l* odd); data were collected on a locally-modified Syntex $P2_1$ diffractometer using a graphite monochromator and MoKα radiation ($\lambda = 0.7107$ Å). The unit cell parameters (Appendix 1) were obtained by least-squares refinement of the average 2θ-values from four sets of thirty reflections: '$\pm 2\theta$' *hkl* and '$\pm 2\theta$' $\overline{hkl}$, $16 < 2\theta < 38°$. The three check reflections indicated some decomposition, the best least-squares fit with a quadratic curve and a maximum decay of 6.8% . The correction for absorption was negligible ($\mu = 0.660$ mm^{-1}, $0.80 < \mu l < 0.92$). The data were averaged over the Laue symmetry and reduced to F_o^2; the form factors for H from Stewart et al. (1965), and the International tables for X-ray Crystallography (1974) for the other atoms; those for Zr, Cl, and Al were corrected for anomalous dispersion. The details of data collection are summarized in Appendix

1. The position of the two independent Zr atoms were derived from the Patterson map, and the Fourier map phased on these two atoms revealed the remainder of the structure. All H-atoms were introduced into the model with fixed coordinates at idealized positions and isotropic U = 0.0756 $Å^2$. Least-squares refinement of the non-hydrogen atoms with anisotropic U_{ij}'s, minimizing $\Sigma w(F_o^2-(F_c/k)^2)_2$, using all the data (3567 reflections), led to S = 1.48, R_F = 0.053, and R'_F = 0.073; final shift/errors <0.10. The maximum deviations found in the $\Delta\rho$ map are close to the t-butyl group in fragment A, and are less than 0.4 e $Å^3$. All calculations were carried out on a Vax 11/780 computer using the CRYRM system of programs.

$[Cp_2Zr(C,O\text{-}\eta^2\text{-}OCHCH_2]_2(\mu\text{-}Cl)(\mu\text{-}AlMe_2)]$ (7b). A suspension of **1b** (0.358 g, 1.11 mmol monomer) in 2 mL of toluene was treated with neat Me_2AlCl (0.05 mL, 0.538 mmol) dropwise via syringe. The resultant deep-yellow solution was stirred 1 h, filtered through Celite on a medium frit and evacuated to dryness. The slightly orange residue was washed with two 5 mL portions of pentane to yield **7b** as an off-white powder (0.130 g, 0.365 mmol). An analytical sample was prepared by crystallization from toluene at -50°C for three weeks. IR (Nujol): 2900 (vs) , 2850 (vs), 1615 ($\nu_{C=C}$, m, br), 1560 (m, br), 1180 (s), 1080 (s), 1010 (s), 905 (s), 800 (vs), 725 (s) cm-1. Anal. Calcd. for $C_{26}H_{30}O_2AlZr_2$: C, 50.43; H, 4.88; Cl, 5.72. Found: C, 50.29; H, 4.79; Cl, 5.83.

$[Cp_2Zr(C,O\text{-}\eta^2\text{-}OCCHCH_2CMe_3)](C_7H_{10}N_2)(AlMe_2Cl)$ (8). A 0.769 g (1.153 mmol) sample of **1a** in 5 mL of toluene was treated with 0.10 mL (1. 153 mmol) of neat $AlMe_2Cl$ via syringe. A solution of 0.422 g (3.460 mmol) of 4-dimethylaminopyridine in toluene was then added via cannula. The solution was stirred for 30 min at 25°C and then evacuated to dryness. The resulting residue was redissolved in 25 mL of toluene, layered with 10 mL of Et_2O and placed in the -50°C freezer to give colorless microcrystals of **8** after 8 h (0.246 g, 0.449 mmol). IR (Nujol): 2900 (vs), 2850 (vs), 1630 (s), 1620 (s), 1550 (m), 1530 (w), 1500 (w), 1290 (w), 1260

(w), 1225 (m), 1180 (w), 1115 (vw), 1065 (m), 103 0 (m), 1020 (s), 990 (m), 820 (m), 815 (s), 800 (s), 680 (s) cm-1. Anal. Calcd. for $C_{26}H_{38}ON_2ClZrAl$: C, 56.96; H, 6.99; N, 5.11. Found: C, 56.99; H, 6.90; N, 4.97. Molecular weight (solution, C_6H_6)[56] Calcd. for $C_{26}H_{38}ON_2ClZrAl$: 548.4. Found: 554.9.

$[Cp_2Zr(C,O\text{-}\eta^2\text{-}OCCHCH_2CMe_3)]_2(\mu\text{-}HAlEt_2)$ (9). Complex **1a** (0.704 g, 1.055 mmol) was dissolved in 10 mL of toluene and treated with neat Et_2AlH (0.23 mL, 2.20 mmol) dropwise via syringe. The light-yellow solution was stirred for 2.5 h and evacuated to dryness. Washing the residue with two 5 mL portions of pentane yielded **9** as an off-white powder (0.320 g, 0.425 mmol). Crystals suitable for structural analysis were obtained by slowly cooling the pentane washings of the crude sample of **9**. IR (Nujol): 2800 (vs), 2870 (vs), 1800 ($\nu_{Zr-H-Al}$, wbr), 1620 (m) ($\nu_{C=C}$), 1360 (m), 1290 (w), 1230 (w), 1220 (w), 1195 (w), 125 0 (w), 1040 (m), 1015 (m), 990 (m), 900 (m), 875 (m) cm-1. Anal. Calcd. for $C_{38}H_{55}O_2Zr_2Al$: C, 60.59; H, 7.36. Found: C, 60.55; H, 7.28.

X-ray Structure Determination of $[Cp_2Zr\ (C,O\text{-}\eta^2\text{-}OCCHCH_2CMe_3)]_2$-$(\mu\text{-}HAlEt_2)$ (9). A crystal 0.01 x 0.28 x 0.76 mm of **9** was mounted in a glass capillary under N_2. Oscillation and Weissenberg photographs indicated monoclinic symmetry and the space group C2/c (*hkl* absent for $h + k$ odd, *h0l* absent for l odd). Data were collected on an Enraf-Nonius CAD4 diffractometer using a graphite monochromator and MoKα radiation ($\lambda = 0.7107$ Å). The unit cell parameters (Appendix 1) were obtained by least-squares refinement of the θ values for 25 reflections in the range: $6.3 < \theta < 15.0$. A complete sphere of data was collected with $\theta < 45°$ yielding 22163 reflections. Three check reflections, recollected after every 10,000 sec of exposure time, showed no significant deviations in their intensities. The data were averaged over the Laue symmetry and reduced to F_o^2. No decay or absorption corrections were deemed necessary. Form factors for H were taken from Stewart et al. (1975) and the International Tables for X-ray Crystallography for the other atoms; those for Zr and Al were corrected for anomolous dispersion.

The position of one of the independent Zr atoms was derived from the Patterson map, and the Fourier map phased on this atom revealed the other Zr atom, the Al atom, and several of the lighter atoms in the coordination spheres of the two Zr atoms. Further structure factor calculations and Fourier maps revealed the remainder of the structure, including the bridging H atom. The remaining H atoms were introduced into idealized positions after verifying their positions on a difference map. The H atoms (except for the bridging hydride atom) were given fixed isotropic U's = 0.063 $Å^2$. Least-squares refinement of all non-hydrogen parameters with anisotropic U's, the scale factor, and the coordinates and isotropic U for the bridging hydride H-atom led to S = 2.80, R_F = 0.067, and R'_F = 0.052; final shift/errors < 0.15. Two peaks approximately 0.8 e $Å^{-3}$ were found in the final difference-Fourier map very near the methyl carbons of the diethylaluminum moiety. All other peaks were less than 0.6 e $Å^{-3}$. All calculations were carried out on a VAX 11/750 computer using the CRYRM system of programs.

$[Cp_2Zr(C,O\text{-}\eta^2\text{-}OCCHCH_2CMe_3)]_2(\mu\text{-}H)(\mu\text{-}AlEt_2)$ (10). A toluene solution of **1a** (1.057 g, 1.58 mmol) was treated with several equivalents (0.400 mL, 3.77 mmol) of neat Et_2AlH. A deep-yellow solution formed and was stirred for 24 h at 80°C. Removal of solvent in vacuo afforded a dark-brown waxy residue, which was washed with four 15 mL portions of cold (-30°C) hexane to yield **10** as a white powder (0.444 g, 0.589 mmol). The dark brown washings were evacuated to dryness, redissolved in toluene, and stirred at 80°C for an additional 6 h. Workup in a similar manner provided an additional 0.094 g (0.125 mmol) of **10**. Recrystallization of 0.100 g of **10** from 5 mL of Et_2O/hexane (3/2) at -20°C afforded crystals suitable for x-ray diffraction. IR (Nujol): 2800 (vs), 2750 (vs), 1630 (m) ($\nu_{C=C}$), 1630 (s), 1310 (m), 1290 (m), 1255 (w), 1195 (w), 1180 (w), 1155 (w), 1020 (m), 1110 (m), 975 (m), 940 (m), 900 (m), 875 (m), 820 (s), 780 (s) cm-1.

X-ray Structure Determination of $[Cp_2Zr\ (C,O\text{-}\eta^2\text{-}OCCHCH_2CMe_3)]_2$-$(\mu\text{-}H)(\mu\text{-}AlEt_2)$ (10). A crystalline block (0.35 x 0.30 x 0.25 mm) of **10** was

mounted approximately along a in a glass capillary under N_2. A series of oscillation and Weissenberg photographs indicated monoclinic symmetry and the space group C2/c (*hkl* absent for $h + k$ odd, *h0l* absent for l odd); data were collected on a Enraf-Nonius CAD-4 diffractometer, using a graphite monochromator and MoKα radiation (λ = 0.7107 Å). The unit cell parameters (Appendix 1) were calculated from the setting angles of 25 reflections in the range $20 < 2\theta < 35°$. A total of 9443 reflections, comprising four symmetry-equivalent data sets, were averaged to give a total of 2845 reflections. The three check reflections, collected every 10,000 seconds of exposure time, showed no significant deviations in their intensities. The correction for absorption was negligible (λ = 0.544 mm^{-1}). The form factors were taken from Table 2.2B, Volume IV, International Tables for X-Ray Crystallography (1974) for all atoms. The position of the Zr atoms was derived from the Patterson map, and the Fourier map phased on this atom revealed the remainder of the structure. All H-atoms were introduced into the model with fixed coordinates at idealized positions and individual isotropic U's equal in magnitude to that of the adjacent heavy atom, plus 10-20% . Least-squares refinement of all non-hydrogen atoms with anisotropic U_{ij}'s, the scale factor, and the two parameters of the hydride H-atom (y-coordinate and U), minimizing $\Sigma w(F_o^2-(F_c/k)^2)_2$, with all the data (2845 reflections) led to S = 1.76, R_F = 0.049, and R_F' = 0.033; final shift/errors <0.10. The maximum deviation found in the ρ map is less than 0.8 e $Å^{-3}$. All calculations were carried out on a Vax 11/750 computer using the CRYRM system of programs.

REFERENCES

1. (a) Blyholder, G.; Emmet, P. H. *J. Phys. Chem.* **1960**, *64*, 470. (b) Ichikawa, M. B.; Sekizawa, K.; Shikakura, K.; Kawai, M. *J. Mol. Cat.* **1981**, *11*, 167. (c) Takeuchi, A.; Katzer, J. R. *J. Phys. Chem.* **1982**, *86*, 2438.

2. (a) Barger, P. T.; Santarsiero, B. D.; Armantrout, J.; Bercaw, J. E. *J. Am. Chem. Soc.* **1984**, *106*, 5178 and references therein. (b) Wolczanski, P. T.; Bercaw, J. E. *Acc. Chem. Res.* **1980**, *13*, 121. (c) Morrison, E. D.; Steinmetz, G. R.; Geoffroy, G. L.; Fultz, W. C.; Rheingold, A. L. *Ibid.* **1984**, *106*, 4783 and references therein. (d) Miyashita, A.; Grubbs, R. H. *Tetrahedron Lett.* **1981**, 1255. Miyashita, A. Abstracts of papers submitted to 3rd China-Japan-U.S. Symposium on Organometallic Chemistry and Catalysis, Santa Cruz, California, August 5, 1984.

3. (a) Dotz, K. H. *Pure Appl. Chem.* **1983**, *55*, 1689. (b) Semmelhack, M. F.; Tamura, R.; Schnatter, W.; Springer, J. *J. Am. Chem. Soc.* **1984**, *106*, 5363.

4. (a) Straus, D. A.; Grubbs, R. H. *J. Am. Chem. Soc.* **1982**, *104*, 5499. (b) Straus, D. A. Ph.D. Thesis, California Institute of Technology, Pasadena, California, 1982. (c) Ho, S. C. H.; Straus, D. A.; Armantrout, J.; Schaefer, W. P.; Grubbs, R. H. *J. Am. Chem. Soc.* **1984**, *106*, 2210. (d) Moore, E. J.; Straus, D. A.; Armantrout, J.; Santarsiero, B. D.; Grubbs, R. H.; Bercaw, J. E. *Ibid.* **1983**, *105*, 2068.

5. Deprotonation of alkyl-acyl metallocenes yields stable metallaenolate anions. The metallaenolate (ketene) anions have been shown to be versatile reagents for the synthesis of binuclear ketene complexes.[4c]

6. Deprotonation of later transition metal acyl complexes generally yields stable enolate complexes: (a) Theopold, K. H.; Becker, P. N.; Bergman, R. G. *J. Am.*

Chem. Soc. **1982**, *104*, 5250. (b) Liebeskind, L. S.; Welker, M. E.; Goedken, V. *Ibid.* **1984**, *106*, 441.(c) Baird , G. J.; Davies, S. G.; Jones, R. H. Prout, K.; Warner, P. *J. Chem. Soc., Chem. Commun.* **1984**, 745.(d) Doney, J. J.; Bergman, R. G.; Heathcock, C. H. *J. Am. Chem. Soc.* **1985**, *107*, 3724.(e) See also: Wulff, W. D.; Gilbertson, S. R. *J. Am. Chem. Soc.* **1985**, *107*, 503.

7. A sequence involving hydrozirconation, carbonylation,[8] and depronation[4] affords zirconocene ketene complexes in yields of 60-70% with defined stereochemistry.

8. (a) Wailes, P. C.; Weigold, H. *J. Organomet. Chem.* **1970**, *24*, 405.(b) Carr, D. B.; Schwartz, J. *J. Am. Chem. Soc.* **1979**, *101*, 3521.(c) Berlelo, C. A.; Schwartz, J. *Ibid.* **1975**, *97*, 228.

9. The use of Lewis acids as activating agents is well established in organic and organometallic chemistry. (a) Richmond, T. G.; Shriver , D. F. *Inorg. Chem.* **1982**, *21*, 1272.(b) Butts, S. B.; Strauss, S. H.; Holt, E. M.; Stinson, R. E.; Alcock, N. W.; Shriver, D. F. *Ibid.* **1980**, *102*, 5093.(c) Negishi, E. *Organometallics in Organic Synthesis* Wiley and Sons: New York, 1980, Vol. 1, p. 350.

10. For the reaction of η^2-(C,C) bound tungsten ketene complexes with Lewis acids see: (a) Kreissl, F. R.; Sieber, W.; Wolfgraber, M. *Angew. Chem., Int. Ed. Eng.* **1983**, *22*, 493. (b) Churchill, M. R.; Wasserman, H. J.; Holmes, S. J.; Schrock, R. R. *Organometallics* **1982**, *1*, 766-768.

11. (a) Wang, H. K.; Chai, H. W.; Muetterties, E. L. *Inorg. Chem.* **1981**, *20*, 2661. (b) Demitras, G.C.; Muetterties, E. L. *J. Am. Chem. Soc.* **1979**, *99*, 2796.

12. Waymouth, R. M.; Santarsiero, B. D.; Grubbs, R. H. *J. Am. Chem. Soc.* **1984**, *106*, 4050.

13. Priorities were assigned according to atomic weight: Zr > O > C > H. See Huggins, J. M.; Bergman, R. G. *J. Am. Chem. Soc.*, **1981**,*103*, 3002. IUPAC

Commission on Nomenclature in Organic Chemistry: *Pure Appl. Chem.*, **1976**, *45*, 11..

14. (a) (Z,Z)-VIIa is obtained stereospecifically from the major isomer of Ia. The chemical shifts for the vinyl protons (H2) (recorded by ^{1}H NMR during the reaction **1a** → **2a** → **(Z,Z)-7a**) fall in the range 5.6-6.2 ppm. However, **(E,Z)-1a** shows a characteristically upfield chemical shift of 4.63 ppm for one of the vinyl proton that we assign to the (E) isomer (Table 2). Moreover, **(E,Z)-7a** prepared from this sample also shows an upfield vinyl proton chemical shift of 4.74 ppm. From these results we conclude that the major isomer of **1a**, from which **(Z,Z)-7a** is obtained, is the (Z,Z) isomer. (b) **(Z,Z)-1a** was used in all further experiments and for the remainder of this discussion will be referred to simply as **1a**.

15. Marsella, J.A.; Moloy, K. G.; Caulton, K. G. *J. Organomet. Chem.* **1980**, *201*, 389.

16. Aluminum has a large quadrupole moment, which often broadens the signal of bound nuclei in the NMR..

17. Hunter, W. E.; Hrncir, D. C.; Bynum, R. V.; Pentilla, R. A.; Atwood, J. L. *Organometallics* **1983**, *2*, 750.

18. Holton, J.; Lappert, M. F.; Pearce, R.; Yarrow, P. I. W. *Chem. Rev.* **1983**, *83*, 135-201.

19. Bridging metal alkyl bonds are typically 0.1-0.2 Å longer than the corresponding terminal bonds. The longest reported terminal Zr-C bond is 2.431(5) Å: Bristow, G. S.; Hitchcock, P. B.; Lappert, M. F. *J. Chem. Soc., Chem. Commun.* **1982**, 462, reference 10..

20. (a) Bristow, G. S.; Hitchcock, P. B.; Lappert, M. F. *J. Chem. Soc., Chem. Commun.* **1982**, 462.(b) Choukroun, R.; Dahan, F.; Gervais, D. *J. Organomet.*

Chem. **1984**, *266*, C33.(c) Engelhardt, L. M.; Jacobsen, G. E.; Raston, C. L.; White, A. H. *J. Chem. Soc., Chem. Commun.* **1984**, 220.(d) Young, S. J.; Hope, H.; Shore, N. E. *Organometallics* **1984**, *3*, 1585-1587.

21. (a) Gambarotta, S.; Pasquali, M.; Floriani, C.; Chiesi-Villa, A.; Guastini, C. *Inorg. Chem.* **1981**, *20*, 1173. (b) Fachinetti, G.; Biran, C.; Floriani, C.; Chiesi-Villa, A.; Guastini, C. *J. Am. Chem. Soc.* **1978**, *78*, 1921. *Inorg. Chem.*, **1978**, *17*, 2995. (c) Meinhart , J. D.; Santarsiero, B. D.; Grubbs, R. H. *J. Am. Chem. Soc.* **1986**, *108*, 3318.

22. (a) Erker, G. *Acc. Chem. Res.* **1984**, *17*, 103-109. (b) Erker, G.; Kropp, K.; Kruger, C.; Chiang, A. *Chem. Ber.* **1982**, *115*, 2447.(c) Erker, G.; Rosenfeldt, F. *J. Organomet. Chem.* **1982**, *224*, 29-42.

23. CO bond lengths for representative complexes: $Cp_2^*Zr(pyr)(OCCH_2)$, 1.338(2) Å;[4d] $[Cp_2Zr(CH_3)(OCCH_2)]^-Na^+\cdot(THF)_2$, 1.339(9) Å;[4c] $(Cp_2ZrCl)_2(\mu\text{-}Ph_2PCH{=}CO)$, 1.330(16) Å;[18d] 1.319(10) Å;[18b] $(Cp_2ZrCl)_2(\mu\text{-}Me_2PCH{=}CO)$, 1.35(2) Å;[18c] $Cp_2^*Zr(H)(OCCHPMe3)$, 1.303(3) Å, Moore, E.J., Ph.D. Thesis, California Institute of Technology, Pasadena, California, 1984..

24. (a) Zaworotko, M. J.; Kerr, C. R.; Atwood, J. L. *Organometallics* **1984**, *4*, 238.(b) Atwood, J. L.; Hrncir, D. C.; Priester, R. D.; Rogers, R. D. *Ibid.* **1983**, *2*, 985. For a survey of bond distances of O-bonded aluminum complexes see: Zaworotko, M. J.; Rogers, R. D. ; Atwood, J. L. *Ibid.*, **1982**, *1*, 1179 and reference 24.

25. Conway, A. J.; Gainsford, G. J.; Schrieke, R. R.; Smith, J. D. *J. Chem. Soc., Dalton Trans.* **1975**, 2499 and references therein.

26. Mole, T.; Jeffrey, E.A. *Organoaluminum Compounds* Elsevier Publishing: New York, 1972..

27. Erker, G.; Kropp, K.; Atwood, J. L.; Hunter, W. E. *Organometallics* **1983**, *2*, 1555-1561 and references therein.

28. (a) Toogood, G. E.; Wallbridge, M. G. H. *Adv. Inorg. Chem. Radiochem.* **1982**, *25*, 267-341.(b) Wailes, P. C.; Coutts, R. S. P.; Weigold, H. *Organometallic Chemistry of Titanium, Zirconium, and Hafnium* Academic Press: New York, 1974.

29. Wolczanski, P. T.; Threlkel, R. S.; Santarsiero, B. D. *Acta Cryst.* **1983**, *C39*, 1330.

30. Jones, S. B.; Petersen, J. L. *Inorg. Chem.* **1981**, *20*, 2889-2894.

31. (a) Teller, R. G.; Bau, R. *Struct. Bonding (Berlin)* **1981**, *44*, 1-82.(a) Bau, R.; Feller, R. G.; Kirtley, S. W.; Koetzle, T. F. *Acc. Chem. Res.* **1979**, *12*, 176.

32. Lobkovskii, E. B.; Soloveichik, G. L.; Sizov, A. I.; Bulychev, B. M. *J. Organomet. Chem.* **1985**, *280*, 53.

33. (a) Kopf, J.; Vollmer, H.-J.; Kaminsky, W. *Cryst. Struct. Commun.* **1980**, *9*, 985.(b) Atwood, J. L.; Hrncir, D. C.; Rogers, R. D.; Howard, J. A. K. *J. Am. Chem. Soc.* **1981**, *103*, 6787.

34. Lauher, J.W.; Hoffmann, R. *J. Am. Chem. Soc.* **1976**, *98*, 1729.

35. (a) Jemmis, E. D.; Chandrasekhar, J.; Schleyer, P. v R. *J. Am. Chem. Soc.* **1979**, *101*, 527.(b) Schleyer, P. v R.; Tidor, B.; Jemmis , E. D.; Chandrasekhar, J.; Wurthwein, E. U.; Kos, A. J.; Luke, B. T.; Pople, J. A. *Ibid.* **1983**, *105*, 484.

36. Schade, C.; Schleyer, P.v R.; Dietrich, H.; Mahdi, W. *J. Am. Chem. Soc.* **1986**, *108*, 2484-2485.

37. (a) Kaminsky, W.; Kopf, J.; Sinn, H.; Vollmer, H. J. *Angew. Chem., Int. Ed. Eng.* **1976**, *15*, 629.(b) Watson, P. L. *J. Am. Chem. Soc.* **1983**, *105*, 6491.(c) Engelhardt, L. M.; Leung, W.; Raston, C. L.; Twiss, P.; White, A. H. *J. Chem. Soc., Dalton, Trans.* **1984**, 321.(d) Atwood, J. L.; Fieldberg, T.; Lappert, M. F.; Luong-Thi, N. T.; Shakir, R.; Thorne, A. J. *J. Chem. Soc., Chem. Commun.*

1984, 1163. (e) Olmstead, M. M.; Power, P. P. *J. Am. Chem. Soc.* **1985**, *107*, 2174, and references therein.

38. (a) Forbus,T. R.; Martin, J. C. *J. Am. Chem. Soc.* **1979**, *101*, 5057.(b) Rhine, W. E.; Stucky, G.; Petersen, S. W. *Ibid.* **1975**, *97*, 6401.

39. Lowry, T. H.; Richardson, K. S. *Mechanism and Theory in Organic Chemistry* Harper and Row: New York, 1981.

40. (a) Fukuto, J.M.; Jensen, F.R. *Acc. Chem. Res.* **1983**, *16*, 177-184. (b) Stille, J. K.; Labadie, J. W. *J. Am. Chem. Soc.* **1983**, *105*, 669.

41. (a) Fritz, H. L.; Espensen, J. H.; Williams, D. A.; Molander, G. A. *J. Am. Chem. Soc.* **1974**, *96*, 2378.(b) Dodd, D.; Johnson, M. D.; Lockman, B. L. *Ibid.* **1977**, *99*, 3664.

42. (a) Gell, K. I.; Posin, B.; Schwartz, J.; Williams, G. M. *J. Am. Chem. Soc.* **1982**, *104*, 1846.(b) Gell, K. I.; Williams, G. M.; Schwartz, J. *J. Chem. Soc., Chem. Commun.* **1980**, 550.

43. (a) Erker G.; Kropp, K. *Chem. Ber.* **1982**, *115*, 2437. (b) Erker, G.; Kropp, K.; Kruger, C.; Chiang, A.-P. *Ibid.* **1982**, *115*, 2447.

44. (a) Gambarotta, S.; Floriani, C.; Chiesi-Villa, A.; Guastini, C. *J. Am. Chem. Soc.* **1983**, *105*, 1690.(b) Fachinetti, G.; Floriani, C.; Roselli, A.; Pucci, S. *J. Chem. Soc., Chem. Commun.* **1978**, 269.

45. We previously proposed a series of rapid transmetallations with inversion to account for stereochemical scrambling of the α-carbon of a titanacyclobutane upon treatment with Me_2AlCl: Ott, K. C.; Lee, J. B.; Grubbs, R. H. *J. Am. Chem. Soc.* **1982**, *104*, 2942.

46. Waymouth, R. M.; Pierre, L.; Grubbs, R. H. Unpublished results.

47. Although comparisons are difficult, alkyl bridges are more labile than chloride or hydride bridges in organoaluminum compounds. (a) Reference 26, p. 32. (b) Eisch, J. J. in *Comprehensive Organometallic Chemistry* Wilkinson, G.; Stone, F. G. A.; Abel, E. W., Eds.; Pergamon Press: Oxford, 1982, Vol. 1.

48. For example, coordinated Me_2AlCl stabilizes the reactive $Cp_2Ti{=}CH_2$ species in the "Tebbe" reagent $Cp_2Ti{=}CH_2{\cdot}AlMe_2Cl$ (a) Tebbe, F. N.; Parshall, G. W.; Reddy, G. S. *J. Am. Chem. Soc.* **1978**, *100*, 3611. (b) Howard, T. R.; Lee, J. B.; Grubbs, R. H. *Ibid.* **1980**, *102*, 6876.

49. Hydrogenolysis of ketene complexes yields aldehydes,[2c,50] alcohols[50] or metal enolates[2a,b] and hydrolysis/alcoholysis yields acetates,[2c] but in only one case[51] has further C-C coupling been observed for a ketene intermediate.

50. Hermann, W.A.; Plank, J. *Angew. Chem., Int. Ed. Eng.* **1978**, *17*, 525.

51. Fagan, P. J.; Manriquez, J. M.; Marks, T. J.; Day, V. W.; Vollmer, S. H.; Day, C. S. *J. Am. Chem. Soc.* **1980**, *102*, 5393.

52. Carbonylation of early transition-metal ketene complexes often leads either to decomposition or displacement of the ketene ligand with concomitant generation of the metallocene dicarbonyl. Meinhart, J. D.; Grubbs, R. H. Unpublished results.

53. (a) Roper M. In *Catalysis in C1 Chemistry* Keim, W., Ed.; D. Reidel Publishing, Dordrecht: 1983, p. 58.(b) Shriver, D. F. In *Catalytic Activation of Carbon Monoxide* Ford, P. C., Ed.; ACS Symposium Series 152, Washington, D.C.: 1981, pp. 1-19.

54. (a) Maruya, K.; Inaba, A.; Maehashi, T.; Domen, K.; Onishi, T. *J. Chem. Soc., Chem. Commun.* **1985**, 487.(b) Saussey, J.; Lavalle y, J-C.; Lamotte, J.; Rais, T. *Ibid.* **1982**, 278.(c) Wang, G.; Hattori, H.; Itoh, H.; Tanabe, K. *Ibid.* **1982**, 1256.

55. *Prudent Practices for Handling Hazardous Chemicals in Laboratories*; National Academy Press: Washington, D. C., 1981.

56. Clark, E. P. *Ind. Eng. Chem., Anal. Ed.* **1941**, *13*, 820.

CHAPTER 3

Reactivity of Group 4 Acyl Complexes with Alkylaluminum Reagents: Synthesis of Zirconium Ketone Complexes

INTRODUCTION

Aluminum reagents are widely used as cocatalysts in a number of industrially important catalytic processes such as Ziegler Natta polymerization[1] and olefin metathesis.[2] Despite the widespread application of catalytic processes employing aluminum cocatalysts, there are very few cases where the role of the cocatalyst is well understood. A notable exception is the olefin metathesis catalyst $Cp_2Ti{=}CH_2{\cdot}AlMe_2Cl$[3] prepared by treating $Cp_2TiMeCl$ with $AlMe_3$. Studies on the synthesis[4] and reactivity[5] of this complex reveal that the alkylaluminum cocatalyst serves a dual role in this system: (1) it acts as a reagent in the formation of the active titanocene methylidene catalyst, and (2) once the alkylidene is formed, $AlMe_2Cl$ coordinates to the reactive $Cp_2Ti{=}CH_2$ fragment and prevents it from dimerizing.

The role of the aluminum reagent in stabilizing the titanocene methylidene prompted us to investigate whether $AlMe_2Cl$ could coordinate to and stabilize other reactive organometallic intermediates. In this chapter we report studies[6] on the synthesis and reactivity of the bis-(cyclopentadienyl) zirconium ketone complexes **2**, which are formally 1:1 adducts between $AlMe_2Cl$ and a zirconium η^2-ketone complex. These complexes, prepared by the reductive alkylation of zirconium acyl complexes by alkylaluminum reagents (eq 1), model intermediates in the catalytic reduction of CO[7] and also promise to be useful reagents for the construction of carbon-carbon bonds.

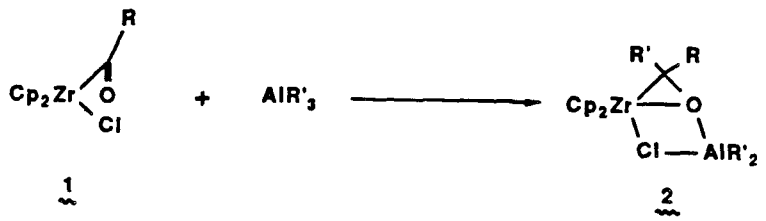

1 2 (1)

Transition metal ketone and aldehyde complexes have been proposed as precursors to branched and linear alcohols formed over metal-oxide CO reduction catalysts.[7] Although the mechanisms of formation of these intermediates is unknown, several recent studies have provided models for the production of ketone[8,9] and aldehyde[10,11] complexes on Fischer-Tropsch catalysts. Herein we report mechanistic studies that provide a good model for the catalytic formation of ketone complexes from transition metal acyl complexes. An important aspect of these studies is the observation that aluminum reagents perform a key role in mediating the formation of the ketone complexes. The role of the aluminum reagent may be of direct relevance to the importance of Lewis-acidic sites on heterogeneous CO reduction catalysts.[12]

Transition metal ketone and aldehyde complexes also show considerable promise as synthetic intermediates. Coordination of an organic ketone or aldehyde to a transition metal center dramatically alters its reactivity and provides a means of coupling the ketone or aldehyde ligand with electrophilic unsaturated substrates such as olefins, acetylenes, and organic carbonyls (Scheme I).

SCHEME I

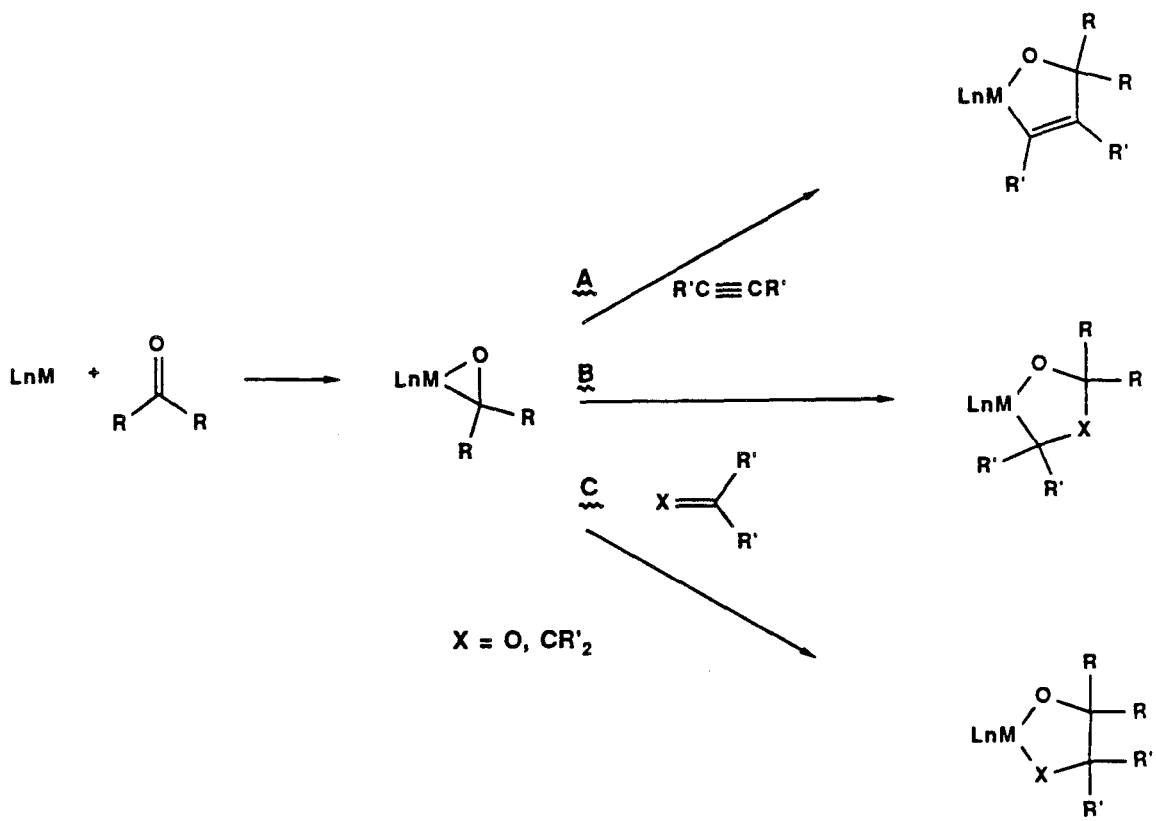

A key question in developing the synthetic utility of these intermediates is the regiochemistry of the coupling step when X = O (paths B and C above). The preferred mode of coupling of organic carbonyl substrates with later transition metal ketone and aldehyde complexes[13] and with titanium[14,15] and rhenium[16] ketene complexes is in a "head-to-tail" fashion (path B). For synthetic applications, the desired pathway is the "head-to-head" reductive coupling of the carbonyls (path C), which results in the formation of a carbon-carbon bond. Herein we report results that demonstrate that the zirconium ketone complexes **2** couple readily with a variety of unsaturated substrates and promote the "head-to-head" coupling of organic ketones to give zirconium diolates. These results suggest that zirconium complexes should prove useful synthetic reagents for the coupling of organic ketones and aldehydes.

RESULTS AND DISCUSSION

Preparation of Zirconium Ketone Complexes. Treatment of the bis-(cyclopentandienyl)zirconium chloro acyl complexes **1** with trialkylaluminum reagents in aromatic solvents affords the ketone complexes **2** in isolated yields of 65-90% (Table 1, eq. 1).[17] Three resonances at 5.57(10H), 1.49(6H), and -0.23(6H) ppm in the ^{1}H NMR spectrum (C_6D_6) of isolated samples of **2a** imply that $AlMe_2Cl$ remains coordinated to the ketone ligand, presumably via Zr-Cl-Al and Zr-O-Al bridging interactions. These complexes were characterized by spectral and analytical techniques, as well as by hydrolysis to the secondary alcohols (see Experimental section). The ketone complexes are thermally sensitive[18] but can be isolated as pale yellow or colorless powders that are stable under an inert atmosphere below 25°C. The reactions in Table 1 were run at 0°C in order to prevent subsequent thermal reactions of the ketone complexes.

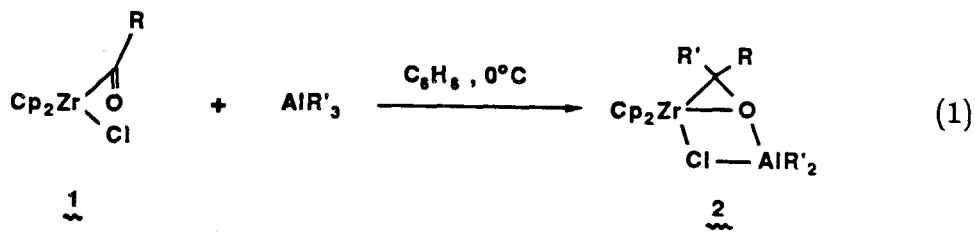

1 2 (1)

The reductive alkylation of zirconium acyl complexes by alkylaluminum reagents occurs readily for primary or secondary aliphatic acyl ligands, with several notable exceptions, as indicated in Table 1. The ethyl methyl ketone complex could not be prepared from the acyl **1a** (R=Me) and $AlEt_3$ (entry 2) although this ketone ligand could be prepared by treating the acyl **1b** (R=Et) with $AlMe_3$ (entry 4). Treatment of **1a** with $AlEt_3$ leads to numerous products, including ethane, suggesting that enolization of the acyl ligand by $AlEt_3$ competes with alkylation in this case. Attempts

Table 1.

Entry	Acyl	R	Reagent	Product	R′	Yield %
1	1a	Me	$AlMe_3$	2a	Me	71
2	1a	Me	$AlEt_3$	-	Et	-
3	1a	Me	$AlR_2CHCHt\text{-}Bu$[a]	-	CHCH*t*-Bu	-
4	1b	Et	$AlMe_3$	2b	Me	85
5	1c	$CH_2CH_2CMe_3$	$AlMe_3$	2c	Me	68
6	1c	$CH_2CH_2CMe_3$	$AlEt_3$	2d	Et	65
7	1d	$c\text{-}C_6H_{11}$	$AlMe_3$	2e	Me	91
8	1e	CHCHPh	$AlMe_3$	-	Me	-

[a]R=*i*-Bu

to prepare vinyl-substituted ketone complexes from either vinyl acyl complexes or vinyl aluminum reagents were unsuccessful (entries 3 and 8).

Zirconium aldehyde complexes are prepared by a similar procedure; treatment of the acyl complex **1b** (R=Et) with diisobutylaluminum hydride gives the aldehyde complex **4a** (80% yield, ^1H NMR, eq 2). The aldehyde complexes were isolated as yellow oils and characterized by spectroscopic comparison with the ketone complexes **2**. The ^1H NMR spectrum of **4a** shows a characteristic[10] resonance at 3.15 (t, J=8.1Hz) due to the aldehydic proton. The chemical shift of this proton in the ^1H NMR spectrum, as well as the ^{13}C chemical shift (ca. 90 ppm) for the carbonyl carbon suggest that both the aldehyde and ketone complexes are best formulated as metallaoxiranes[8,10c-g] rather than π-complexes.

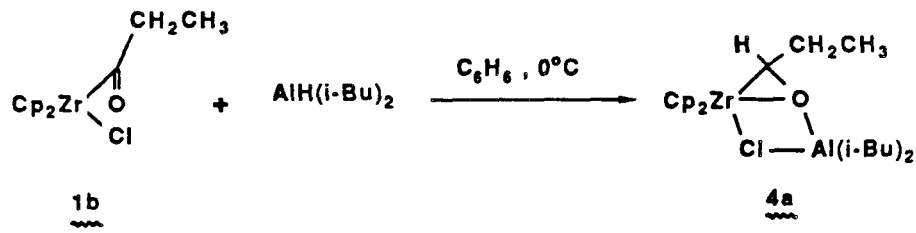

1b **4a** (2)

Oligomeric zirconium aldehyde complexes are prepared in lower yields (ca. 20%) by treating the acyl complexes with $LiBEt_3H$ (eq 3). In contrast to the dialkylalu-

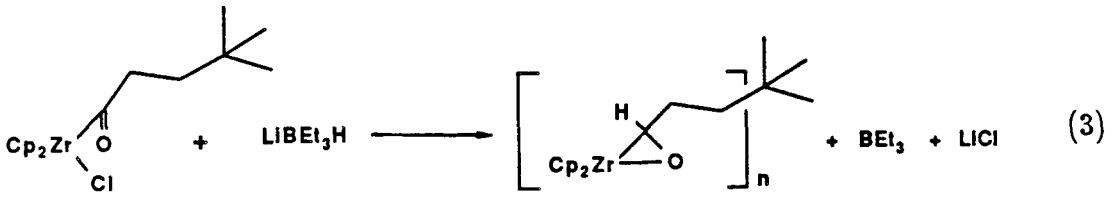

(3)

minum chloride, the trialkylborane generated in this reaction does not coordinate to the aldehyde ligand. Once formed, these aldehyde complexes most likely oligomerize.

Mechanism. We envision two possible mechanisms for the formation of the ketone complexes **2**. The simplest mechanism (mech. A, eq 4) involves the direct reductive alkylation of the acyl ligand by $AlMe_3$.[19] Similar mechanisms have been proposed for reductions of acyl ligands by boranes,[20] metal hydrides,[10] and zirconium alkyls.[21] Another mechanistic possibility (mech. B, eq 5) involves a stepwise pathway proceeding by initial transmetallation to give the alkyl acyl complex **3**, followed by a 1,2-migration of the alkyl group to the acyl ligand. Transmetallations between zirconium and aluminum complexes are facile,[17,22] but the coupling of alkyl and acyl ligands at group 4 metal centers requires elevated temperatures.[8] Thus, formation of the ketone complexes by the latter mechanism at 0°C would require that the aluminum reagent accelerate this latter coupling step.

Prior to this work there was little precedent for Lewis-acid induced couplings of an alkyl and an acyl ligand at a transition metal center. The demonstration of such an effect would not only be directly relevant to the mechanism of reaction (1), but might also have important implications for the effects of Lewis acids in CO reduction systems. Mechanistic studies were therefore initiated in an attempt to (1) demonstrate whether aluminum reagents promote the reductive coupling of alkyl and acyl ligands, and (2) establish the mechanism by which the ketone complexes **2** are formed when the chloro acyl complexes **1** are treated with alkylaluminum reagents.

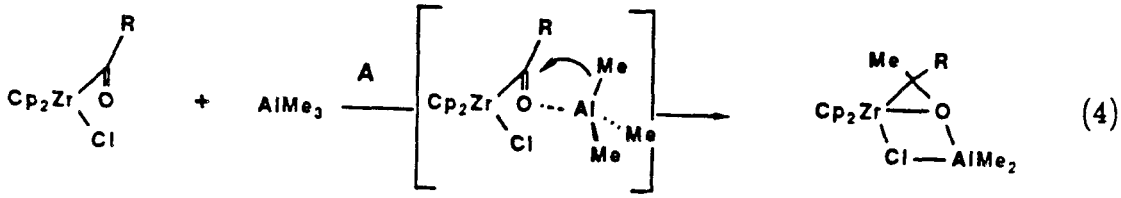

(4)

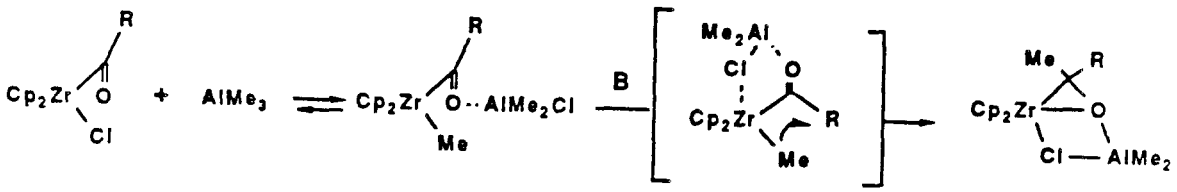

(5)

The approach for the mechanistic studies was first to establish that aluminum reagents promote the intramolecular reductive coupling of alkyl and acyl ligands by investigating the reactivity of the alkyl acyl complex **3** with alkylaluminum chlorides. Treatment of the zirconocene methyl acetyl complex **3** with dimethylaluminum chloride at 0°C in toluene yielded the ketone complex **2a** in 60% yield by ^{1}H NMR (eq 6). Higher yields of ketone products (> 85%, ^{1}H NMR, eq 7) were observed when diisobutylaluminum chloride was used as the aluminum reagent instead of dimethylaluminum chloride.

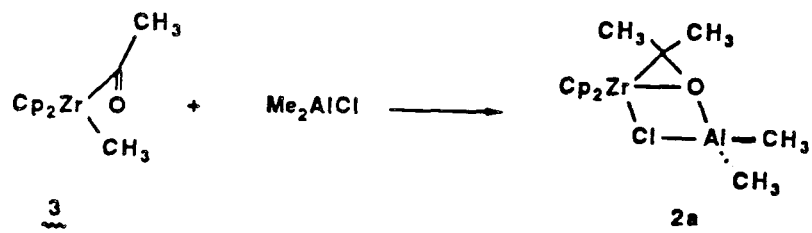

3 **2a**

(6)

Isotopic labeling was employed to probe the mechanisms of these reactions. The results from crossover experiments clearly demonstrate that the ketone complexes are

formed at one zirconium center. Treatment of the doubly-labeled **3-d$_6$-^{13}C** and **3** with diisobutylaluminum chloride yielded the ketone complexes **6-d$_6$-^{13}C** and **6** (eq 8). No crossover products were detected by ^{1}H and ^{13}C NMR of the ketone complexes or by G.C.-mass spectroscopy of the alcohols generated upon hydrolysis of the reaction mixture.

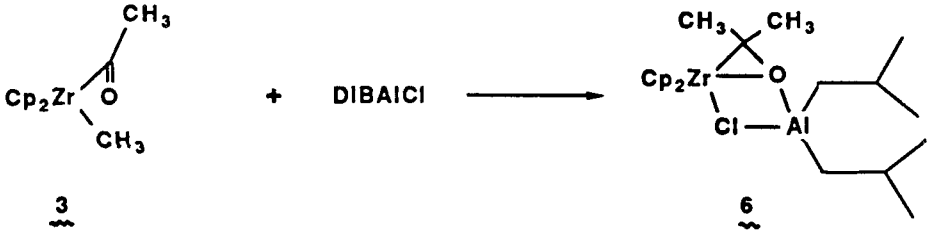

3 6 (7)

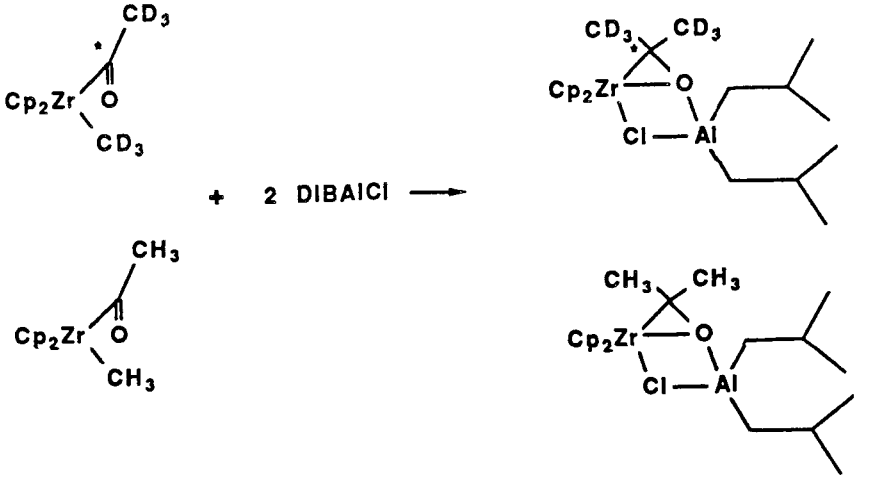

(8)

Deuterium labeling studies further establish the mechanism of formation of the ketone complexes **2** from the alkyl acyl complexes **3**. Treatment of the acyl **3-d$_6$** with $AlMe_2Cl$ in C_7D_8 at 0°C produced the ketone complexes **7** and **8** in a ratio of 4:1 and an overall yield of 60% (as determined by ^{1}H, ^{2}H , and ^{13}C NMR, eq 9).

The observed product ratio clearly establishes that the predominant pathway for this reaction (eq. 9) involves intramolecular migration of the methyl group to the acyl ligand and not transmetallation to **1** followed by direct alkylation by $Al(CH_3)_2CD_3$.

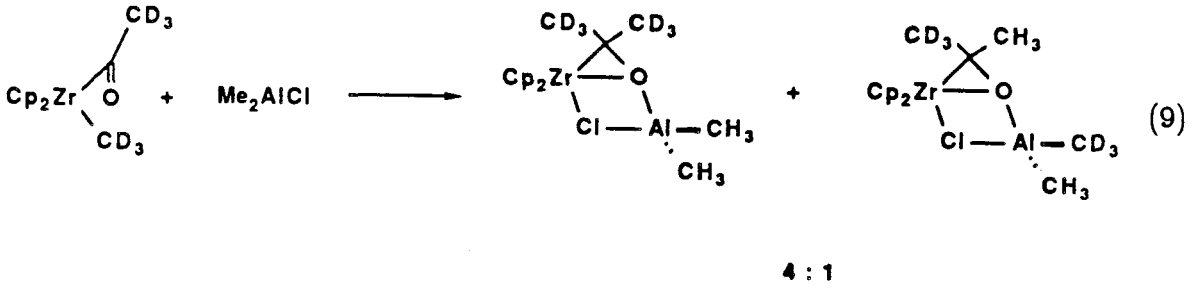

As seen in Scheme II, the acyl intermediates of the two previously discussed mechanisms are related by transmetallation between the chloro acyl $AlMe_3$ adduct **9** and the alkyl acyl $AlMe_2Cl$ adduct **10**. Treatment of **3** with $AlMe_2Cl$ should initially produce **10**. Transmetallation to **9** followed by alkylation by $Al(CH_3)_2CD_3$ would produce **7** and **8** in a statistical ratio of 1:2 due to scrambling of the labeled methyl groups at the aluminum center. The experimentally observed ratio of 4:1 (**7**:**8**) rules out mechanism A as the dominant pathway and implies that the major pathway involves the Lewis-acid assisted reductive coupling of the alkyl and acyl ligands.

SCHEME II

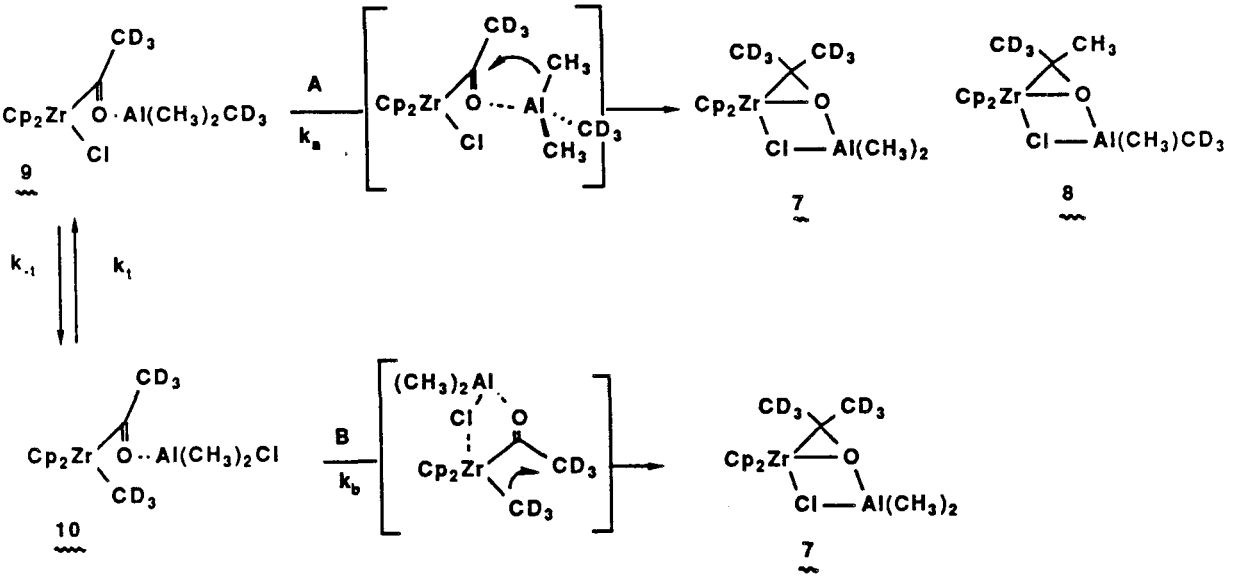

The observation of a small amount of the d_3-ketone complex **8** indicates that

transmetallation to form **9** is competitive with the rate of reductive coupling of the alkyl and acyl ligands of **10**. The d_3-ketone complex **8** could be formed from **9** in one of two ways: (1) direct alkylation of the acyl ligand of **9** by $Al(CH_3)_2CD_3$ or (2) transmetallation back to **10** (with scrambling of the labeled methyl groups) followed by reductive coupling of the alkyl and acyl ligands.

The mechanistic studies outlined above demonstrate for the first time that Lewis acids promote the intramolecular reductive coupling of alkyl and acyl ligands. These studies clearly establish the mechanism of ketone formation from the reaction of the alkyl acyl complexes **3** with dialkylaluminum chloride reagents. Whether a similar mechanism is followed for the formation of the ketone complexes from the chloro acyl complexes **1** and trialkylaluminum reagents cannot be established at this time since no direct information is available concerning the relative rates of direct alkylation of the acyl ligand (path A) vs. transmetallation from **9** to **10** (k_a vs. k_{-t}, Scheme II). If, for example, transmetallation from **9** to **10** were faster than alkylation (i.e., $k_{-t} > k_a$), then path B would be the major pathway for formation of the ketone complexes from the chloro acyl complexes **1** (as it is for the alkyl acyl complexes **3**), since we have shown that $k_b > k_t$. If however, the rate of direct alkylation (path A) were faster than transmetallation from **9** to **10** (i.e., $k_a > k_{-t}$), then path A would be the dominant mechanism.

Although we cannot yet rule out a direct alkylation pathway, we have been able to establish the viability of a stepwise mechanism for reductions of transition metal acyl complexes.[23] A significant result of these studies is the demonstration that dialkylaluminum reagents accelerate the rate of migration of an alkyl group to a cis acyl ligand. Erker has shown that in the absence of $AlMe_2Cl$, the acyl $Cp_2Zr(Ph)COPh$ isomerizes to the benzophenone complex $[Cp_2ZrOCPh_2]_2$ upon thermolysis of the acyl at 70°C for one hour (eq 10). In contrast, the acyl complex **3** rearranges rapidly at -30°C to give the ketone complexes **2** in the presence of AlR_2Cl (eq 11). Thus, the

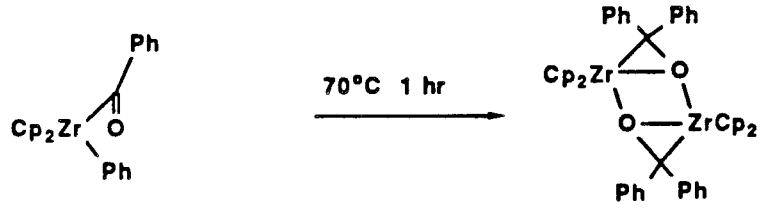

(10)

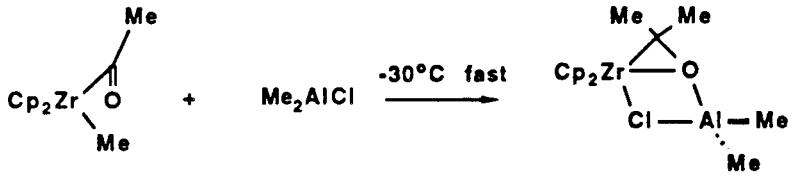

(11)

interaction of the aluminum reagent with the acyl complex **3** lowers the free energy of activation for the migration reaction by at least 6-7 kcal/mol.[24]

The role of dialkylaluminum chlorides in accelerating these migration reactions is not yet clear. Based on our experimental results and on theoretical calculations reported by Hoffmann et al.,[25] it is likely that the aluminum reagent performs a dual role in these reactions: (1) to break up the stable η^2-coordination of the acyl ligand, thereby facilitating rotation of the acyl ligand to a geometry favorable for the migration reaction, and (2) to lower the barrier for migration of the alkyl group through electronic effects on the acyl ligand as shown below.

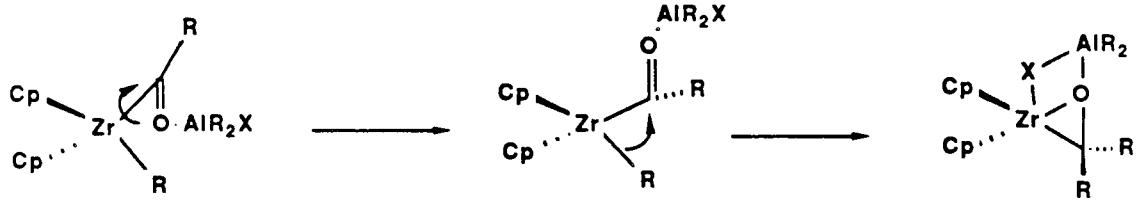

Implications. The role of the aluminum reagent in the isomerization of the

alkyl acyl **3** to the ketone complexes **2** has important implications for the role of Lewis-acidic sites in CO reduction. Lewis-acidic metal oxides are widely used to support heterogeneous CO reduction catalysts, but the role of the support continues to be a matter of considerable debate.[26] The effects of molecular Lewis acids on the reactivity of metal centers and coordinated ligands provide a good model for Lewis-acidic effects of metal oxide catalyst supports. Shriver[12] has demonstrated that molecular Lewis acids and aluminum oxides promote the migratory insertion of CO to give acyl complexes (eq 12). Our results imply that Lewis acids also promote further reduction of the acyl ligand. The implications of these studies are that localized Lewis-acidic effects may not only affect the reactivity of metal centers, but also the reactivity of carbon monoxide and ligands derived from carbon monoxide.

(12)

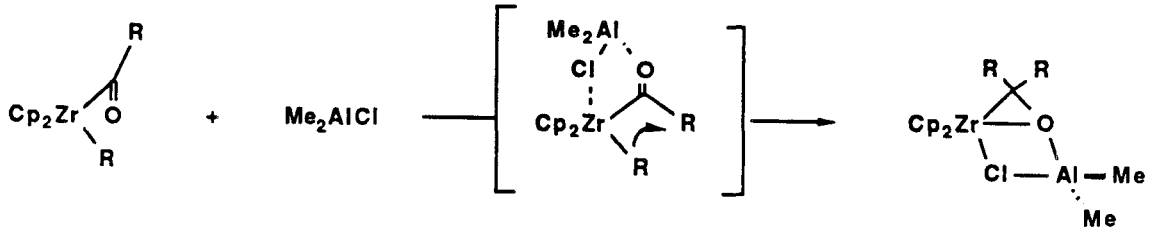

A related observation concerns the role of transition metal ketone complexes as models for intermediates formed on Fischer-Tropsch catalysts. Mazenec[7] has recently proposed that metal ketone complexes are important precursors to branched alcohols formed on metal oxide CO reduction catalysts. The present results provide a good

model for the formation of ketone complexes from acyl intermediates on Lewis-acidic metal oxide surfaces.

Reactivity of Ketone Complexes. The ketone complexes **2** are formally 1:1 adducts of a zirconium ketone complex and $AlMe_2Cl$. Lewis bases such as pyridine have been used successfully to remove coordinated $AlMe_2Cl$ from the Tebbe reagent $Cp_2Ti{=}CH_2{\cdot}AlMe_2Cl$,[3-5] and thus it was anticipated that strong Lewis bases would react with these ketone complexes to generate the pyridine·$AlMe_2Cl$ adduct and a monomeric ketone complex, which might then be trapped by added substrates such as olefins or acetylenes. In contrast to our expectations, treatment of the ketone complexes with pyridine produces the stable adduct **11** (eq 13). Coordinated $AlMe_2Cl$ could not be displaced even when pyridine was used as a solvent; the adduct **11** slowly crystallizes from pyridine solutions of **2a**.[27]

$$\underset{\underset{\sim}{2}}{Cp_2Zr(OCMe_2)\cdot AlMe_2Cl} + \text{pyr} \longrightarrow \underset{\underset{\sim}{11}}{Cp_2Zr(OCMe_2)\cdot AlMe_2Cl\cdot pyr} \quad (13)$$

The pyridine adduct **11** is unstable in benzene solution and slowly reacts to form the trinuclear Zr_2Al μ-ketone complex **12** (eq 14). Thermolysis of **11** for 45 min at 68°C yielded **12** in 62% yield. The trinuclear ketone complex **12** was characterized by ^1H and ^{13}C NMR as well as microanalysis. The ^1H NMR spectrum of **12**, consisting of 3 resonances at 5.71 (20H), 1.70 (12H), and -0.28 (6H) ppm, implies that this molecule has a symmetric structure similar to the trinuclear Zr_2Al bridging ketene complexes discussed in Chapter 2. This compound is considerably more stable than

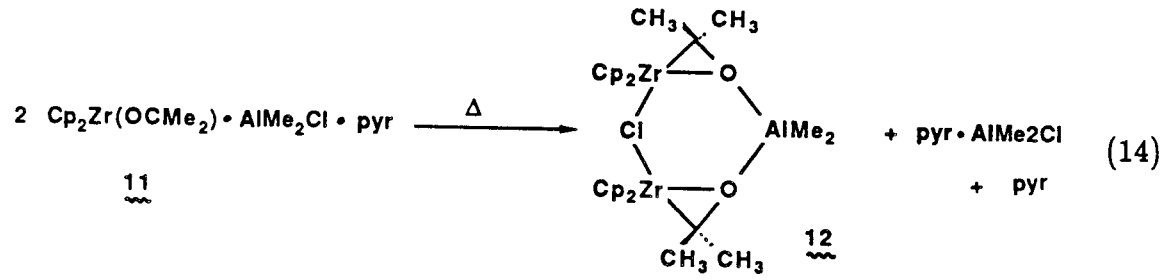

(14)

the 1:1 ZrAl ketone complexes **2**; thermolysis of **12** for 8 hours at 85°C did not result in significant decomposition.

Although a coordinatively unsaturated zirconium ketone monomer could not be generated by treatment of the ketone complexes with pyridine, the ketone complexes **2** are sufficiently reactive with unsaturated substrates such as olefins, alkynes, and ketones that removal of coordinated $AlMe_2Cl$ is unneccessary. Ethylene inserts readily (< 5 min, 25°C) into the Zr-C bond of the ketone complex to give the oxymetallacyclopentane complexes **13**, which were isolated in 60-70% yields and fully characterized by ^1H and ^{13}C NMR, microanalysis, and hydrolysis to the tertiary alcohols. ^1H NMR and microanalytical data indicate that $AlMe_2Cl$ remains coordinated to the oxymetallacycle ligand, presumably via reciprocal Zr-O-Al and Al-Cl-Zr bridging interactions.[28] Attempts to obtain the substituted oxymetallacyclopentanes by treatment of the ketone complexes with higher olefins were unsuccessful. Solutions of **2a** in C_7D_8 did not react with propene, ethyl vinyl ether, or diethyl fumarate after days at room temperature.

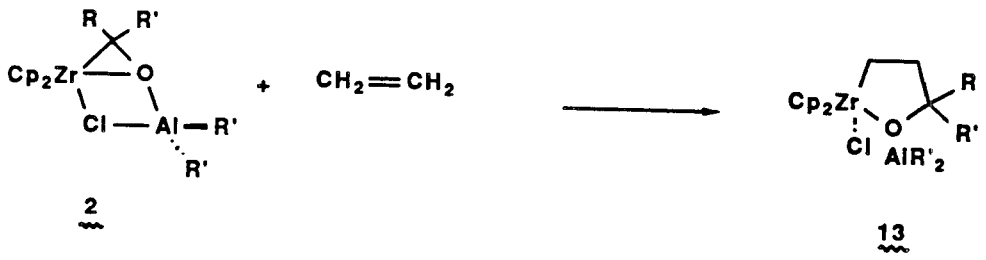

(15)

Alkynes react readily with the ketone complexes (< 5 min, 25°C) to yield the oxymetallacyclopentenes **14** (eq 16, Table 2). These complexes were isolated in yields of 50-70% and were characterized by ^{1}H, ^{13}C NMR, microanalysis, and by hydrolysis to the tertiary allyl alcohols. Terminal alkynes react regioselectively to give oxymetallacyclopentenes with the substituent in the α position relative to the metal center. Internal alkynes react more slowly and with limited regioselectivity. For example, treatment of **2a** with methylphenylacetylene yielded a 1.7:1 ratio of the regioisomeric oxymetallacyclopentenes **14e,f** after 2 hr at room temperature (Table 2).

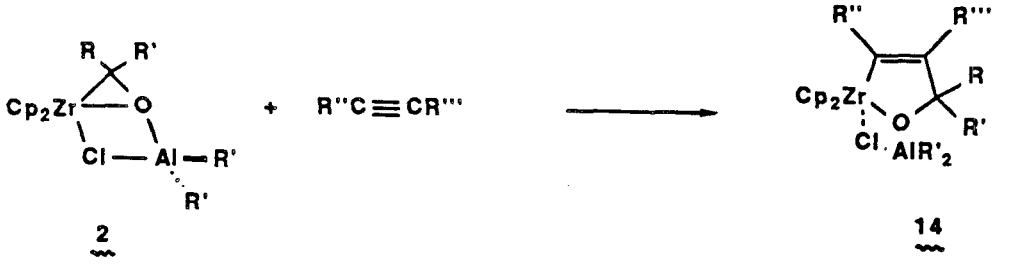

(16)

Table 2.

Complex	R	R′	Alkyne	Product	R″	R‴	Yield %
2a	Me	Me	HCCH	14a	H	H	52
2b	Me	Et	PhCCH	14b	Ph	H	71
2a	Me	Me	MeCCMe	14c	Me	Me	95[a]
2a	Me	Me	PhCCPh	14d	Ph	Ph	95[a]
2a	Me	Me	PhCCMe	14e,f	Ph(Me)	Me(Ph)	95[a,b]

[a] ^{1}H NMR Yield. [b] Ratio 14e:14f, 1.7:1

Insertion of aryl and α,β-unsaturated organic ketones into the ketone ligand generates the diolate complexes **15**. Treatment of **2a** with acetophenone affords the diolate **15a** (eq 17). This compound was not isolated but was characterized by ^{1}H, ^{13}C NMR and by hydrolysis to the 1,2-diol **16**. The 1,2-diol **16** could be prepared in one pot from the acyl **1a** (R=Me) in 50% isolated yield.

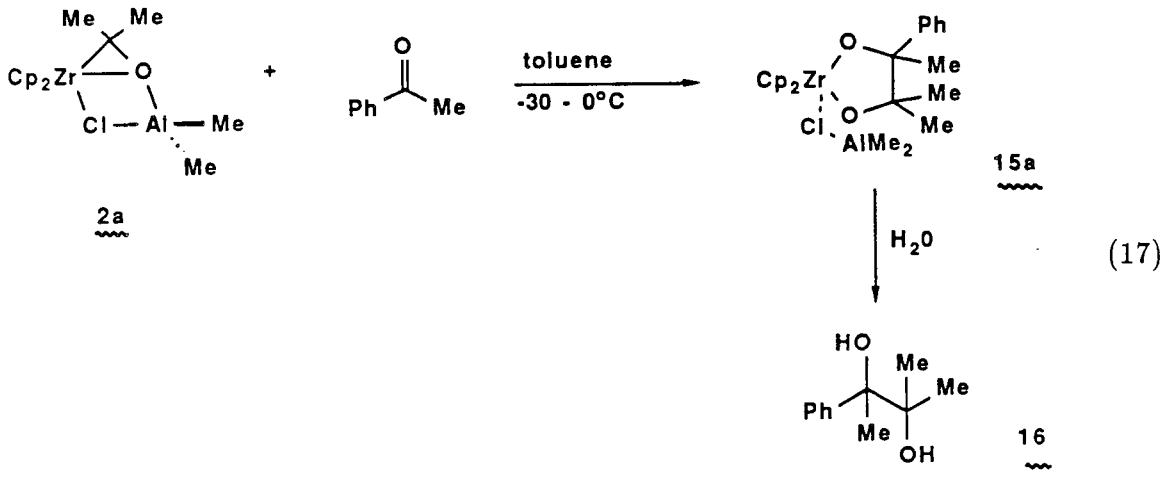

(17)

Treatment of **2a** with methyl vinyl ketone or 3-pentene-2-one yielded the vinyl substituted diolates **15b** and **15c**, respectively (eq 18). These compounds are unstable above 5°C and were not isolated but were characterized by spectroscopic comparison with the diolate **15a**. Aliphatic ketones and esters did not react with the ketone complexes **2** at 25°C after 24 hrs. Aldehydes react readily at room temperature to give what appear to be similar diolate products by ^{1}H NMR, but these products have not yet been fully characterized.[29]

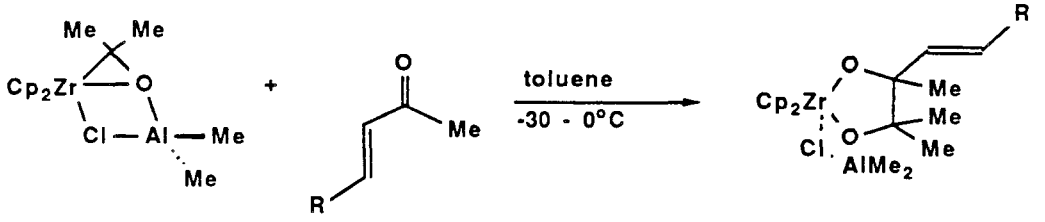

(18)

Summary and Implications. The ketone and aldehyde complexes described herein should find important applications as reagents in organic synthesis. As outlined in Scheme III, the reactivity of these complexes provides the basis for a synthetic strategy to convert olefins to tertiary allyl alcohols and 1,2-diols.

Scheme III

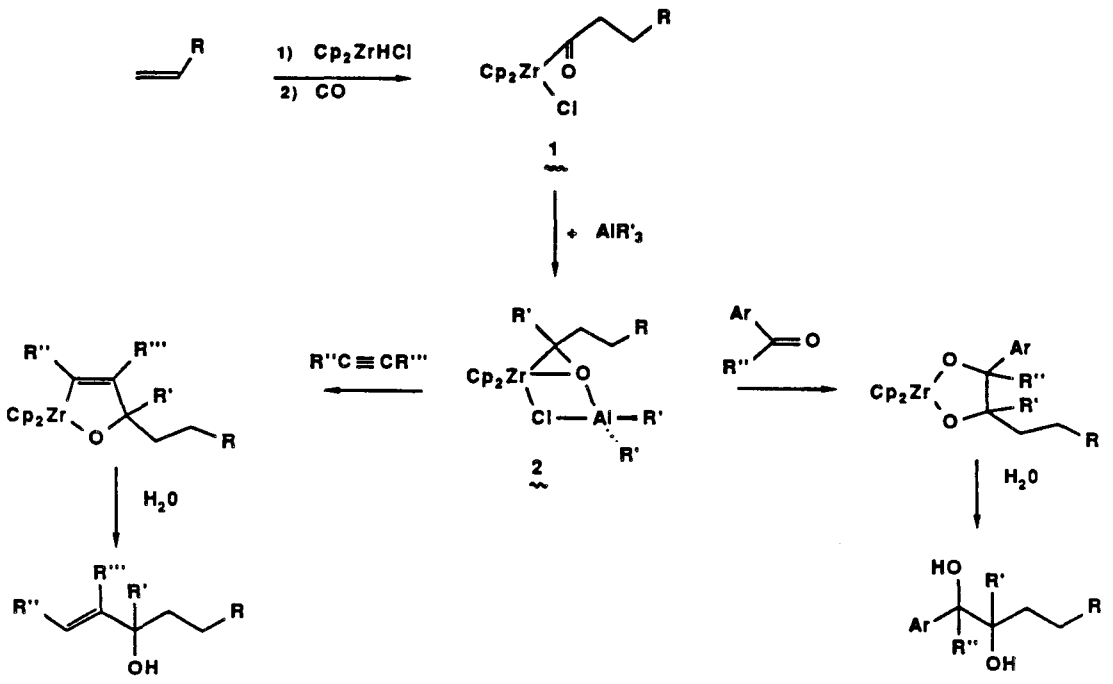

Hydrozirconation of olefins, followed by carbonylation produces zirconium acyl complexes in high yields ($\geq$ 90%).[17,30] Reductive alkylation of the acyl complexes by alkylaluminum reagents yields the ketone complexes **2**, which can be isolated, or more conveniently, generated in situ and treated with the appropriate unsaturated substrate. Treatment of the ketone complexes with alkynes generates oxymetallacyclopentenes, which can be hydrolyzed to tertiary allyl alcohols. Treatment of the ketone complexes with ketones affords diolates, which can be hydrolyzed to 1,2-diols. These reactions can be conveniently run in one pot;[29] thus, olefins can be converted to allyl alcohols or 1,2-diols in a one step procedure via a series of metal mediated carbon-carbon forming reactions.

A significant feature of the above studies is the observation that the ketone complexes **2** couple with organic ketones to give diolates. As mentioned in the Intro-

duction section, later transition metal ketone complexes generally couple with organic carbonyl substrates in a "head-to-tail" fashion (path B, Scheme I),[13] a transformation of limited synthetic utility since no carbon-carbon bond is formed. The fact that diolates are produced in the present case demonstrates that under the appropriate conditions, zirconium reagents can promote the "head-to-head" coupling of carbonyl substrates.

At the present time, the features of the metal center and/or ligand environment that govern the regiochemistry of the reductive coupling of carbonyl substrates is unclear.[32] For the ketone complexes **2**, it may be that the coordinated $AlMe_2Cl$ plays an important role in favoring the formation of the zirconium diolates. The role of the aluminum reagent in mediating the reactivity of the ketone ligand is not well understood. Nevertheless, it is clear that the 1:1 ZrAl ketone complexes **2** are more reactive than the dimeric zirconium ketone complexes reported by Erker.[8] For example, reaction of the dimeric benzophenone complex **17** with acetylenes requires 2 hours at 90°C, whereas the ketone complexes **2** react rapidly with acetylenes at 0°C (eqs 19,20). Thus, the aluminum reagent not only prevents dimerization of the ketone complexes, but it may also affect the inherent reactivity of the ketone ligand.

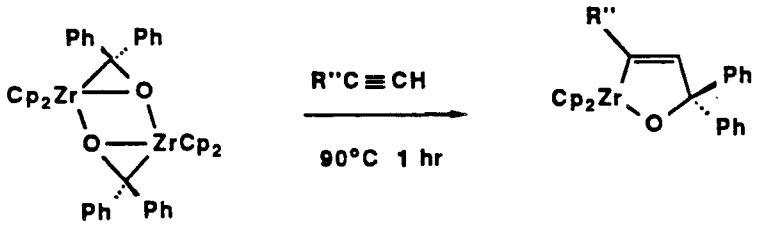

(19)

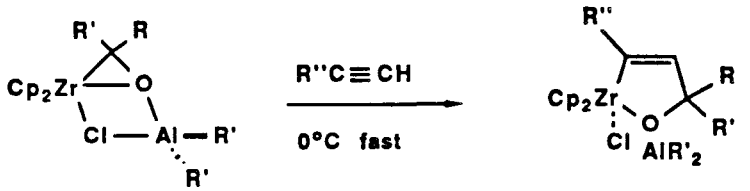

(20)

Trinuclear Zr_2Al Ketone Complexes. During the course of the mechanistic studies on the reactivity of the alkyl acyl complexes **3** with dialkylaluminum chlorides, unusual products were observed when the acyl complexes were treated with less than one molar equivalent of the aluminum reagent. For example, treatment of the methyl acyl complex **3** with 0.5 equivalent of diisobutylaluminum chloride resulted in the formation of the trinuclear ketone complex **18** (eq 21). The ^1H NMR spectrum of **18** suggests a structure similar to that of **12** and the trinuclear ketene complexes discussed in Chapter 2. As with **12**, the ketone complex **18** is thermally stable; thermolysis for 10 hours at 80°C did not result in significant decomposition of the complex.

(21)

Trinuclear ketone complexes with bridging methyl rather than bridging chloride ligands can also be prepared by treating the acyl complexes with 0.5 equiv of $AlMe_3$. Treatment of the acyl **3** with 0.5 equiv. of $AlMe_3$ produced the trinuclear bridging ketone complex **19** (eq 22). A significant amount of Cp_2ZrMe_2 is observed unless the reactions are run under an atmosphere of carbon monoxide. The ^1H NMR (C_6D_6) of the sparingly soluble complex **19** displays resonances at 5.56 (s, 20H), 1.67 (s, 12H), -0.37 (s, 6H), and -0.50 (s, 3H) ppm, implying a structure similar to that of the trinuclear bridging ketene complex **3** discussed in Chapter 2. The low solubility of this compound has precluded a complete characterization; nevertheless, the spectroscopic and analytical data are consistent with the structure given below.

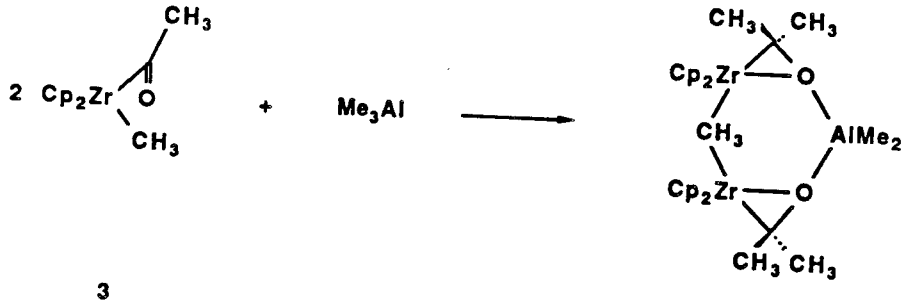

(22)

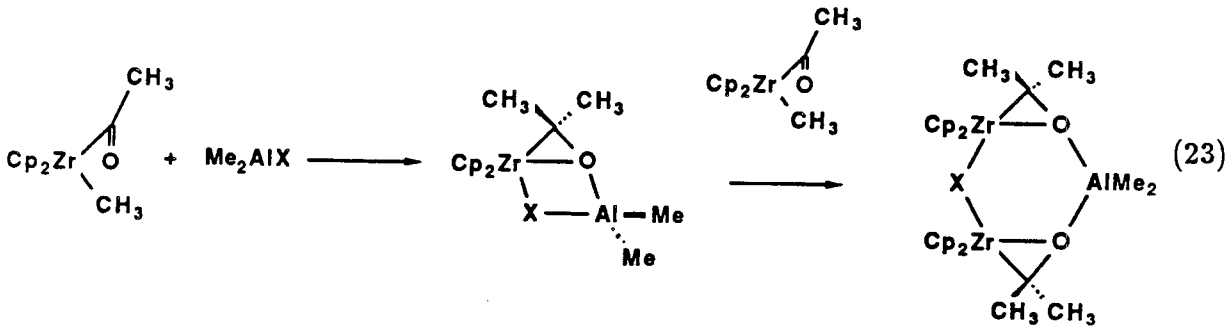

(23)

The simplest mechanism for formation of the trinuclear ketone complexes **18** and **19** is a stepwise pathway involving initial formation of the ketone complex $Cp_2Zr(OCMe_2)\cdot AlR_2X$, followed by reaction with excess **3** (eq 23). This mechanism was investigated by studying the reactions of the ketone complexes **2** with the methyl acyl complexes **3**. Treatment of a C_6D_6 solution of the ketone complex **2a** with the acyl complex **3** yielded the trinuclear ketone complex **12** quantitatively (eq 24). This result establishes that the ZrAl ketone complexes **2** are intermediates in the formation of the trinuclear Zr_2Al ketone complexes, since we have shown that treatment of the methyl acyl complex **3** with AlR_2Cl gives **2**. Treatment of the ketone complex **2c** ($R=CH_2CH_2CMe_3$) with the methyl acyl **3** afforded the trinuclear ketone complex **20** (eq 25). None of the ketone complex **12** was observed, which rules out dissociative mechanisms and implies that the trinuclear complexes are formed by a stepwise pathway involving initial formation of the ketone complex $Cp_2Zr(OCMe_2)\cdot AlR_2X$, followed by a simple bimolecular reaction with the acyl complex **3** (eq 23).

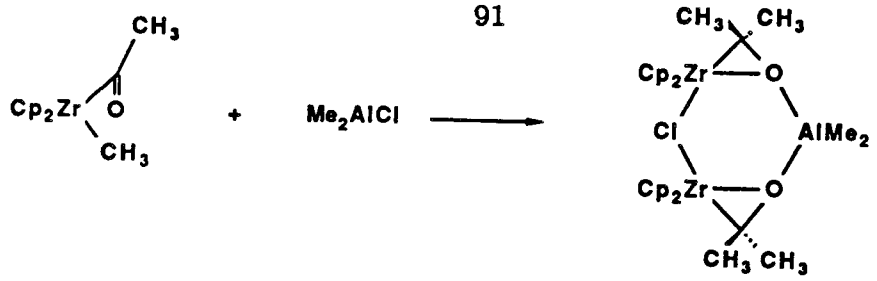

(24)

3 12

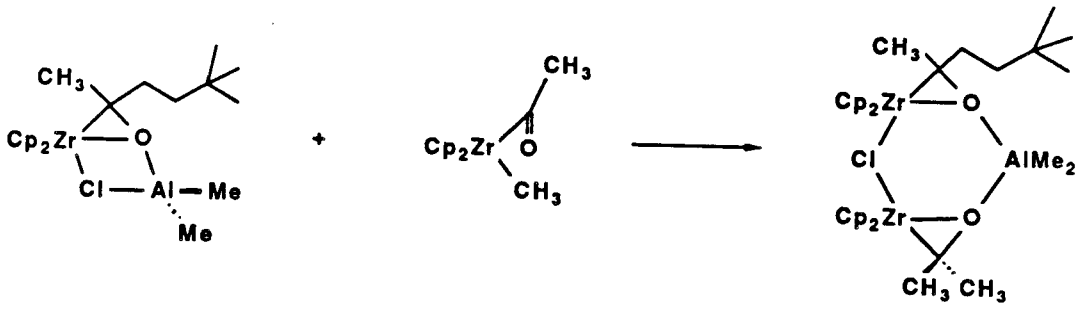

(25)

2 3 20

One of the implications of these studies is that the ketone complexes **2** can function as Lewis acids to induce the reductive coupling of zirconium alkyl and acyl ligands. This result suggests that other Lewis acidic metal centers might also promote the formation of zirconium ketone complexes in their coordination sphere. This strategy could prove useful for the preparation of heterobimetallic bridging ketone complexes.

CONCLUSIONS

We have demonstrated that zirconium acyl complexes react with alkylaluminum reagents to give zirconium ketone complexes. The reactivity of zirconium acyl complexes with aluminum reagents is sensitive to the nature of the acyl complex and the aluminum reagent. The reaction of zirconium chloro acyl complexes with trialkylaluminum reagents or zirconium alkyl acyl complexes with dialkylaluminum chloride reagents produces zirconium ketone complexes. In contrast, Schwartz has shown[17] that treatment of zirconium chloro acyl complexes with aluminum trichlorides results in transmetallation of the acyl to the aluminum center. These results point out the dramatic effects that the zirconium and aluminum ligands have on transmetallation equilibria between these two metal centers.

The complexity of bimetallic zirconium-aluminum systems render mechanistic studies difficult.[1a,33] A number of competing pathways are generally involved, and their relative rates are sensitive to the types of ligands on the zirconium and aluminum centers. Thus, mechanistic descriptions of these systems must take into account a number of possible reaction pathways. For the systems described in this chapter, we have shown conclusively that treatment of zirconium alkyl acyl complexes with alkylaluminum chlorides produces zirconium ketone complexes via a mechanism involving reductive coupling of zirconium alkyl and acyl ligands. Whether the same path is followed for zirconium chloro acyl complexes and trialkylaluminum reagents could not be established unequivocally since the relative rates of reductive alkylation of zirconium acyl complexes vs. transmetallation (k_a vs. k_{-t}, Scheme II) are unknown. Nevertheless, since we have shown that transmetallation occurs in this system, both direct alkylation (path A, Scheme II) and transmetallation-reductive coupling (path B) have to be considered in a generalized mechanistic scheme for the formation of ketone and aldehyde complexes. The course for a given reaction will depend on the relative rates of direct alkylation, transmetallation, and reductive coupling, and

these rates will depend on the nature of the zirconium acyl ligand and the aluminum reagent. For example, it is possible that formation of ketone complexes from zirconium chloro acyl complexes and aluminum alkyls involves transmetallation followed by reductive coupling (Path B), whereas the path for formation of the aldehyde complexes involves direct reduction of the acyl ligand by the aluminum hydride (Path A). Further mechanistic investigations of this system are certainly warranted.

The reductive coupling of zirconium alkyl and acyl ligands induced by alkylaluminum reagents has important implications for the reactivity of acyl intermediates and the role of Lewis acids in CO reduction. This work provides an effective model for the mechanism of formation of ketone intermediates on metal oxide CO reduction catalysts.

Coordination of an organic ketone or aldehyde to an early transition metal center dramatically affects the reactivity of the organic substrate and provides a means of coupling ketone ligands with electrophilic substrates such as olefins, alkynes, aldehydes or ketones. The formation of zirconium diolates from the reaction of the ketone complexes **2** with organic ketones suggests that bimetallic zirconium-aluminum complexes might be developed into useful reagents for the cross-coupling of organic ketones and aldehydes.

EXPERIMENTAL SECTION

General Procedures. The general experimental techniques and procedures were described in Chapter 2. The acyl complexes **1a-1e**[17], **3** and **3-d_6-^{13}C**[33] were prepared by literature procedures. $AlMe_3$ was used neat (Alfa), or as 2M solutions in toluene (Aldrich). Et_3Al, $AlMe_2Cl$, diisobutylaluminum chloride, and diisobutylaluminum hydride were obtained neat from Texas Alkyls and were used without further purification. Mesitylene was dried over calcium hydride, vacuum transferred, and stored in the drybox. NMR solvents were purified as described in Chapter 2. All NMR chemical shifts are reported in ppm relative to TMS and were recorded at 25°C unless otherwise indicated. Mass Spectra were obtained at the UC Riverside Mass Spectra facility.

$Cp_2Zr(C,O\text{-}\eta^2\text{-}OCCMe_2)\cdot AlMe_2Cl$ 2a. In a typical procedure, 0.563 gm of **1a** (1.88 mmol) was suspended in 10 ml of 1/1 benzene/hexane and cooled to 0°C in an ice bath. This suspension was treated with 1 ml of a 2M solution of $AlMe_3$ to give a yellow solution. Solvent was removed in vacuo at 0°C and the pale-yellow residue washed with two 5 ml portions of pentane to give **2a** as a pale yellow powder (0.465 gm, 1.31 mmol, 70%). ^{1}H NMR(C_6D_6): δ 5.57 (s, 10H), 1.49 (s, 6H), -0.28 (s, 6H). ^{13}C NMR(C_6D_6): δ 109.9, 80.9, 33.5, -6.32. Anal. calcd. for $C_{15}H_{22}OClZrAl$: C, 48.4; H, 6.0; Cl, 9.5. Found: C, 48.47; H, 5.96; Cl, 9.61.

$Cp_2Zr(C,O\text{-}\eta^2\text{-}OC(Me)CH_2CH_3)\cdot AlMe_2Cl$ 2b. The acyl **1b** (0.690 gm, 2.204 mmol) was treated with $AlMe_3$, using the procedure described for **2a** to give **2b** as a pale yellow powder (0.728 gm, 1.89 mmol, 86%) ^{1}H NMR(C_6D_6): δ 5.61 (s, 5H), 5.59 (s, 5H), 1.92 (q, J=6.35Hz, 1H), 1.43 (s, 3H), 0.884 (t, J=7.37Hz, 3H), -0.25 (s, 6H). ^{13}C NMR(C_6D_6): δ 110.0, 109.9, 86.6, 38.9, 29.9, 12.4.

$Cp_2Zr(C,O\text{-}\eta^2\text{-}OC(Me)CH_2CH_2CMe_3)\cdot AlMe_2Cl$ 2c. The acyl **1c** (0.500 gm, 1.36mmol) was treated with $AlMe_3$, using the procedure described for **2a** to give

2c as a yellow powder (0.450 gm, 1.02 mmol, 75%). ^{1}H NMR(C_6D_6): δ 5.68 (s, 5H), 5.61 (s, 5H), 1.97 (m, 2H), 1.47 (s, 3H), 1.35 (m, 2H), 0.94 (s, 9H), -0.22 (s, 3H), -0.29 (s, 3H). ^{13}C NMR(C_6D_6): δ 110.0, 109.8, 85.5, 41.4, 40.8, 30.9, 30.5, 29.7, 6.13. Anal. calcd. for $C_{20}H_{32}OClZrAl$: C, 54.31; H, 7.30. Found: C, 54.25; H, 7.26.

$Cp_2Zr(C,O\text{-}\eta^2\text{-}OC(Et)CH_2CH_2CMe_3)\cdot AlEt_2Cl$ 2d. Neat $AlEt_3$ (0.395 ml, 2.8 mmol) was dissolved in benzene and cannulated dropwise into a precooled (0°C) benzene solution of the acyl **1c** (1.043 gm, 2.82 mmol). Solvent was removed in vacuo to afford a waxy yellow solid, which was washed with three 5 ml portions of pentane to give **2d** as a light yellow powder (0.880 gm, 64%). ^{1}H NMR(C_6D_6): δ 5.68 (s, 5H), 5.64 (s, 5H), 1.94 (q, J=7.32Hz, 2H), 1.68 (t, J=7.32Hz, 2H), 1.39 (m, 3H), 0.96 (s, 9H), 0.35 (m, 4H). Anal. calcd. for $C_{23}H_{38}OClZrAl$: C, 57.05; H, 7.91; Cl, 7.32. Found: C, 56.98; H, 7.89; Cl, 7.41.

$Cp_2Zr(C,O\text{-}\eta^2\text{-}OC(Me)CH(CH_2)_5)\cdot AlMe_2Cl$ 2e. The acyl **1e** was treated with $AlMe_3$, using the procedure described for **2a** to give **2e** as a light yellow powder (0.734 gm, 1.668 mmol, 91%). ^{1}H NMR(C_6D_6): δ 5.63 (s, 5H), 5.62 (s, 5H), 1.69 (m, 5H), 1.47 (m, 1H), 1.36 (s, 3H), 1.20 (m, 5H), -0.29 (s, 3H), -0.38 (s, 3H).

$Cp_2Zr(C,O\text{-}\eta^2\text{-}OC(H)CH_2CH_3)\cdot Al(i\text{Bu})_2Cl$ 4a. The acyl **1b** (0.766 gm, 2.44 mmol) was suspended in 10 ml of 1/1 benzene/hexane and cooled to 0°C. Neat diisobutylaluminum hydride (0.352 gm, 2.47 mmol) was dissolved in hexane and cannulated into the acyl suspension to give a yellow solution. This solution was stirred for 15 min and evacuated to give **4a** as a yellow oil, which turned brown upon standing. ^{1}H NMR(C_6D_6): δ 5.59 (s, 10H), 3.15 (dd, J=8.1Hz, J=8.3Hz, 1H), 2.15 (m, 2H), 1.80 (m, 1H), 1.59 (m, 1H), 1.20 (d, J=7.32Hz, 12H), 1.04 (t, J=7.32Hz, 3H), 0.36 (d, J=7.32Hz, 4H). ^{13}C NMR(C_6D_6): δ 109.2, 109.1, 82.8, 32.4, 28.95, 28.90, 26.8, 15.9.

$Cp_2Zr(C,O\text{-}\eta^2\text{-}OC(H)CH_2CH_2CMe_3)\cdot Al(i\text{-}Bu)_2Cl$ 4b. Diisobutylaluminum hydride was dissolved in benzene and added to a precooled (0°C) benzene/hexane

solution of the acyl **1c** (0.600 gm, 1.62 mmol). The resulting pale-yellow solution was stirred for 15 min and evacuated to yield **4b** as a yellow oil. ^{1}H NMR(C_6D_6): δ 5.65 (s, 5H), 5.62 (s, 5H), 3.17 (m, 1H), 1.20 (d, 12H), 0.97 (s, 9H), 0.39 (s, 2H), 0.32 (s, 2H).

$[Cp_2Zr(C,O\text{-}\eta^2\text{-}OC(H)CH_2CH_2CMe_3)]_n$ 5. 2.9 ml of a 1M THF solution of $LiBEt_3H$ was added to a precooled (0°C) toluene solution of the acyl **1c** (0.954 gm 2.57 mmol). The resulting yellow solution was allowed to warm to room temperature and filtered through a pad of Celite on a fine frit. Removal of solvent in vacuo followed by washing with pentane afforded **5** as a yellow powder (0.170 gm, 0.506 mmol, 20%). ^{1}H NMR(C_6D_6): δ 5.83 (s, 5H), 5.74 (s, 5H), 2.49 (m, 1H), 1.88 (m, 1H), 1.74 (m, 1H), 1.43 (m, 1H), 1.32 (m, 1H), 1.08 (s, 9H). ^{13}C NMR(C_6D_6): δ 108.3 (d, J=150Hz, Cp), 108.2 (d, J=150Hz, Cp), 80.4 (d, J=140.6Hz, CHO), 46.9 (t, J=121.8, CH_2), 34.1 (t, J=123.9Hz, CH_2), 31.1 (s, CMe_3), 30.5 (q, J=123.2Hz, CH_3).

Formation of the Ketone Complex 6 from the Acyl 3. The acyl **3** (28 mg, 0.10 mmol) was weighed into an NMR tube modified with a 14/20 joint and dissolved in 0.500 ml of toluene-d_8 containing 5μL of mesitylene as an internal standard. Diisobutylaluminum chloride (0.02 ml) and 3 atm of CO were condensed into the NMR tube at 77K and the tube sealed with a torch. The solution was allowed to thaw at -50°C and the NMR spectra were recorded at -10°C. Integration of the cyclopentadienyl and mesitylene resonances in the ^{1}H NMR spectrum indicated an 87% yield of the ketone complex **6**. ^{1}H NMR(C_7D_8): δ 5.57 (s, 10H), 1.50 (s, 6H), 1.35 (m, 2H), 1.21 (d, J=6.6Hz, 12H), 0.33 (d, J=7.08Hz, 4H). ^{13}C NMR(C_7D_8): δ 109.3, 80.3, 33.5, 28.5, 26.5, 21.2.

Crossover Experiment. The acyl **3** (8 mg, 0.029 mmol) and the doubly-labeled acyl **3-d_6-^{13}C** (9 mg, 0.031 mmol) were weighed into an NMR tube modified with a 14/20 joint. A side arm addition tube was charged with 5 μL of mesitylene, 0.14 ml (0.072 mmol) of neat diisobutylaluminum chloride and 0.500 ml of toluene-d_8 and

attached to the NMR tube. The contents of the side arm were added to the sample at 77K and the NMR tube sealed under 3 atm of CO. The sample was thawed at -50°C and placed in a precooled -30°C NMR probe. **6,6-d_6-^{13}C** ^{1}H NMR (C_7D_8, -30°C): δ 5.57 (s, 20H), 1.51 (s, 6H), 1.26 (d, J=6.5Hz, 24H), 0.38 (d, J=6.5Hz, 8H). ^{13}C NMR (C_7D_8 , -30°C): δ 79.7. The NMR tube was then cracked open and the sample hydrolyzed with 0.12 ml of water to afford the labeled and unlabeled isopropanols: ^{1}H NMR(C_7D_8): δ 3.58 (m, J=6.1Hz, 1H), 0.94 (d, J=6.1Hz, 6H). ^{13}C NMR(C_7D_8): δ 63.3 (d, J=140.1Hz). G.C.-mass spectroscopy of the hydrolyzed samples yielded peaks at 49 ($CD_3{}^{13}CHOH^+$) and at 45 ($CH_3{}^{12}CHOH^+$), but none at 48 ($CD_3{}^{12}CHOH^+$) or at 46 ($CH_3{}^{13}CHOH^+$).

Labeling Studies. An NMR tube, modified with a 14/20 joint, was charged with 13 mg (0.045 mmol) of the doubly-labeled acyl **3-d_6-^{13}C**, fitted with a side-arm addition tube and a gas bulb adapter. To the side-arm addition tube were added 0.17 ml of a 2.6M C_6D_6 solution of $AlMe_2Cl$, 0.500 ml of C_7D_8, and 5 μL of mesitylene as an internal standard. The contents of the side arm were added to the acyl at 77K, the NMR tube sealed with a torch under 3 atm of CO and the NMR spectra recorded at 0°C. ^{1}H NMR(C_7D_8): δ 5.51 (s, 20H), 1.48 (d, J=5.37Hz, 0.63H), -0.21 (s, 11H). ^{13}C NMR(C_7D_8): δ 79.7. ^{2}D NMR (C_7H_8): δ 1.43.

$Cp_2Zr(C,O\text{-}\eta^2\text{-}OCMe_2)\cdot AlMe_2Cl\cdot pyr$ 11. The ketone complex **2a** (0.700 gm, 1.88 mmol) was dissolved in benzene and treated with excess pyridine via syringe. The resulting pale-yellow solution was filtered through a pad of Celite on a fine frit and evacuated to give **11** as a yellow powder (0.556 gm, 1.24 mmol, 66%). A sample suitable for analysis was obtained by dissolving **2a** in a minimum of pyridine, layering with Et_2O and slowly cooling to -50°C. ^{1}H NMR(C_6D_6): δ 8.40 (m, 2H), 6.80 (m, 1H), 6.5 (m, 2H), 5.76 (s, 10H), 1.73 (s, 6H), -0.12 (s, 6H). ^{13}C NMR(C_6D_6): δ 148.2, 138.9, 124.3, 109.8, 78.1, 35.3. Anal. calcd. for $C_{20}H_{27}OClZrAl$: C, 53.25; H, 6.03; N, 3.11; Cl, 7.86. Found: C, 53.25; H, 6.06; N, 3.21; Cl, 7.93.

$[Cp_2Zr(C,O\text{-}\eta^2\text{-}OCMe_2)]_2(\mu\text{-}AlMe_2)(\mu\text{-}Cl)$ 12. Method A: The pyridine adduct **11** (0.178 gm, 0.395 mmol) was dissolved in 6 ml of toluene and placed in an oil bath kept at 68°C for 45 min. The bath was turned off and the solution allowed to cool slowly to room temperature and then placed in a -20°C freezer to yield **12** as colorless needles (0.080 gm, 0.234 mmol, 62%). ^{1}H NMR(C_6D_6): δ 5.71 (s, 20H), 1.70 (s, 12H), -0.28 (s, 6H). Anal. calcd. for $C_{28}H_{38}O_2ClZr_2Al$: C, 51.62; H, 5.88. Found: C, 51.50; H, 6.05.

$[Cp_2ZrOC(Me)(CH_2CH_3)CH_2CH_2]\cdot AlMe_2Cl$ 13a. The ketone complex **2b** (0.297 gm, 0.771 mmol) was dissolved in 6 ml of toluene and placed under an atm of ethylene that had been passed through a -78°C trap. The resulting yellow solution was allowed to stir for 40 min and evacuated to dryness. This residue was washed with three 5 ml portions of pentane to yield **12a** as a pale-yellow powder (0.200 gm, 0.484 mmol, 63%). ^{1}H NMR(C_6D_6): δ 5.67 (s, 5H), 5.66 (s, 5H), 2.16 (m, 1H), 2.06 (m, 1H), 1.86 (m, 2H), 1.14 (s, 3H), 1.12 (m, 2H), -0.26 (s, 6H). ^{13}C NMR(C_6D_6): δ 112.0, 11.9, 89.3, 41.9, 40.9, 36.3, 27.1. Hydrolysis of **12a** with 5% HCl yielded 3-methyl-pentane-3-ol in 45% yield by cap G.C.

$[Cp_2ZrOC(Me)(CH_2CH_2CMe_3)CH_2CH_2]\cdot AlMe_2Cl$ 13b. The acyl complex **1c** (0.500 gm, 1.36 mmol) was dissolved in 15 ml of benzene, treated with 1 ml of a 2M toluene solution of $AlMe_3$ and placed under an atmosphere of ethylene, which had been passed through a -78°C trap. The resulting yellow solution was stirred for 4 hours and evacuated to give a glassy yellow oil. This material was dissolved in pentane and the pentane removed in vacuo at -50°C to give **12b** as an off-white powder (0.475 gm, 1.01 mmol, 74%). ^{1}H NMR(C_6D_6): δ 5.73 (s, 5H), 5.70 (s, 5H), 1.93 (m, 2H), 1.74 (m, 2H), 1.22 (t, 2H), 1.20 (s, 3H), 1.00 (m, 2H), 0.90 (s, 9H), -0.23 (s, 3H), -0.25 (s, 3H). ^{13}C NMR(C_6D_6): δ 112.5, 89.0, 42.5, 41.0, 39.5, 31.0, 30.0, 27.5. Anal. calcd. for $C_{22}H_{36}OClAlZr$: C, 56.20; H, 7.72; Cl, 7.54. Found: C, 56.21; H, 7.32; Cl, 8.47.

$[Cp_2ZrOC(Me)_2CHCH]\cdot AlMe_2Cl$ 14a. The ketone complex **2a** (0.423 gm, 1.14 mmol) was dissolved in 10 ml of hexane and 2 ml of toluene and placed under an atmosphere of acetylene that had been passed through a -78°C trap. The resulting suspension was stirred for 30 min and evacuated to give an off-white powder. This material was redissolved in a minimum of toluene, layered with Et_2O and cooled slowly to -50°C to afford **13a** as colorless microcrystals (0.230 gm, 0.578 mmol, 50%). ^1H NMR(C_6D_6): δ 6.35 (d, J=10.9Hz, 1H), 5.71 (d, J=10.9Hz, 1H), 5.68 (s, 10H), 1.24 (s, 6H), -0.24 (s, 6H). ^{13}C NMR(C_6D_6): δ 175.5, 140.4, 112.1, 90.8, 29.3, -4.13. Anal. calcd. for $C_{17}H_{24}OClAlZr$: C, 51.30; H, 6.08; Cl, 8.91. Found: C, 51.26; H, 6.10; Cl, 8.98. Hydrolysis of **13a** with H_2O afforded 2-methyl-3-butene-2-ol in 70% yield by cap. G.C.

$[Cp_2ZrOC(CH_3)(CH_2CH_3)CHCPh]\cdot AlMe_2Cl$ 14b. The acyl **1b** (0.654 gm, 2.089 mmol) was suspended in 6 ml of benzene and 5 ml of pentane and cooled to 0°C. To this solution was added 1.1 ml of a 2M toluene solution of $AlMe_3$ followed by 0.240 ml (2.18 mmol) of phenylacetylene. The resulting tan yellow solution was stirred briefly a 0°C and evacuated to dryness. The resulting light brown-residue was washed with three 5 ml portions of pentane to yield **14b** as a lemon-yellow powder (0.725 gm, 1.49 mmol, 71%). ^1H NMR(C_6D_6): δ 7.24 (m, 2H), 7.12 (m, 3H), 5.85 (s, 5H), 5.75 (s, 5H), 5.43 (s, 1H), 1.68 (m, J=7.08Hz, 3H), 1.29 (s, 3H), -0.21 (s, 3H). ^{13}C NMR(C_6D_6): δ 186.0 (C), 154.0 (Ph), 139.0 (CH), 126.2 (Ph), 113.2 (Cp), 112.6 (Cp), 92.1 (CO), 36.8 (CH_3), 28.9 (CH_2), 10.56 (CH_3). Anal. calc. for $C_{24}H_{30}OClZrAl$: C, 59.05; H, 6.19. Found: C, 59.14; H, 6.30. The stereochemistry of the product was assigned by difference NOE: irradiation of the methyl resonance at 1.29 ppm led to enhancement of the methine signal at 5.43 ppm. Irradiation of the Cp resonance at 5.85 ppm led to enhancement of the aryl resonances at 7.24 and 7.12 ppm.

Reaction of 2a with 2-butyne. The ketone complex **2a** (12 mg, 0.045 mmol) was dissolved in C_6D_6 in an NMR tube and treated with 5μL (0.066 mmol) of 2-butyne to give **14c** in > 85% yield (determined by integration of the Cp region). ^{1}H NMR(C_6D_6): δ 5.76 (s, 10H), 1.51 (s, 3H), 1.30 (s, 3H), 1.27 (s, 6H), -0.22 (s, 6H).

Reaction of 2a with diphenylacetylene. The ketone complex **2a** (28 mg, 0.075 mmol) and diphenylacetylene (20 mg, 0.11 mmol) were dissolved in C_6D_6 in an NMR tube to give **14d** after 2 hr at room temperature (> 90% yield). ^{1}H NMR(C_6D_6): δ 7.50 (m, 2H), 6.98 (m, 3H), 5.85 (s, 10H), 1.40 (s, 6H), -0.19 (s, 6H).

Reaction of 2a with 1-phenyl-1-propyne. The ketone complex **2a** (0.053 mmol) was dissolved in C_7D_8 in an NMR tube and treated with 1-phenyl-1-propyne which had been passed through a plug of silica gel. Integration of the Cp region in the ^{1}H NMR spectrum indicated a 1.7:1 ratio of regioisomers **14e,f**. ^{1}H NMR (C_6D_6) major isomer: δ 7.3 (m, 5H), 5.80 (s, 10H), 1.33 (s, 3H), 1.28 (s, 6H), -0.28 (s, 6H). ^{1}H NMR(C_6D_6) minor isomer: δ 7.21 (m, 5H), 5.76 (s, 10H), 1.32 (s, 6H), 1.13 (s, 3H), -0.26 (s, 6H).

$[Cp_2\overline{ZrOC(Me)(Ph)C(Me)_2O}]\cdot AlMe_2Cl$ 15a. An NMR tube was charged with 24 mg (0.064 mmol) of the ketone complex **2a**, cooled to 0°C and treated with 7.5 μL of acetophenone. The ^{1}H NMR spectrum, recorded at 0°C, indicated the immediate formation of **15a**. ^{1}H NMR(C_6D_6): δ 7.24 (m, 5H), 6.05 (s, 5H), 6.02 (s, 5H), 1.46 (s, 3H), 1.43 (s, 3H), 0.88 (s, 3H), -0.14 (s, 3H), -0.21 (s, 3H).

$Me(Ph)C(OH)C(OH)Me_2$ 16. The acyl **1a** (0.715 gm, 2.39 mmol) was suspended in toluene in a medium Schlenk tube, cooled to 0°C and treated with 1.20 ml of a 2M toluene solution of $AlMe_3$ to give a yellow solution. This solution was cooled to -78°C, treated with 0.32 ml (2.74 mmol) of acetophenone and allowed to stir at 0°C for 30 min. The reaction mixture was hydrolyzed with water, filtered through a coarse frit, and extracted with ether. The organic layer was separated, washed with

brine, dried over $MgSO_4$, and rotoevaporated to give an off white waxy solid. Flash chromatography (30% EtOAc/pet. ether) afforded 0.200 gm (1.11 mmol 48%) of **16**. Recrystallization from pet ether yielded colorless crystals of **16** suitable for analysis. Anal. ($C_{11}H_{16}O_2$) C, H. M.p. 80-81°C, uncorr.; lit. m.p. 83-84°C.[35]

$[Cp_2\overline{ZrOC(Me)(CHCH_2)C(Me)_2O}]\cdot AlMe_2Cl$ 15b. The ketone complex **2a** was dissolved in C_6D_6, frozen in liquid nitrogen and treated with 3.4 μL of methyl vinyl ketone. This sample was allowed to thaw and the NMR spectrum recorded at 0°C. ^{1}H NMR(C_6D_6): δ 5.97 (s, 10H), 5.46 (d, J=9.28Hz, 1H), 5.36 (d, J=3.9Hz, 1H), 4.93 (dd, J=9.28Hz, J=3.9Hz, 1H), 1.17 (s, 3H), 1.14 (s, 3H), 1.11 (s, 3H), -0.19 (s, 6H).

$[Cp_2\overline{ZrOC(Me)(CHCHMe)C(Me)_2O}]\cdot AlMe_2Cl$ 15c. The diolate **15c** was produced by a procedure similar to that for **15b** by treating 21 mg (0.057 mmol) of **2a** with 5.5μL of 3-pentene-2-one. ^{1}H NMR(C_7D_8, 0°C): δ 5.98 (s, 5H), 5.97 (s, 5H), 5.66 (dq, J=14.9Hz, J=6.4Hz, 1H), 5.20 ppm (d, J=14.89Hz, 1H), 1.65 (d, J=6.4Hz, 1H), 1.19 (s, 3H), 1.18 (s, 3H), 1.13 (s, 3H), -0.23 (s, 3H), -0.24 (s, 3H). ^{13}C NMR(C_7D_8, 0°C): δ 121.6 (CH), 115.8 (CH), 114.7 (Cp), 114.0 (Cp), 88.8 (CO), 88.6 (CO), 27.9 (CH_3), 26.8 (CH_3), 25.2 (CH_3), 18.43 (CH_3).

$[Cp_2Zr(C,O\text{-}\eta^2\text{-}OCMe_2)](\mu\text{-}Al(CH_2CHMe_2)(\mu\text{-}Cl)$ 17. The acyl **3** (0.357 gm, 1.277 mmol) was dissolved in benzene and cooled to 0°C. A benzene solution of dimethylaluminum chloride (0.124 ml, 0.638 mmol) was added slowly via cannula to the acyl solution. The resulting yellow solution was stirred as it warmed to room temperature and evacuated to dryness. The residue was washed with 6 ml of pentane to give **17** as a yellow powder (0.308 gm, 0.419 mmol, 66%). ^{1}H NMR(C_6D_6): δ 5.71 (s, 20H), 2.28 (m, J=6.6Hz, 2H), 1.70 (s, 12H), 1.31 (d, J=6.6Hz, 12H), 0.30 (d, J=6.8Hz, 4H). ^{13}C NMR(C_6D_6): δ 109.3, 80.3, 33.5, 28.5, 26.4. Anal. calcd. for $C_{37}H_{50}O_2ClAlZr_2$: c, 55.51; H, 6.80; Cl, 4.82. Found: C, 55.35; H, 6.93; Cl, 4.03.

$[Cp_2Zr(C,O\text{-}\eta^2\text{-}OCMe_2)](\mu\text{-}AlMe_2)(\mu\text{-}CH_3)$ 19. The acyl **3** (0.858 gm, 3.06 mmol) was dissolved in a minimum of toluene, placed under an atmosphere of CO and cooled to 0°C. A toluene solution of $AlMe_3$ (0.138 gm, 1.91 mmol) was prepared and cannulated into the acyl solution. The solution was stirred briefly at 0°C after which **19** precipitated as yellow microcrystals. After the solution was cooled at -20°C for 4 hours, the dark yellow supernatant was cannulated off and the resulting yellow solid washed with two 10 ml portions of cold toluene to give **19** as a yellow powder, which was only sparingly soluble in aromatic solvents or THF. ^{1}H NMR(C_6D_6): δ 5.57 (s, 2H), 1.67 (s, 12H), -0.37 (s, 6H), -0.50 (s, 3H). ^{1}H NMR(THF): δ 5.86 (s, 20H), 1.55 (s, 12H), -0.28 (s, 3H), -0.88 (s, 6H). Anal. calc. for $C_{29}H_{41}O_2AlZr_2$: C, 55.19; H, 6.55. Found: C, 55.22; H, 6.66.

Formation of 12 from 2a and 3. Addition of a benzene-d_6 solution of the alkyl acyl **3a** to the ketone complex **2a** led to the immediate precipitation of **12** as a yellow microcrystalline material.

$[Cp_2Zr(C,O\text{-}\eta^2\text{-}OCMe_2)][Cp_2Zr(OC(Me)CH_2CH_2CMe_3)](\mu\text{-}AlMe_2)(\mu\text{-}Cl)$ 20. The ketone complex **2c** and the acyl **3** were dissolved in toluene to give a yellow solution, which was stirred briefly and evacuated to give **18** as a yellow powder (0.276 gm, 0.383 mmol, 52%). ^{1}H NMR(C_6D_6): δ 5.86 (s, 5H), 5.75 (s, 5H), 5.73 (s, 5H), 5.69 (s, 5H), 2.60 (td, ^{3}J=12.7Hz, ^{2}J=3.9Hz, 1H), 1.75 (s, 3H), 1.65 (s, 3H), 1.61 (s, 3H), 1.39 (td, ^{3}J=13.2, ^{2}J=3.9Hz, 1H), 1.27 (td, ^{3}J=13.2Hz, ^{2}J=4.6Hz, 1H), 1.01 (s, 9H), -0.23 (s, 3H), -0.28 (s, 3H). ^{13}C NMR(C_6D_6): δ 110.1, 109.9, 109.7, 109.6, 83.9, 77.9, 42.4, 41.8, 34.5, 33.8, 32.5, 30.6, 30.0.

REFERENCES

1. (a) Sinn, H.; Kaminsky, W. *Adv. Organomet. Chem.* **1980**, *18*, 99-149. (b) Pino, P.; Mulhaupt, R. *Angew. Chem., Int. Ed. Eng.* **1980**, *19*, 857-875. (c) Boor, J. *Ziegler-Natta Catalysis and Polymerizations* Academic Press: London; 1983.

2. (a) Ivin, K.J. *Olefin Metathesis* Academic Press: London; 1983. (b) Grubbs, R.H. *Comprehensive Organometallic Chemistry* Wilkinson, G.; Stone, F.G.A.; Abel, E.W., Eds.; Pergamon Press: Oxford, 1982, Vol 9, pp. 499.

3. (a) Tebbe, F.N.; Parshall, G.W.; Reddy, G.S. *J. Am. Chem. Soc.* **1978**, *100*, 3611. (b) Tebbe, F.N.; Parshall, G.W.; Ovenall, D.W. *Ibid.* **1979**, *101*, 5074. (c) Howard, T.R.; Lee, J.B.; Grubbs, R.H. *Ibid.* **1980**, *102*, 6876. (d) Ott, K.C.; Lee, J.B; Grubbs, R.H. *Ibid.* **1982**, *104*, 2942.

4. Ott, K.C.; deBoer, E.J.M.; Grubbs, R.H. *Organometallics* **1984**, *3*, 223.

5. (a) Stille, J.R.; Grubbs, R.H. *J. Am. Chem. Soc.* **1986**, *108*, 855-856. (b) Cannizzo, L.F.; Grubbs, R.H. *J. Org. Chem.* **1985**, *50*, 2316, 2386. (c) Pine, S.H.; Pettit, R.J.; Geib, G.D.; Cruz, S.G.; Gallego, C.H.; Tijernia, T.; Pine, R.D. *J. Org. Chem.* **1985**, *50*, 1212. (d) Clawson, L.; Buchwald, S.L.; Grubbs, R.H. *Tetrahedron Lett.* **1984**, 5733. (e) Brown-Wensley, K.A.; Buchwald, S.L.; Cannizzo, L.F.; Clawson, L. E.; Ho, S.C.H.; Meinhart, J.D.; Stille, J.R.; Straus, D.A.; Grubbs, R.H. *Pure Appl. Chem.* **1983**, *55*, 1733.

6. A preliminary account of a portion of this work has appeared: Waymouth, R.M.; Klauser, K.R.; Grubbs, R.H. *J. Am. Chem. Soc.* **1986**, *108*, 6385.

7. Mazenec, T.J. *J. Catal.* **1986**, *98*, 115.

8. (a) Erker, G.; Dorf, U.; Czisch, P.; Peterson, J.L. *Organometallics* **1986**, *5*, 668. (b) Erker, G.; Rosenfeldt, F. *J. Organomet. Chem.* **1982**, *224*, 29. (c) Rosenfeldt, F.; Erker, G. *Tetrahedron Lett.* **1980**, *21*, 1637.

9. (a) Wood, C.D.; Schrock, R.R. *J. Am. Chem. Soc.* **1979**, *101*, 5421. (b) Evitt, E.R.; Bergman, R.G. *Ibid.* **1980**, *102*, 7003. (c) Manriquez, J.M.; McAlister, D.R.; Sanner, R.D.; Bercaw, J.E. *Ibid.* **1978**, *100*, 2716. (d) Demerseman, B.; Bouquet, B.; Bigorgne, M. *J. Organomet. Chem.* **1975**, *93*, 199. (e) Fachinetti, G.; Floriani, C. *J. Chem. Soc., Chem. Commun.* **1972**, 654. (f) Suggs, J.W.; Wovkulich, M.J.; Cox, S.D. *Organometallics* **1985**, *4*, 1101.

10. (a) Gambarotta, S.; Floriani, C.; Chiesi-Villa, A.; Guastini, C. J. *J. Am. Chem. Soc.* **1983**, *105*, 1690. (b) Fachinetti, G.; Floriani, C.; Roselli, A.; Pucci, S. *J. Chem. Soc., Chem. Commun.* **1978**, 278. (c) Erker, G. *Acc. Chem. Res.* **1984**, *17*, 103. (d) Erker, G.; Kropp, K. *Chem. Ber.* **1982**, *115*, 2437. (e) Skibbe, V.; Kropp, K.; Erker, G. *Tetrahedron* **1982**, *38*, 1285. (f) Kropp, K.; Skibbe, V.; Erker, G. *J. Am. Chem. Soc.* **1983**, *105*, 3353. (g) Skibbe, V.; Erker, G. *J. Organomet. Chem.* **1983**, *241*, 15. (h) Roddick, D.M. Ph.D. Thesis, California Institute of Technology, Pasadena, California, 1984. (i) Gell, K.I.; Posin, B.; Schwartz, J.; Williams, G.M. *J. Am. Chem. Soc.* **1982**, *104*, 1846. (j) See also: Marsella, J.A.; Folting, K.; Huffman, J.C.; Caulton, K.G. *J. Am. Chem. Soc.* **1981**, *103*, 5596.

11. **V:** (a) Gambarotta, S.; Floriani, C.; Chiesi-Villa, A.; Guastini, C. *J. Am. Chem. Soc.* **1982**, *104*, 2019. **Mo:** (b) Gambarotta, S.; Floriani, C.; Chiesi-Villa, A.; Guastini, C. *Ibid.* **1984**, *107*, 2985. (c) Adams, H.; Bailey, N.A.; Gauntlett, J.T.; Winter, M.J. *J. Chem. Soc., Chem. Commun.* **1984**, 1360. (d) Brunner, H.; Wachter, J.; Bernal, I.; Creswick, M. *Angew. Chem., Int. Ed. Eng.* **1979**, *18*, 861. **Re:** (e) Buhro, W.E.; Patton, A.T.; Strouse, C.E.; Gladysz, J.A. *J. Am. Chem. Soc.* **1983**, *105*, 1056. **Fe:** (f) Berke, H.; Huttner, G.; Weiler, G.; Zsolnai, L. *J. Organomet. Chem.* **1984**, *B39*, 1380. **Ru:** (g) Chaudret, B.N.; Cole-Hamilton, D.J.; Nohr, R.S.; Wilkinson, G. *J. Chem. Soc., Dalton Trans.* **1977**, 1546. **Os:** (h) Headford, C.E.L., Roper, W.R. *J. Organomet. Chem.* **1983**,

244, C53. **Ni:** (i) Walther, D. *Ibid.* **1980**, *190*, 393. **Pt:** (j) Green, M.; Howard, J.A.K.; Laguna, A.; Smart, L.E.; Spencer, J.L.; Stone, F.G.A. *J. Chem. Soc., Dalton Trans.* **1977**, 278.

12. (a) Horwitz, C.P.; Shriver, D.F. *Adv. Organomet. Chem.* **1984**, *23*, 219-305. (b) Richmond, T.G.; Shriver, D.F. *Inorg. Chem.* **1982**, *21*, 1272. (c) Butts, S.B.; Strauss, S. H.; Holt, E.M.; Stimson, R.E.; Alcock, N.W.; Shriver, D.F. *J. Am. Chem. Soc.* **1980**, *102*, 5093. (d) Correa, F.; Nakamura, R.; Stimson, R.E.; Burwell, Jr., R.L.; Shriver, D.F. *Ibid.* **1980**, *102*, 5112. (e) Shriver, D.F. In *Catalytic Activation of Carbon Monoxides* Ford, P.C., Ed.; ACS Symposium Series 152: Washington, D.C., 1981, pp.1-19. (f) Labinger, J.A.; Miller, J.S. *J. Am. Chem. Soc.* **1982**, *104*, 6856.

13. (a) Browning, J.; Empsall, H.D.; Green, M.; Stone, F.G.A. *J. Chem. Soc., Dalton Trans.* **1973**, 381 and refs. therein. (b) Hunt, M.M.; Kemmitt, R.D.; Russell, D.R; Tucker, P.A. *J. Chem. Soc., Dalton Trans.* **1979**, 287.

14. (a) Fachinetti, G.; Biran, C.; Floriani, C.; Chiesi-Villa, A.; Guastini, C. *J. Am. Chem. Soc.* **1978**, *100*, 1921-1922. (b) Fachinetti, G.; Biran, C.; Floriani, C.; Chiesi-Villa, A.; Guastini, C. *Inorg. Chem.* **1978**, *17*, 2995-3002.

15. (a) Pasquali, M.; Floriani, C.; Chiesi-Villa, A.; Guastini, C. *J. Am. Chem. Soc.* **1979**, *101*, 4740-4742. (b) Pasquali, M.; Floriani, C.; Chiesi-Villa, A.; Guastini, C. *Inorg. Chem.* **1981**, *20*, 349-355.

16. Casey, C.P.; O'Connor, J.M.; Haller, K.J. *J. Am. Chem. Soc.* **1985**, *107*, 3172.

17. Treatment of the acyl complexes **1** with $AlCl_3$ results in transmetallation of the acyl ligand from zirconium to aluminum. Carr, D.B.; Schwartz, J. *J. Am. Chem. Soc.* **1979**, *101*, 3521.

18. The ketone complexes **2** begin to decompose in solution or in the solid state at temperatures higher than 30°C.

19. This mechanism is similar to that proposed for the reductive alkylation of organic carbonyl substrates by alkylaluminum reagents. Eisch, J.J. In "Comprehensive Organometallic Chem.; Wilkinson, G., Stone, F.G.A.; Abel, E.W., Eds.; Pergamon Press: Oxford, 1982, Vol 9, pp. 499.

20. (a) Van Doorn, J.A.; Masters C.; Vogler, H. C. *J. Organomet. Chem.* **1976**, *105*, 245.(b) Casey, C.P.; Neumann, S.M.; Andrews, M.A.; McAlister, D.R. *Pure Appl. Chem.* **1980**, *52*, 625.(c) Gladysz, J.A. *Aldrichimica Acta* **1979**, *12*, 13.

21. Martin, B.D.; Matchett, S.A.; Norton, J.R.; Anderson, O.P. *J. Am. Chem. Soc.* **1985**, *107*, 7952.

22. Mole, T.; Jeffery, E.A. *Organoaluminum Compounds* Elsevier Publishing: New York, 1972.

23. This mechanism might also be considered for reductions observed when acyl complexes are treated with metal alkyl or hydrido reagents (refs. 10,20,21).

24. Assuming a unimolecular half-life of 1 min at -30°C for reaction (11), one can calculate a rate constant $k=1.2\times10^{-2}s^{-1}$ which translates to a free energy of activation $\Delta G\simeq18.3$ kcal/mol (-30°C). The experimentally determined free energy of activation for the formation of the benzophenone complex is $\Delta G= 25.1$ kcal/mol (65°C, ref 8).

25. (a) Tatsumi, K.; Nakamura, A.; Hofmann, P.; Stauffert, P.; Hoffmann, R. *J. Am. Chem. Soc.* **1985**, *107*, 4440. (b) Hofmann, P.; Stauffert, P.; Tatsumi, K., Nakamura, A.; Hoffmann, R. *Organometallics* **1985**, *4*, 404-406.

26. (a) Baker, R.J.; Tauster, S.J.; Eds. *Strong Metal Support Interactions* ACS Symposium Series 298: Washington D.C., 1986. (b) Imelik, B.; Naccache, C.; Condurier, G.; Praliand. H.; Meriandeau, P.; Martin, G.A.; Vedrine, J.C.; Eds., *Metal Support and Metal Additive Effects in Catalysis* Elsevier Publishing: New York, 1982.

27. The difference in reactivity between the ketone complexes **2** and the Tebbe reagent $Cp_2TiCH_2{=}CH_2{\cdot}AlMe_2Cl$ towards pyridine probably arises from the strong Zr-O-Al interactions in the former complexes.

28. In the absence of coordinated $AlMe_2Cl$, zirconocene oxymetallacyclopentanes dimerize. Takaya, H.; Yamakawa, M.; Mashima, K. *J. Chem. Soc., Chem. Commun.* **1983**, 1283.

29. Wysong, E.B.; Grubbs, R.H., unpublished results.

30. (a) Wailes, P.C.; Weigold, H. *J. Organomet. Chem.* **1970**, *24*, 405. (b) Bertelo, C.A.; Schwartz, J. *Ibid.* **1975**, *97*, 228.

31. The coupling of trimethylsilylketene at a bis(pentamethylcyclopentadienyl)zirconium center occurs in a head-to-head fashion. In this case, it is likely that steric effects are important in determining the regiochemistry of coupling. Moore, E.J., PhD Thesis, California Institute of Technology, Pasadena, CA, 1984.

32. Floriani has previously observed competitive head-to-head vs. head-to-tail coupling of organic carbonyl substrates at titanium centers.[14,15] Diphenylketene couples in a head-to-tail fashion at titanium centers, while diethylketomalonate couples in a head-to-head fashion. Floriani attributed the difference in the regiochemistry of coupling to one- and two-electron reductive coupling processes. Carbonyl substrates that can be reduced by Ti(II) to the dianion (a two-electron process) will produce metallacycles of structure **A**. Less reducible substrates should proceed via a radical-type mechanism and give rise to metallacycles of structure **B**.

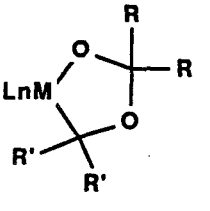

A

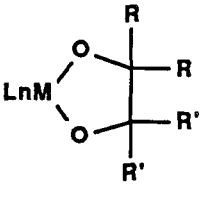

B

33. (a) Negishi, E.; Van Horn, D.E.; Yoshida, T. *J. Am. Chem. Soc.* **1985**, *107*, 6639-6647.(b) Negishi, E.; Takahashi, T. *Aldrichimica Acta* **1985**, *18*, 31-47.

34. See Chapter 2 of this thesis.

35. Roger, R. *J. Chem. Soc.* **1925**, *124*, 518.

Appendix

Crystal Structure Data

Table 1. Summary of Crystal Data for **3, 7a, 9, and 10.**

compd	**3**	**7a**	**9**	**10**
formula	$C_{37}H_{53}Zr_2O_2Al$	$C_{36}H_{50}Zr_2O_2AlCl$	$C_{38}H_{55}Zr_2O_2Al$	$C_{38}H_{55}Zr_2O_2Al$
mol wt	739.2	759.57	753.27	753.27
space group	$P2_1/c$	$P2_1/c$	$C2/c$	$C2/c$
a, Å	10.2089(7)	10.2193(14)	11.777(5)	18.219(2)
b, Å	20.214(3)	20.237(3)	19.998(4)	10.3644(9)
c, Å	18.421(2)	18.458(3)	32.636(11)	20.273(2)
β, deg	94.375(8)	94.303(14)	96.83(5)	94.565(8)
V, Å^3	3790.4(7)	3802.8(10)	7632(4)	3815.8(7)
Z	4	4	8	4
λ, Å	0.7107	0.7107	0.7107	0.7107
scan mode	0-2θ	0-2θ	ω	ω
scan range, deg	2.0 (in 2θ)	2.0 (in 2θ) plus dispersion	1.0 (in ω)	1.0 (in ω)
reflectns	$+h \pm k \pm l$	$+h \pm k \pm l$	$\pm h \pm k \pm l$	$\pm h \pm k \pm l$
collect.	10114	8116	22163	9443
av	6573	3567	4989	2845
	(5216I>0)	(3332I>0)	(4369I>0)	(2845I>0)
	(3380I>3σI)	(2596I>3σI)	(3651I>3σI)	(1848I>3σI)

Table 2. Bond Lengths(Å) and Angles(°) for 3.

	Fragment A	Fragment B
Zr–C	2.559(7)	2.456(7)
Zr–O(1)	2.179(4)	2.183(4)
Zr–C(1)	2.187(6)	2.183(6)
Zr–C(11)	2.522(8)	2.551(10)
Zr–C(12)	2.480(9)	2.516(11)
Zr–C(13)	2.509(9)	2.502(10)
Zr–C(14)	2.526(8)	2.490(9)
Zr–C(15)	2.535(8)	2.494(9)
Zr–C(21)	2.475(9)	2.492(11)
Zr–C(22)	2.487(8)	2.526(10)
Zr–C(23)	2.520(8)	2.517(9)
Zr–C(24)	2.512(8)	2.524(9)
Zr–C(25)	2.500(8)	2.490(11)
Al–O	1.818(4)	1.805(4)
Al–C	3.739(8)	
Al–C(8)	1.948(8)	1.951(8)
C(1)–O	1.398(7)	1.413(7)
C(1)–C(2)	1.323(9)	1.330(9)
C(2)–C(3)	1.501(10)	1.498(10)
C(3)–C(4)	1.493(11)	1.529(10)
C(4)–C(5)	1.472(15)	1.540(12)
C(4)–C(6)	1.458(15)	1.517(12)
C(4)–C(7)	1.497(13)	1.511(12)
C(11)–C(12)	1.395(12)	1.397(15)
C(12)–C(13)	1.390(13)	1.316(15)
C(13)–C(14)	1.367(12)	1.300(14)
C(14)–C(15)	1.387(11)	1.342(13)
C(15)–C(11)	1.358(11)	1.394(13)
C(21)–C(22)	1.378(12)	1.382(15)
C(22)–C(23)	1.360(11)	1.334(13)
C(23)–C(24)	1.373(11)	1.337(13)
C(24)–C(25)	1.386(11)	1.323(14)
C(25)–C(21)	1.376(12)	1.397(15)
C–H(1)	0.94(5)	
C–H(2)	0.98(5)	
C–H(3)	0.86(5)	
O–Al–O	98.0(2)	
Zr–C–Zr	147.8(3)	
C–Zr–C(1)	113.2(2)	113.5(2)
C–Zr–O	75.9(2)	75.9(2)
C(1)–Zr–O	37.3(2)	37.8(2)

Zr–C(1)–O	71.0(3)	71.1(3)
Zr–O–C(1)	71.6(3)	71.1(3)
Zr–O–Al	152.6(2)	159.6(2)
Al–O–C(1)	127.1(4)	128.5(4)
O–C(1)–C(2)	124.7(6)	122.2(6)
C(1)–C(2)–C(3)	123.4(6)	122.6(6)
C(2)–C(3)–C(4)	117.8(6)	114.9(6)
O(1)–Al–C(8)	108.8(3)	109.0(3)
O(2)–Al–C(8)	107.9(3)	110.3(3)
C(8)–Al–C(8)	120.5(3)	
H(1)–C–H(2)	119(4)	
H(1)–C–H(3)	117(4)	
H(2)–C–H(3)	122(4)	
Zr–C–H(1)	74(3)	80(3)
Zr–C–H(2)	99(3)	111(3)
Zr–C–H(3)	81(3)	93(3)
Al–C–Zr(1)	73.5(2)	
Al–C–Zr(2)	75.5(2)	

Table 3. Atom Coordinates ($\times 10^5$) and U_{eq}'s ($Å^2$, $\times 10^4$) for 3.

	x	y	z	U_{eq}
Zr(1)	13502(6)	15168(3)	13002(3)	380(2)
Zr(2)	−16921(6)	33391(3)	12983(3)	414(2)
C	−2489(74)	24081(36)	16718(40)	466(19)
Al	7816(20)	28959(10)	−1583(11)	453(5)
O(1)	14944(40)	22907(20)	4865(21)	475(12)
O(2)	−5376(39)	31755(20)	3646(20)	468(12)
C(1A)	23892(62)	17910(29)	3493(33)	451(18)
C(2A)	32459(68)	18214(32)	−1535(35)	556(20)
C(3A)	42228(71)	12848(35)	−2723(38)	643(22)
C(4A)	42986(82)	10325(39)	−10296(41)	751(26)
C(5A)	30130(129)	7501(70)	−12794(64)	1934(57)
C(6A)	45819(147)	15685(66)	−15235(57)	2019(58)
C(7A)	52718(108)	4829(52)	−10750(51)	1459(43)
C(8A)	32(85)	24318(39)	−10124(38)	846(28)
C(1B)	−14902(59)	36672(31)	1835(34)	457(18)
C(2B)	−15806(66)	39691(34)	−4599(36)	545(20)
C(3B)	−25887(70)	44904(33)	−6566(38)	597(22)
C(4B)	−34823(78)	43469(38)	−13430(43)	707(24)
C(5B)	−44644(101)	49196(47)	−14801(51)	1253(38)
C(6B)	−27271(85)	42922(43)	−20184(46)	921(30)
C(7B)	−42535(88)	37168(48)	−12626(47)	1067(33)
C(8B)	20458(74)	36071(36)	−2626(41)	758(25)
C(11A)	2142(89)	4261(37)	14700(46)	843(31)
C(12A)	10234(80)	3539(38)	8982(62)	977(38)
C(13A)	4926(89)	7337(44)	3191(47)	888(30)
C(14A)	−5948(78)	10500(37)	5371(45)	719(26)
C(15A)	−7619(72)	8524(36)	12450(46)	688(25)
C(21A)	30548(88)	9626(40)	21137(46)	839(29)
C(22A)	22440(83)	12788(45)	25676(40)	792(28)
C(23A)	23784(75)	19445(41)	24965(42)	734(25)
C(24A)	32805(79)	20549(40)	19935(45)	773(27)
C(25A)	37137(70)	14459(51)	17618(39)	805(30)
C(11B)	−32222(73)	23410(36)	12862(80)	1175(56)
C(12B)	−35633(96)	27071(67)	6569(57)	1255(43)
C(13B)	−40666(78)	32734(56)	8518(59)	1081(39)

C(14B)	−40506(77)	33056(46)	15571(57)	923(30)
C(15B)	−35163(83)	27538(53)	18575(47)	898(31)
C(21B)	−19169(94)	44456(53)	18718(73)	1271(43)
C(22B)	−8551(133)	45100(37)	14546(48)	1148(63)
C(23B)	1098(86)	41237(44)	17424(53)	879(31)
C(24B)	−2662(103)	38295(38)	23427(47)	848(32)
C(25B)	−14870(121)	40135(52)	24325(49)	1077(38)
H(1)	−606(50)	2248(25)	1218(29)	450(181)
H(2)	−516(52)	2203(26)	2122(30)	522(186)
H(3)	451(45)	2643(22)	1668(24)	229(149)

Table 4. Atom Coordinates ($\times 10^4$) of Hydrogen Atoms for 3.

	x	y	z
H(2A)	3252	2227	−484
H(3A1)	4045	899	65
H(3A2)	5152	1452	−97
H(5A1)	3065	250	−1465
H(5A2)	2989	640	−1943
H(5A3)	2235	1100	−1293
H(5A4)	2674	328	−1049
H(5A5)	2289	753	−932
H(5A6)	2541	985	−1759
H(6A1)	5496	1826	−1260
H(6A2)	3489	1822	−1696
H(6A3)	4453	1377	−2072
H(7A1)	6202	687	−904
H(7A2)	5449	351	−1512
H(7A3)	5276	187	−536
H(8A1)	100	2700	−1460
H(8A2)	479	1985	−1087
H(8A3)	−948	2321	−976
H(2B)	−961	3831	−840
H(3B1)	−2132	4931	−706
H(3B2)	−3167	4538	−227
H(5B1)	−3978	5391	−1053
H(5B2)	−5038	4950	−948
H(5B3)	−5163	4847	−1395
H(5B4)	−4417	5431	−1483
H(5B5)	−4602	5036	−1852
H(5B6)	−3978	5301	−1861
H(6B1)	−2376	4747	−2176
H(6B2)	−1942	3994	−1947
H(6B3)	−3396	4107	−2469
H(7B1)	−3694	3343	−1240
H(7B2)	−4736	3742	−785
H(7B3)	−4978	3671	−1669
H(7B4)	−5241	3838	−1215
H(7B5)	−3970	3506	−825

H(7B6)	−4220	3420	−1679
H(8B1)	2710	3620	150
H(8B2)	2486	3542	−732
H(8B3)	1559	4045	−304
H(21A)	369	196	1987
H(22A)	1831	57	882
H(23A)	851	786	−195
H(24A)	−1188	1391	234
H(25A)	−1518	1006	1557
H(26A)	3187	456	2076
H(27A)	1593	1047	2895
H(28A)	1888	2313	2760
H(29A)	3623	2501	1812
H(30A)	4388	1356	1378
H(21B)	−2824	1877	1306
H(22B)	−3462	2561	126
H(23B)	−4433	3674	532
H(24B)	−4356	3694	1898
H(25B)	−3340	2624	2406
H(26B)	−2807	4682	1768
H(27B)	−780	4812	989
H(28B)	1043	4060	1545
H(29B)	281	3505	2707
H(30B)	−2095	3870	2838

Table 5. **Gaussian amplitudes ($\times 10^4$) for 3.**

	U_{11}	U_{22}	U_{33}	U_{12}	U_{13}	U_{23}
Zr(1)	416(4)	340(4)	388(4)	9(3)	59(3)	−14(3)
Zr(2)	411(4)	417(4)	425(4)	28(3)	95(3)	−70(3)
C	545(47)	450(46)	421(45)	−28(37)	151(37)	−15(34)
Al	509(13)	465(14)	402(13)	88(10)	146(10)	31(10)
O(1)	584(30)	436(30)	432(28)	153(23)	208(23)	31(21)
O(2)	465(27)	589(32)	361(27)	151(23)	106(22)	34(22)
C(1A)	583(45)	314(41)	472(44)	49(33)	144(35)	−17(31)
C(2A)	719(51)	504(48)	470(45)	158(38)	217(39)	35(35)
C(3A)	704(54)	637(55)	609(52)	230(42)	194(43)	−40(39)
C(4A)	935(68)	738(64)	616(58)	353(51)	292(50)	−61(45)
C(5A)	1588(122)	2639(161)	1571(121)	369(116)	86(98)	−1506(113)
C(6A)	3144(181)	2013(137)	1074(91)	1100(132)	1294(109)	542(90)
C(7A)	1827(118)	1650(107)	960(83)	1160(92)	498(76)	−80(70)
C(8A)	1123(73)	877(66)	539(56)	137(56)	72(53)	−112(45)
C(1B)	406(40)	464(47)	502(45)	66(32)	32(34)	−68(34)
C(2B)	524(46)	623(53)	480(47)	169(38)	−15(37)	11(37)
C(3B)	649(52)	507(50)	612(53)	87(39)	−93(41)	−5(38)
C(4B)	693(59)	681(59)	740(61)	121(46)	8(48)	48(47)
C(5B)	1453(96)	1106(87)	1131(87)	703(73)	−354(71)	5(64)
C(6B)	945(72)	1000(76)	801(68)	73(56)	−47(56)	184(54)
C(7B)	888(71)	1367(93)	894(72)	−241(64)	−269(57)	222(63)
C(8B)	763(57)	634(59)	908(64)	−17(44)	265(49)	185(46)
C(21A)	917(71)	491(58)	1085(82)	−255(50)	−160(60)	245(50)
C(22A)	656(63)	439(57)	1818(114)	66(45)	−31(66)	−445(63)
C(23A)	876(73)	897(77)	924(75)	−384(56)	286(58)	−504(56
C(24A)	718(60)	586(59)	817(64)	−167(44)	−182(50)	−30(46)
C(25A)	582(54)	505(54)	989(69)	−190(41)	144(50)	−60(46)
C(26A)	965(74)	750(67)	752(67)	315(54)	−269(55)	−94(50)
C(27A)	925(69)	992(73)	461(53)	16(56)	73(48)	82(48)
C(28A)	660(57)	783(64)	732(62)	228(48)	−117(47)	−268(49)
C(29A)	649(60)	774(66)	847(68)	−314(49)	−260(50)	88(51)
C(30A)	458(49)	1445(93)	504(52)	148(55)	−11(39)	−77(56)
C(21B)	380(51)	363(58)	2819(160)	−99(40)	359(81)	−76(75)
C(22B)	738(79)	1645(123)	1439(102)	−745(78)	457(71)	−922(88)
C(23B)	473(55)	1667(112)	1083(85)	−85(65)	−70(58)	605(80)
C(24B)	612(57)	951(78)	1267(84)	38(54)	474(61)	−151(66)
C(25B)	689(65)	1028(83)	973(75)	−289(58)	45(55)	401(61)
C(26B)	904(79)	1062(94)	1769(125)	437(69)	−408(79)	−1095(85)
C(27B)	2190(134)	200(51)	947(80)	−77(63)	−572(84)	1(47)
C(28B)	941(72)	707(70)	1005(80)	−418(55)	180(62)	−277(55)
C(29B)	1298(90)	521(58)	654(65)	−6(57)	−381(60)	−170(46)
C(30B)	1417(105)	1172(98)	707(71)	−432(76)	507(71)	−540(62)

Table 6. Bond Lengths(Å) and Angles(°) for 7a

	Fragment A	Fragment B
Zr–Cl	2.636(2)	2.632(2)
Zr–O	2.172(4)	2.147(4)
Zr–C(1)	2.170(6)	2.173(6)
Zr–C(11)	2.486(10)	2.490(11)
Zr–C(12)	2.517(9)	2.514(11)
Zr–C(13)	2.506(8)	2.521(12)
Zr–C(14)	2.508(8)	2.516(11)
Zr–C(15)	2.500(10)	2.483(10)
Zr–C(21)	2.487(10)	2.490(19)
Zr–C(22)	2.527(9)	2.487(15)
Zr–C(23)	2.495(9)	2.507(14)
Zr–C(24)	2.479(9)	2.510(12)
Zr–C(25)	2.453(10)	2.469(14)
Al–O	1.809(4)	1.818(4)
Al–C(8)	1.941(8)	1.950(8)
C(1)–O	1.390(7)	1.393(7)
C(1)–C(2)	1.319(9)	1.339(9)
C(2)–C(3)	1.493(9)	1.492(10)
C(3)–C(4)	1.498(11)	1.519(10)
C(4)–C(5)	1.441(18)	1.503(12)
C(4)–C(6)	1.477(18)	1.516(12)
C(4)–C(7)	1.516(14)	1.514(12)
C(11)–C(12)	1.399(14)	1.333(16)
C(12)–C(13)	1.357(12)	1.325(17)
C(13)–C(14)	1.374(12)	1.396(16)
C(14)–C(15)	1.374(13)	1.417(15)
C(15)–C(11)	1.399(14)	1.351(15)
C(21)–C(22)	1.366(13)	1.376(24)
C(22)–C(23)	1.383(13)	1.298(20)
C(23)–C(24)	1.390(13)	1.304(18)
C(24)–C(25)	1.344(14)	1.330(19)
C(25)–C(21)	1.340(14)	1.397(24)
O(A)–Al–O(B)	98.6(2)	
Zr–Cl–Zr	134.87(7)	
Cl–Zr–C(1)	117.7(2)	118.4(2)
Cl–Zr–O	80.5(1)	80.8(1)
C(1)–Zr–O	37.4(2)	37.6(2)
Zr–C(1)–O	71.4(3)	70.2(3)
Zr–O–C(1)	71.3(3)	72.2(3)
Zr–O–Al	151.0(2)	159.4(2)
Al–O–C(1)	125.3(4)	126.6(4)

O–C(1)–C(2)	125.4(6)	124.8(6)
C(1)–C(2)–C(3)	124.3(6)	123.2(6)
C(2)–C(3)–C(4)	117.2(6)	115.4(6)
O(A)–Al–C(8)	109.6(3)	109.2(3)
O(B)–Al–C(8)	107.3(3)	109.5(3)
C(8)–Al–C(8)	120.4(3)	

Table 7. Atom Coordinates ($\times 10^5$) and U_{eq}'s ($Å^2$, $\times 10^4$) for 7a.

	x	y	z	U_{eq}
Zr(1)	13579(6)	34989(3)	13117(3)	406(1)
Zr(2)	−17356(6)	16685(3)	12796(3)	444(1)
Cl	−2579(18)	26353(8)	18368(8)	566(4)
Al	7846(21)	21271(9)	−1288(10)	498(5)
O(A)	15219(40)	27050(18)	5299(19)	456(10)
O(B)	−5878(42)	18595(20)	3726(20)	544(11)
C(1A)	24012(65)	32031(28)	3807(32)	479(16)
C(2A)	32578(71)	31750(30)	−1196(35)	597(18)
C(3A)	42169(73)	37100(33)	−2555(35)	664(20)
C(4A)	42731(97)	39406(42)	−10246(44)	836(25)
C(5A)	45807(184)	34014(71)	−14940(67)	2426(65)
C(6A)	29886(163)	42316(83)	−12693(69)	2245(67)
C(7A)	52776(114)	44885(54)	−10651(53)	1506(41)
C(8A)	603(86)	26044(38)	−9801(34)	845(25)
C(1B)	−14964(60)	13686(30)	1651(34)	510(18)
C(2B)	−15864(67)	10656(33)	−4825(34)	584(19)
C(3B)	−25662(70)	5364(33)	−6813(37)	653(20)
C(4B)	−34583(79)	6665(36)	−13627(40)	724(22)
C(5B)	−26884(95)	7217(45)	−20237(43)	1043(30)
C(6B)	−42687(97)	12868(47)	−12831(49)	1123(31)
C(7B)	−43853(98)	858(49)	−14779(48)	1235(33)
C(8B)	19824(80)	13877(35)	−2322(40)	818(22)
C(11A)	9792(89)	46347(39)	8241(69)	951(33)
C(12A)	2161(105)	45934(39)	14224(51)	906(31)
C(13A)	−7433(81)	41431(38)	12538(47)	718(24)
C(14A)	−6330(83)	39047(37)	5632(49)	734(23)
C(15A)	4285(111)	42074(50)	2881(44)	917(29)
C(21A)	22338(91)	37969(55)	25642(44)	847(28)
C(22A)	24375(89)	31309(51)	25226(44)	797(27)
C(23A)	33241(95)	30181(43)	20045(52)	820(27)
C(24A)	36965(77)	36324(60)	17521(39)	789(28)
C(25A)	30131(112)	40841(41)	21029(55)	904(29)
C(11B)	−40870(85)	17007(54)	15510(69)	987(33)
C(12B)	−41192(86)	16927(60)	8269(72)	1027(37)
C(13B)	−36293(105)	22573(72)	6027(57)	1020(35)
C(14B)	−32524(78)	26507(37)	12046(94)	1070(47)
C(15B)	−35498(91)	22700(63)	18162(50)	927(30)
C(21B)	−17533(206)	8962(91)	23309(98)	1478(53)
C(22B)	−5031(213)	11519(49)	23477(74)	1266(51)
C(23B)	558(98)	9183(64)	17920(95)	1059(38)
C(24B)	−7338(175)	5367(48)	13920(52)	992(34)
C(25B)	−18709(141)	5126(52)	16990(96)	1120(42)

Table 8. Atom Coordinates ($\times 10^4$) of Hydrogen Atoms for 7a.

	x	y	z
H(2A)	3267	2763	−445
H(2B)	−972	1204	−864
H(11A)	1769	4941	792
H(12A)	370	4847	1913
H(13A)	−1469	4004	1589
H(14A)	−1219	3546	294
H(15A)	781	4131	−220
H(21A)	1585	4033	2884
H(22A)	1990	2775	2818
H(23A)	3645	2569	1836
H(24A)	4368	3729	1375
H(25A)	3101	4588	2046
H(31A)	5137	3560	−73
H(32A)	4005	4107	63
H(51A)	4275	3016	−1311
H(52A)	5583	3364	−1478
H(53A)	4251	3510	−1961
H(61A)	2489	4260	−877
H(62A)	2595	3910	−1617
H(63A)	3150	4617	−1527
H(71A)	5070	4820	−747
H(72A)	6111	4310	−923
H(73A)	5230	4639	−1552
H(81A)	−582	2910	−818
H(82A)	748	2831	−1188
H(83A)	−332	2286	−1315
H(11B)	−4400	1339	1894
H(12B)	−4465	1311	508
H(13B)	−3542	2389	58
H(14B)	−2862	3117	1173
H(15B)	−3350	2439	2336
H(21B)	−2417	1013	2715
H(22B)	−14	1453	2740
H(23B)	1036	1007	1641
H(24B)	−563	274	910

H(25B)	−2729	263	1534
H(31B)	−3129	482	−257
H(32B)	−2077	109	−743
H(51B)	−1972	988	−1913
H(52B)	−2428	278	−2156
H(53B)	−3262	921	−2405
H(61B)	−4676	1263	−840
H(62B)	−3740	1648	−1336
H(63B)	−4960	1290	−1674
H(71B)	−5143	132	−1225
H(72B)	−3937	−359	−1278
H(73B)	−4602	27	−1974
H(81B)	2308	1250	238
H(82B)	1511	1045	−478
H(83B)	2681	1541	−528

Table 9. Gaussian amplitudes ($\times 10^4$) for 7a

	U_{11}	U_{22}	U_{33}	U_{12}	U_{13}	U_{23}
Zr(1)	489(4)	350(3)	384(4)	−11(3)	58(3)	11(3)
Zr(2)	459(4)	435(4)	447(4)	−33(3)	87(3)	73(3)
Cl	699(12)	573(10)	447(10)	−171(9)	164(9)	−43(8)
Al	589(14)	514(12)	409(11)	−105(10)	148(10)	−55(9)
O(A)	570(29)	414(24)	408(24)	−153(23)	183(21)	−24(19)
O(B)	565(30)	677(29)	409(25)	−151(25)	146(23)	−69(21)
C(1A)	581(46)	426(38)	439(40)	−72(36)	79(37)	51(30)
C(2A)	741(53)	516(42)	565(43)	−144(38)	243(42)	1(33)
C(3A)	786(56)	721(49)	501(44)	−256(43)	137(40)	74(36)
C(4A)	1001(73)	841(58)	704(58)	−357(55)	311(53)	−18(47)
C(5A)	4059(245)	1857(126)	1643(115)	−1262(151)	2070(150)	−459(105)
C(6A)	1996(157)	3227(207)	1508(117)	−692(149)	93(112)	1716(135)
C(7A)	1817(128)	1655(101)	1112(81)	−961(94)	543(79)	233(71)
C(8A)	1201(72)	891(56)	443(44)	−117(53)	61(46)	33(39)
C(1B)	388(42)	560(43)	576(46)	−123(35)	−15(34)	61(36)
C(2B)	549(49)	740(47)	461(43)	−159(39)	16(37)	−63(38)
C(3B)	620(52)	682(47)	644(49)	−120(41)	−39(41)	−67(38)
C(4B)	733(59)	743(51)	676(52)	−149(47)	−89(47)	−97(41)
C(5B)	1201(83)	1266(76)	653(56)	−299(64)	9(57)	−135(51)
C(6B)	981(74)	1320(83)	1012(68)	165(65)	−310(58)	−225(60)
C(7B)	1201(83)	1454(87)	974(69)	−713(73)	−430(62)	126(61)
C(8B)	919(63)	663(49)	919(56)	−61(45)	370(49)	−234(42)
C(11A)	774(70)	473(50)	1603(98)	−15(47)	63(72)	452(60)
C(12A)	973(74)	462(51)	1260(85)	220(51)	−82(68)	−224(51)
C(13A)	700(61)	572(50)	901(65)	186(47)	184(49)	7(45)
C(14A)	663(60)	708(52)	809(61)	170(46)	−91(49)	75(49)
C(15A)	1158(89)	946(70)	664(59)	408(63)	177(60)	469(55)
C(21A)	881(70)	1118(80)	544(54)	69(61)	51(51)	−211(51)
C(22A)	767(65)	1044(77)	542(52)	−274(54)	−221(48)	396(49)
C(23A)	785(67)	792(64)	823(64)	348(53)	−344(55)	−160(51)
C(24A)	504(54)	1345(86)	517(48)	−125(56)	20(39)	7(58)
C(25A)	1089(82)	749(60)	820(68)	−314(63)	−287(62)	12(56)
C(11B)	570(59)	1128(88)	1318(90)	−86(56)	432(59)	118(72)
C(12B)	517(59)	1259(98)	1282(96)	89(62)	−87(60)	−386(81)
C(13B)	637(70)	1242(91)	1201(88)	418(67)	182(62)	476(82)
C(14B)	352(54)	466(53)	2388(137)	103(41)	68(76)	107(81)
C(15B)	663(65)	1107(77)	1028(75)	83(58)	170(56)	−428(69)
C(21B)	2048(168)	1320(125)	1203(108)	750(112)	1026(122)	943(96)
C(22B)	2415(188)	605(64)	675(76)	251(96)	−567(98)	38(58)
C(23B)	767(73)	815(80)	1546(114)	128(65)	−241(86)	424(72)
C(24B)	1442(109)	516(57)	984(72)	245(66)	−137(89)	73(54)
C(25B)	937(93)	648(66)	1714(131)	−270(63)	−309(86)	694(76)

Table 10. Bond Lengths(Å) and Angles(°) for 9

	FragmentA	*FragmentB*
Zr–Zr	4.263(1)	
Zr–O	2.160(4)	2.194(4)
Zr–C(1)	2.198(6)	2.175(5)
Al–C(8)	1.933(9)	1.965(8)
O–C(1)	1.406(7)	1.372(1)
C(1)–C(2)	1.308(8)	1.318(8)
C(2)–C(3)	1.496(8)	1.496(8)
C(3)–C(4)	1.527(9)	1.539(10)
C(4)–C(5)	1.506(10)	1.488(11)
C(4)–C(6)	1.501(10)	1.514(12)
C(4)–C(7)	1.492(11)	1.516(12)
C(8)–C(9)	1.512(15)	1.538(13)
C(11)–C(12)	1.374(12)	1.360(17)
C(11)–C(15)	1.357(12)	1.348(16)
C(12)–C(13)	1.385(12)	1.350(17)
C(13)–C(14)	1.360(12)	1.355(16)
C(14)–C(15)	1.369(12)	1.312(16)
C(21)–C(22)	1.355(15)	1.350(16)
C(21)–C(25)	1.350(16)	1.355(18)
C(22)–C(23)	1.344(14)	1.352(15)
C(23)–C(24)	1.346(15)	1.362(16)
C(24)–C(25)	1.371(16)	1.379(18)
Zr(1)–O(B)	2.193(4)	
Zr(2)–H	2.015(34)	
Al–O(A)	1.778(4)	
Al–H	1.704(34)	
O–Zr–C(1)	37.6(2)	36.6(2)
O(A)–Al–C(8)	111.5(3)	109.5(3)
C(8)–Al–H	100.2(12)	107.1(12)
Zr–O–C(1)	72.7(3)	70.9(3)
Zr–C(1)–O	69.7(3)	72.5(3)
Zr–C(1)–C(2)	166.5(5)	160.2(5)
Al–C(8)–C(9)	118.2(7)	110.9(6)
C(2)–C(1)–O	123.8(5)	127.2(5)
C(3)–C(2)–C(1)	122.6(5)	120.7(5)
C(4)–C(3)–C(2)	117.3(5)	117.3(5)
C(5)–C(4)–C(3)	109.9(6)	111.4(6)
C(6)–C(4)–C(3)	109.0(5)	109.7(6)
C(7)–C(4)–C(3)	110.3(6)	107.7(6)
C(6)–C(4)–C(5)	108.7(6)	108.5(7)
C(7)–C(4)–C(5)	108.7(6)	110.5(7)

C(7)–C(4)–C(6)	110.1(6)	109.0(7)
C(15)–C(11)–C(12)	109.7(8)	108.6(11)
C(13)–C(12)–C(11)	106.8(7)	106.7(11)
C(14)–C(13)–C(12)	107.2(8)	107.4(11)
C(15)–C(14)–C(13)	109.8(8)	109.6(10)
C(14)–C(15)–C(11)	106.5(8)	107.7(10)
C(25)–C(21)–C(22)	106.5(10)	108.7(11)
C(23)–C(22)–C(21)	109.7(9)	108.9(10)
C(24)–C(23)–C(22)	107.7(9)	107.3(10)
C(25)–C(24)–C(23)	107.5(10)	108.2(11)
C(24)–C(25)–C(21)	108.6(10)	106.8(12)
O(A)–Zr(1)–O(B)	77.0(1)	
O(B)–Zr(1)–C(1A)	114.5(2)	
O(B)–Zr(2)–H	86.2(10)	
C(1B)–Zr(2)–H	122.8(10)	
O(A)–Al–H	101.4(11)	
C(8A)–Al–C(8B)	124.2(4)	
Zr(1)–O(A)–Al	153.5(2)	
Al–O(A)–C(1A)	131.3(3)	
Zr(1)–O(B)–Zr(2)	152.7(2)	
Zr(1)–O(B)–C(1B)	136.4(3)	
Zr(2)–H–Al	147.8(20)	

Table 11. Atom Coordinates ($\times 10^5$) and U_{eq}'s (Å^2, $\times 10^4$) for 9

	x	y	z	U_{eq}
Zr(1)	604(5)	21049(3)	37890(2)	436(2)
Zr(2)	35508(5)	22597(3)	35733(2)	461(2)
Al	19868(17)	36560(10)	38966(6)	537(5)
O(A)	8129(32)	30907(18)	38404(11)	517(11)
O(B)	18015(30)	19335(17)	36367(11)	408(10)
C(1A)	-2936(49)	31414(29)	39584(17)	434(17)
C(2A)	-7421(50)	37010(29)	40699(18)	469(17)
C(3A)	-19206(52)	37382(30)	41962(18)	527(18)
C(4A)	-20623(56)	41095(33)	45956(19)	547(19)
C(5A)	-16400(70)	48172(40)	45707(23)	913(26)
C(6A)	-33071(64)	41250(38)	46540(23)	857(24)
C(7A)	-13910(74)	37716(46)	49537(22)	1078(35)
C(8A)	18615(78)	43149(37)	34600(31)	1218(38)
C(9A)	14796(107)	50129(55)	35579(38)	1826(51)
C(1B)	24070(48)	14027(29)	35080(15)	376(19)
C(2B)	20456(51)	7834(30)	34463(17)	463(17)
C(3B)	28243(55)	2552(30)	33137(18)	570(19)
C(4B)	23730(73)	-1739(35)	29380(21)	735(25)
C(5B)	20265(82)	2482(39)	25688(23)	1099(35)
C(6B)	13440(94)	-5721(42)	30341(26)	1252(37)
C(7B)	33158(88)	-6536(41)	28553(25)	1241(35)
C(8B)	23951(63)	38662(44)	44838(24)	1027(29)
C(9B)	34551(102)	43208(47)	45467(30)	1470(41)
C(11A)	-2462(63)	18235(55)	30308(21)	775(29)
C(12A)	-6204(74)	24705(42)	30598(21)	701(25)
C(13A)	-15863(71)	24469(45)	32635(25)	780(26)
C(14A)	-17587(63)	17955(55)	33583(25)	833(28)
C(15A)	-9295(82)	14056(38)	32189(27)	810(27)
C(21A)	-3829(129)	20345(47)	45221(27)	977(34)
C(22A)	7468(96)	19000(54)	45291(23)	883(34)
C(23A)	8848(90)	13102(56)	43442(28)	864(29)
C(24A)	-1614(132)	10733(43)	42069(27)	1003(35)
C(25A)	-9474(75)	15247(76)	43172(34)	1051(36)
C(11B)	40703(70)	19367(88)	43108(26)	979(38)
C(12B)	46568(123)	25132(56)	42670(37)	1074(38)
C(13B)	54280(82)	23798(66)	40034(38)	1020(36)
C(14B)	53157(86)	17258(67)	38983(28)	916(32)
C(15B)	45029(105)	14552(43)	40852(39)	954(34)
C(21B)	31528(124)	21130(66)	28120(23)	1031(40)
C(22B)	28990(77)	27577(70)	28833(26)	945(31)
C(23B)	38741(122)	30847(43)	30228(27)	933(29)
C(24B)	47481(83)	26368(84)	30312(29)	1109(37)
C(25B)	42915(144)	20215(66)	29130(35)	1176(39)
H[a]	3054(29)	3168(17)	3750(11)	9(10)

[a] Hydrogen atom coordinates $\times 10^4$, isotropic U $\times 10^3$.

Table 12. Atom Coordinates ($\times 10^4$) and U ($\times 10^4$) of Hydrogen Atoms for 9

	x	y	z	U
H(2A)	-302	4099	4072	63
H(3A1)	-2184	3293	4224	63
H(3A2)	-2396	3956	3979	63
H(5A1)	-1747	5048	4818	63
H(5A2)	-852	4814	4536	63
H(5A3)	-2061	5036	4342	63
H(6A1)	-3399	4351	4905	63
H(6A2)	-3723	4358	4430	63
H(6A3)	-3590	3683	4666	63
H(7A1)	-1510	3996	5201	63
H(7A2)	-1641	3319	4968	63
H(7A3)	-603	3778	4920	63
H(8A1)	2562	4607	3496	63
H(8A2)	1253	4648	3513	63
H(9A1)	1741	5147	3824	63
H(9A2)	1670	5294	3355	63
H(9A3)	635	4977	3536	63
H(2B)	1283	671	3485	63
H(3B1)	3002	-38	3541	63
H(3B2)	3499	471	3251	63
H(5B1)	1872	-29	2333	63
H(5B2)	2637	546	2529	63
H(5B3)	1368	498	2610	63
H(6B1)	855	-661	2786	63
H(6B2)	933	-327	3218	63
H(6B3)	1589	-986	3160	63
H(7B1)	3279	-730	2566	63
H(7B2)	3221	-1065	2992	63
H(7B3)	4036	-465	2953	63
H(8B1)	1904	3898	4685	63
H(8B2)	3128	4078	4591	63
H(9B1)	3477	4498	4823	63
H(9B2)	4098	4036	4539	63
H(9B3)	3409	4649	4354	63
H(11A)	398	1689	2900	63
H(12A)	-283	2858	2958	63
H(13A)	-2038	2815	3327	63
H(14A)	-2364	1634	3499	63
H(15A)	-851	933	3248	63
H(21A)	-713	2410	4640	63
H(22A)	1351	2182	4647	63
H(23A)	1595	1101	4317	63

H(24A)	-320	666	4061	63
H(25A)	-1753	1487	4258	63
H(11B)	3458	1878	4474	63
H(12B)	4541	2928	4397	63
H(13B)	5953	2688	3909	63
H(14B)	5759	1498	3717	63
H(15B)	4264	1000	4063	63
H(21B)	2617	1783	2708	63
H(22B)	2157	2950	2843	63
H(23B)	3940	3541	3102	63
H(24B)	5536	2732	3105	63
H(25B)	4699	1611	2904	63

Table 13. Gaussian Amplitudes ($\times 10^4$) for 9

	U_{11}	U_{22}	U_{33}	U_{12}	U_{13}	U_{23}
Zr(1)	444(4)	509(4)	358(4)	-3(3)	64(3)	-20(3)
Zr(2)	437(4)	545(4)	397(4)	-10(3)	33(3)	-17(3)
Al	577(13)	519(13)	518(13)	-52(10)	81(10)	-91(10)
O(A)	513(27)	512(26)	538(29)	13(21)	108(22)	-92(21)
O(B)	407(23)	462(25)	346(23)	9(20)	9(18)	-38(20)
C(1A)	412(39)	589(44)	313(35)	40(33)	96(30)	37(31)
C(2A)	448(40)	472(41)	494(42)	42(33)	90(32)	-70(32)
C(3A)	535(43)	593(43)	441(41)	71(34)	4(33)	-46(33)
C(4A)	573(46)	639(48)	439(43)	88(37)	99(35)	-60(36)
C(5A)	1115(68)	966(64)	722(58)	19(54)	372(50)	-337(48)
C(6A)	773(58)	1025(63)	819(60)	118(48)	280(47)	-164(47)
C(7A)	1274(77)	1557(85)	393(48)	433(63)	57(48)	-56(51)
C(8A)	1430(87)	449(51)	1889(103)	328(53)	665(76)	243(57)
C(9A)	1996(127)	1353(102)	2120(142)	-213(93)	211(105)	411(92)
C(1B)	524(40)	445(40)	154(31)	99(33)	14(28)	4(28)
C(2B)	596(44)	411(40)	375(38)	66(33)	23(32)	-7(31)
C(3B)	782(50)	509(42)	397(40)	96(37)	-18(36)	-10(32)
C(4B)	1176(69)	480(47)	492(48)	146(47)	-135(46)	-151(38)
C(5B)	1930(99)	821(60)	474(51)	337(62)	-154(56)	-151(44)
C(6B)	1898(108)	890(67)	837(69)	-327(69)	-377(69)	-244(53)
C(7B)	1964(105)	890(65)	749(62)	472(67)	-333(64)	-425(51)
C(8B)	694(55)	1527(80)	865(63)	-555(54)	119(46)	-772(58)
C(9B)	2078(120)	1158(82)	1086(83)	183(80)	-182(80)	-305(64)
C(11A)	570(52)	1327(82)	385(46)	152(57)	-121(38)	-312(50)
C(12A)	746(60)	891(64)	398(45)	-3(48)	-219(41)	64(40)
C(13A)	558(55)	967(68)	735(58)	242(49)	-248(44)	-317(49)
C(14A)	441(50)	1146(75)	900(65)	-230(53)	27(43)	-179(58)
C(15A)	848(66)	647(57)	857(66)	14(51)	-224(52)	-268(48)
C(21A)	1661(112)	824(71)	558(58)	449(77)	594(67)	223(49)
C(22A)	1239(85)	1067(82)	327(46)	72(64)	29(49)	185(47)
C(23A)	1146(83)	871(72)	631(60)	468(64)	334(57)	343(52)
C(24A)	1602(108)	640(64)	801(69)	-256(73)	286(77)	180(49)
C(25A)	720(67)	1558(109)	946(82)	99(74)	391(59)	579(75)
C(11B)	540(57)	1889(120)	470(54)	159(75)	-93(43)	259(68)
C(12B)	1105(95)	981(84)	983(85)	300(71)	-508(68)	-396(65)
C(13B)	608(64)	1093(88)	1252(91)	-430(59)	-338(59)	233(69)
C(14B)	563(60)	1188(90)	959(72)	284(58)	-66(53)	-161(66)
C(15B)	812(76)	779(68)	1116(89)	-65(61)	-523(62)	254(64)
C(21B)	1750(120)	1051(88)	334(45)	-536(89)	299(61)	-41(53)
C(22B)	903(71)	1357(91)	576(55)	-82(75)	90(49)	514(62)
C(23B)	1249(84)	812(67)	787(63)	-350(69)	324(65)	138(49)
C(24B)	715(69)	1766(121)	899(72)	-312(82)	310(55)	270(80)
C(25B)	1558(113)	1283(101)	851(78)	406(94)	820(83)	212(69)

Table 14. Bond Lengths(Å) and Angles(°) for 10

Zr–C(1)	2.188(4)
Zr–O	2.195(2)
Zr–H	2.01(4)
Zr–C(11)	2.511(5)
Zr–C(12)	2.505(6)
Zr–C(13)	2.515(7)
Zr–C(14)	2.506(6)
Zr–C(15)	2.513(5)
Zr–C(21)	2.512(5)
Zr–C(22)	2.483(7)
Zr–C(23)	2.508(7)
Zr–C(24)	2.531(7)
Zr–C(25	2.517(6)
Al–O	1.812(3)
Al–C(8)	1.956(5)
C(1)–O	1.392(4)
C(1)–C(2)	1.315(5)
C(2)–C(3)	1.501(6)
C(3)–C(4)	1.519(6)
C(4)–C(5)	1.461(8)
C(4)–C(6)	1.496(8)
C(4)–C(7)	1.477(8)
C(11)–C(12)	1.391(8)
C(12)–C(13)	1.386(9)
C(13)–C(14)	1.363(9)
C(14)–C(15)	1.377(8)
C(15)–C(11)	1.379(7)
C(21)–C(22)	1.384(8)
C(22)–C(23)	1.378(10)
C(23)–C(24)	1.387(10)
C(24)–C(25)	1.386(9)
C(25)–C(21)	1.385(8)
Zr–Zr'	3.976(1)
Al–H	3.94(4)
Zr–Al	3.766(2)
O–Al–O	94.40(12)
Zr–H–Zr'	163(2)
H–Zr–C(1)	113.9(11)
H–Zr–O	77.1(11)
C(1)–Zr–O	37.04(11)
Zr–C(1)–O	71.77(18)
Zr–C(1)–C(2)	162.5(3)
Zr–O–C(1)	71.18(18)

Zr–O–Al	139.89(13)
Al–O–C(1)	132.8(2)
O–C(1)–C(2)	125.5(3)
C(1)–C(2)–C(3)	122.0(4)
C(2)–C(3)–C(4)	118.0(4)
O–Al–C(8)	109.39(17)
C(8)–Al–C(8')	116.8(2)
Al–H–Zr(1)	81.5(12)

Table 15. Atom Coordinates ($\times 10^5$) and U_{eq}'s (Å^2, $\times 10^4$) for 10

	x	y	z	U_{eq}
Zr	6870(2)	15034(4)	17857(2)	523(1)
Al	0(0)	45893(16)	25000(0)	447(4)
O	1700(13)	34024(23)	18745(11)	462(6)
C(1)	5955(19)	34184(41)	13336(18)	470(11)
C(2)	6470(21)	43920(41)	9236(19)	530(12)
C(3)	10802(24)	42999(45)	3254(20)	659(13)
C(4)	16717(25)	53033(48)	2415(21)	661(13)
C(5)	21991(35)	53853(76)	8422(34)	1595(28)
C(6)	20374(35)	50513(66)	−3818(30)	1364(23)
C(7)	13284(38)	65893(67)	1762(39)	1541(27)
C(8)	−8840(26)	55803(46)	22158(24)	803(15)
C(9A)	−10786(56)	67442(103)	25787(80)	814(41)
C(9B)	−8543(57)	67659(95)	18967(79)	1086(43)
C(11)	15682(25)	20262(60)	27649(24)	725(15)
C(12)	16267(28)	7038(64)	26597(30)	889(19)
C(13)	19394(33)	5337(64)	20634(38)	1017(21)
C(14)	20586(26)	17158(77)	17999(26)	930(20)
C(15)	18393(25)	26410(48)	22311(29)	721(15)
C(21)	2134(36)	10778(49)	6086(23)	790(16)
C(22)	7815(32)	2161(72)	7624(31)	941(19)
C(23)	5548(47)	−6481(56)	12216(35)	1082(24)
C(24)	−1508(41)	−3181(62)	13688(28)	969(20)
C(25)	−3569(30)	7548(55)	9905(28)	778(16)
H	0(0)	1203(39)	2500(0)	545(141)

Table 16. Atom Coordinates ($\times 10^4$) and U ($\times 10^4$) of Hydrogen Atoms for 10

	x	y	z	U
H(2)	410	5187	1001	759
H(31)	740	4352	−54	569
H(32)	1314	3480	337	569
H(51)	1989	5359	1233	823
H(52)	2490	4486	787	823
H(53)	2552	5985	771	823
H(61)	1673	5065	−730	848
H(62)	2398	5706	−429	848
H(63)	2271	4231	−337	848
H(71)	1098	6801	570	886
H(72)	1690	7243	109	886
H(73)	971	6594	−188	886
H(81A)	−834	5838	1772	1519
H(82A)	−1290	5007	2227	1519
H(81B)	−1175	5038	1921	1519
H(82B)	−1135	5727	2603	1519
H(91A)	−641	7230	2677	1519
H(92A)	−1422	7226	2302	1519
H(93A)	−1284	6487	2970	1519
H(91B)	−530	6702	1561	1646
H(92B)	−680	7396	2219	1646
H(93B)	−1336	6989	1723	1646
H(11)	1379	2425	3137	1013
H(12)	1475	46	2947	1013
H(13)	2048	−287	1884	823
H(14)	2255	1865	1390	1013
H(15)	1868	3551	2174	911
H(21)	212	1765	299	1013
H(22)	1245	207	580	1013
H(23)	836	−1356	1406	1076
H(24)	−441	−745	1673	1519
H(25)	−815	1200	992	1203

Table 17. Gaussian amplitudes ($\times 10^4$) for **10**

	U_{11}	U_{22}	U_{33}	U_{12}	U_{13}	U_{23}
Zr	511(3)	527(3)	520(3)	105(2)	−29(2)	−96(2)
Al	452(11)	423(10)	472(10)	0(0)	67(8)	0(0)
O	474(16)	494(16)	427(15)	39(14)	92(12)	6(13)
C(1)	397(23)	634(28)	381(24)	47(23)	48(19)	−133(23)
C(2)	470(27)	667(31)	462(26)	60(23)	90(21)	20(23)
C(3)	599(31)	875(35)	509(28)	−5(27)	82(24)	−5(25)
C(4)	552(31)	861(36)	589(30)	−57(28)	165(25)	34(26)
C(5)	1087(54)	2071(80)	1549(63)	−733(53)	−379(48)	449(56)
C(6)	1188(52)	1927(72)	1057(47)	−418(49)	594(41)	−85(46)
C(7)	1289(58)	1041(51)	2404(85)	−94(46)	835(57)	369(54)
C(8)	812(37)	648(34)	939(38)	237(29)	14(29)	−11(31)
C(9A)	542(71)	650(84)	1257(142)	201(57)	114(69)	−147(74)
C(9B)	785(76)	819(83)	1613(152)	−113(57)	−152(78)	522(76)
C(11)	552(32)	1006(43)	587(33)	117(30)	−146(25)	−108(31)
C(12)	663(38)	1022(50)	931(46)	164(35)	−246(33)	296(38)
C(13)	781(43)	958(48)	1261(58)	475(38)	−237(39)	−344(44)
C(14)	476(31)	1513(62)	798(39)	287(38)	30(26)	−136(44)
C(15)	436(29)	816(37)	883(39)	54(27)	−130(28)	−41(34)
C(21)	925(42)	848(41)	578(32)	−70(36)	−53(32)	−272(27)
C(22)	839(44)	1093(51)	883(45)	116(41)	13(36)	−549(38)
C(23)	1527(71)	622(41)	1039(52)	284(45)	−257(48)	−342(37)
C(24)	1265(57)	712(42)	924(44)	−270(40)	56(41)	−334(36)
C(25)	815(41)	715(38)	769(38)	−37(32)	−149(33)	−330(30)